US009075185B2

(12) **United States Patent**
Kumano et al.

(10) **Patent No.: US 9,075,185 B2**
(45) **Date of Patent: Jul. 7, 2015**

(54) **HOLE-ASSISTED OPTICAL FIBER**

(71) Applicants: **FURUKAWA ELECTRIC CO., LTD.**, Tokyo (JP); **NIPPON TELEGRAPH AND TELEPHONE CORPORATION**, Chiyoda-ku (JP)

(72) Inventors: **Naomi Kumano**, Tokyo (JP); **Iwao Shimotakahara**, Tokyo (JP); **Ryuichi Sugizaki**, Tokyo (JP); **Takeshi Yagi**, Tokyo (JP); **Tomoya Shimizu**, Ibaraki (JP); **Takashi Matsui**, Ibaraki (JP); **Yukihiro Goto**, Ibaraki (JP); **Toshio Kurashima**, Ibaraki (JP); **Kazuhide Nakajima**, Ibaraki (JP)

(73) Assignees: **FURUKAWA ELECTRIC CO., LTD.**, Tokyo (JP); **NIPPON TELEGRAPH AND TELEPHONE CORPORATION**, Tokyo (JP)

(*) Notice: Subject to any disclaimer, the term of this patent is extended or adjusted under 35 U.S.C. 154(b) by 351 days.

(21) Appl. No.: **13/754,963**

(22) Filed: **Jan. 31, 2013**

(65) **Prior Publication Data**

US 2013/0136409 A1 May 30, 2013

Related U.S. Application Data

(63) Continuation of application No. PCT/JP2011/068073, filed on Aug. 8, 2011.

(30) **Foreign Application Priority Data**

Aug. 9, 2010 (JP) 2010-179058

(51) **Int. Cl.**

G02B 6/032 (2006.01)
G02B 6/02 (2006.01)
G02B 6/036 (2006.01)

(52) **U.S. Cl.**

CPC ***G02B 6/032*** (2013.01); ***G02B 6/02333*** (2013.01); ***G02B 6/02366*** (2013.01); *G02B 6/03627* (2013.01)

(58) **Field of Classification Search**

CPC G02B 6/02333
See application file for complete search history.

(56) **References Cited**

U.S. PATENT DOCUMENTS

7,228,040 B2 6/2007 Nakajima et al.
2010/0215329 A1 * 8/2010 Bickham et al. 385/123

FOREIGN PATENT DOCUMENTS

JP 2004-226540 A 8/2004
JP 3854627 B2 9/2006

OTHER PUBLICATIONS

International Search Report mailed Sep. 6, 2011 in PCT/JP2011/068073 filed Aug. 8, 2011 (with English translation).

(Continued)

Primary Examiner — Uyen Chau N Le
Assistant Examiner — Chad Smith
(74) *Attorney, Agent, or Firm* — Oblon, McClelland, Maier & Neustadt, L.L.P.

(57) **ABSTRACT**

A hole-assisted optical fiber includes a core portion and a cladding portion that includes an inner cladding layer, an outer cladding layer, and holes formed around the core portion. A diameter of the core portion is 3 μm to 9.8 μm, a relative refractive index difference of the core portion relative to the outer cladding layer is 0.11% to 0.45%, an outside diameter of the inner cladding layer is 53 μm or less, a relative refractive index difference of the inner cladding layer relative to the outer cladding layer is a negative value, −0.30% or more, a diameter of each hole is 2.4 μm to 4.0 μm, a hole occupancy rate is 17% to 48%, a bending loss at a wavelength of 1625 nm when bent at a radius of 5 mm is 1 dB/turn or less, and a cut-off wavelength is 1550 nm or less.

3 Claims, 49 Drawing Sheets

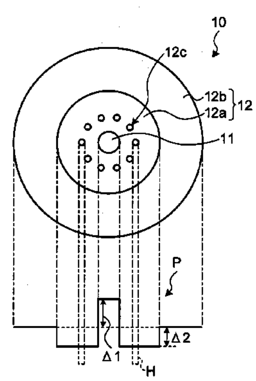

(56) **References Cited**

OTHER PUBLICATIONS

International Written Opinion mailed Sep. 6, 2011 in PCT/JP2011/068073 filed Aug. 8, 2011.
Kazuhide, Nakajima, et al., Single-Mode Hole-Assisted Fiber with Low Bending Loss Characteristics, Proc Int Wire Cable Symp, vol. 58, 2009, pp. 264-269.
Takatoshi Kato et al., "Dispersion Shifted Fiber for WDM Transmission", IEICE Technical Report OCS96-51 to 59, vol. 96, No. 335, Nov. 1, 1996, pp. 43-48 (with English translation).
Tomoyo Shimizu et al., "A Study on Cutoff Wavelength Characteristics in Hole-Assisted Fiber", Proceedings of the 2009 IEICE General Conference, Mar. 4, 2009, pp. 512, B-13-24 (with English translation).
Takashi Matsui et al., "A Study on Bending-Loss and Dispersion Properties of Hole-Assisted Fibers", Proceedings of the 2010 IEICE General Conference, Mar. 2, 2010, pp. 521, B-13-26 (with English translation).
M.-J. Li et al., Ultra-Low Bending Loss Single-Mode Fiber for FTTH, Journal of Lightwave Technology, vol. 27, No. 3, Feb. 18, 2009, pp. 376-382.

* cited by examiner

FIG.1

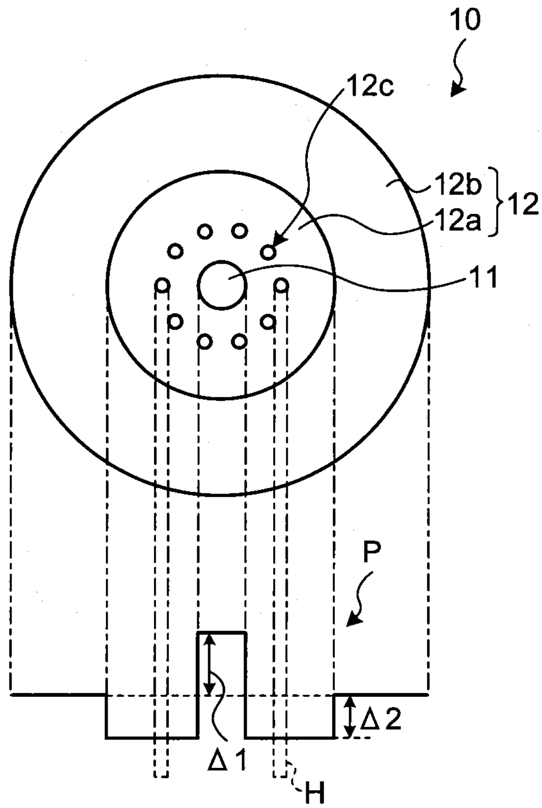

FIG.2

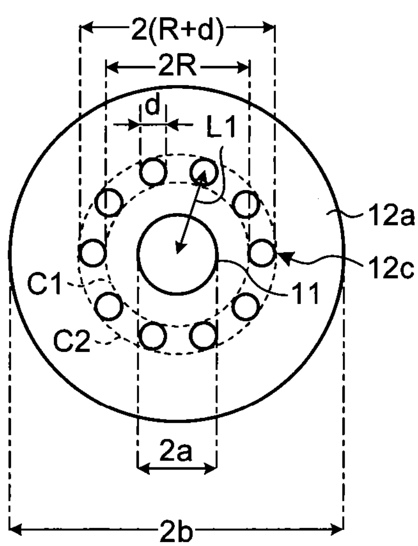

FIG.3A

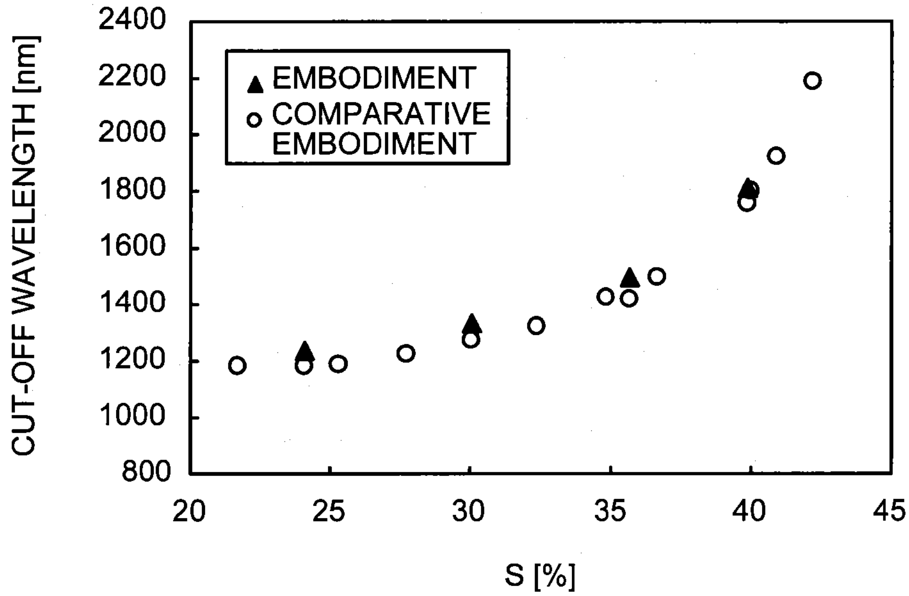
2400
2200
2000
1800
1600
1400
1200
1000
800
CUT-OFF WAVELENGTH [nm]
EMBODIMENT
COMPARATIVE EMBODIMENT
20
25
30
35
40
45
S [%]

FIG.3B

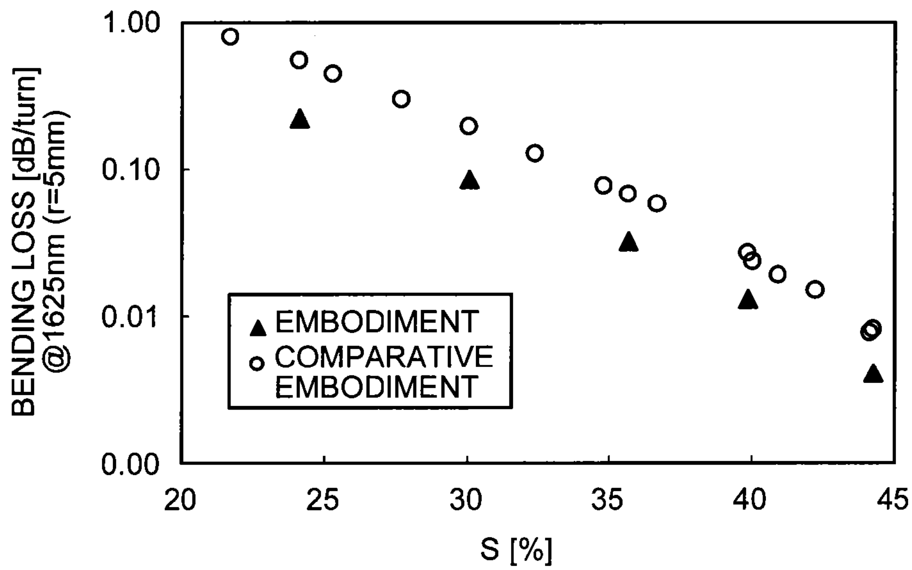
1.00
0.10
0.01
0.00
BENDING LOSS [dB/turn] @1625nm (r=5mm)
EMBODIMENT
COMPARATIVE EMBODIMENT
20
25
30
35
40
45
S [%]

FIG.4A

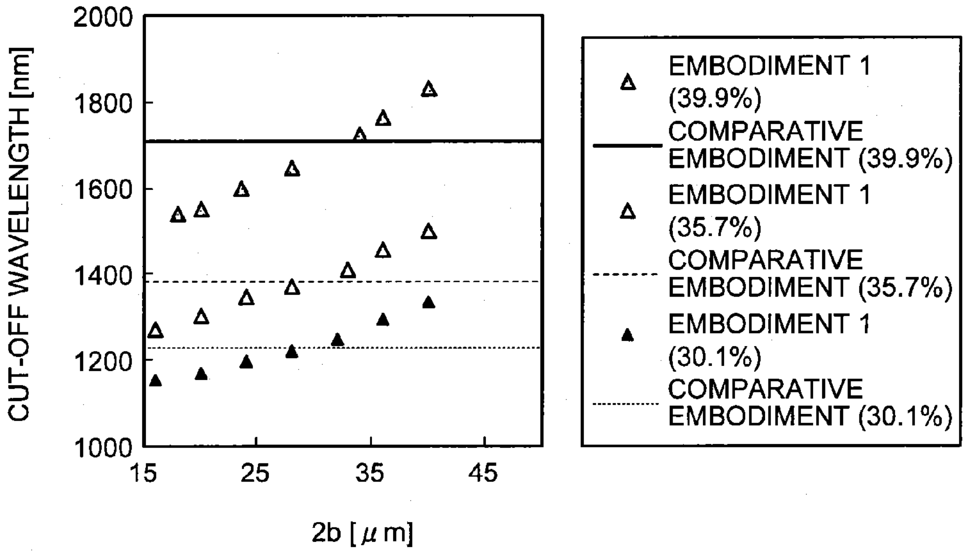
2000
1800
1600
1400
1200
1000
CUT-OFF WAVELENGTH [nm]
15
25
35
45
2b [μm]
EMBODIMENT 1 (39.9%)
COMPARATIVE EMBODIMENT (39.9%)
EMBODIMENT 1 (35.7%)
COMPARATIVE EMBODIMENT (35.7%)
EMBODIMENT 1 (30.1%)
COMPARATIVE EMBODIMENT (30.1%)

FIG.4B

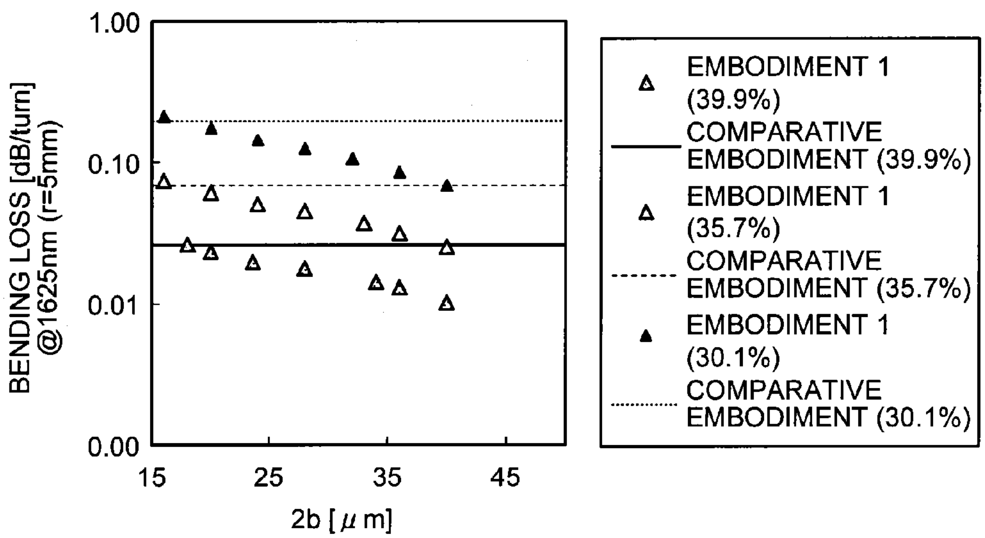
1.00
0.10
0.01
0.00
BENDING LOSS [dB/turn] @1625nm (r=5mm)
15
25
35
45
2b [μm]
EMBODIMENT 1 (39.9%)
COMPARATIVE EMBODIMENT (39.9%)
EMBODIMENT 1 (35.7%)
COMPARATIVE EMBODIMENT (35.7%)
EMBODIMENT 1 (30.1%)
COMPARATIVE EMBODIMENT (30.1%)

FIG.4C

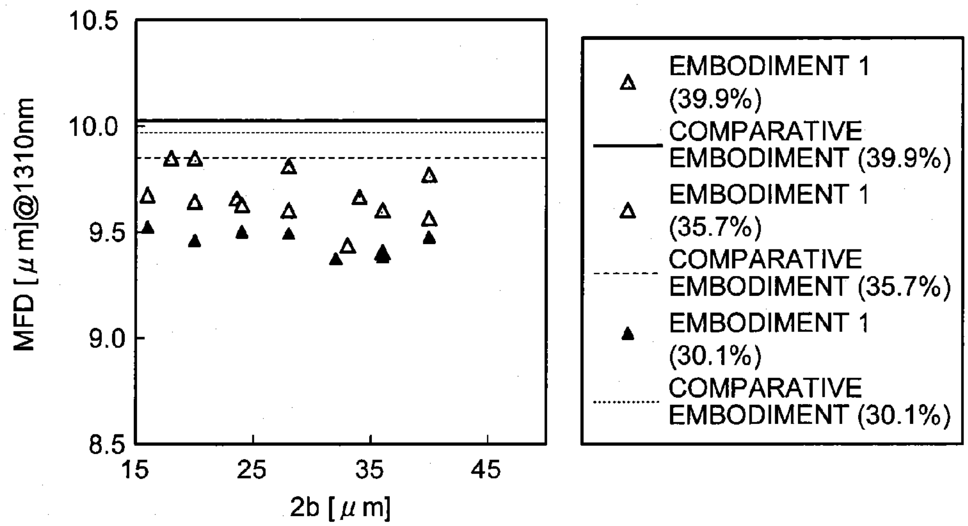

10.5
10.0
9.5
9.0
8.5
MFD [μ m]@1310nm
15
25
35
45
2b [μ m]
EMBODIMENT 1 (39.9%)
COMPARATIVE EMBODIMENT (39.9%)
EMBODIMENT 1 (35.7%)
COMPARATIVE EMBODIMENT (35.7%)
EMBODIMENT 1 (30.1%)
COMPARATIVE EMBODIMENT (30.1%)

FIG.4D

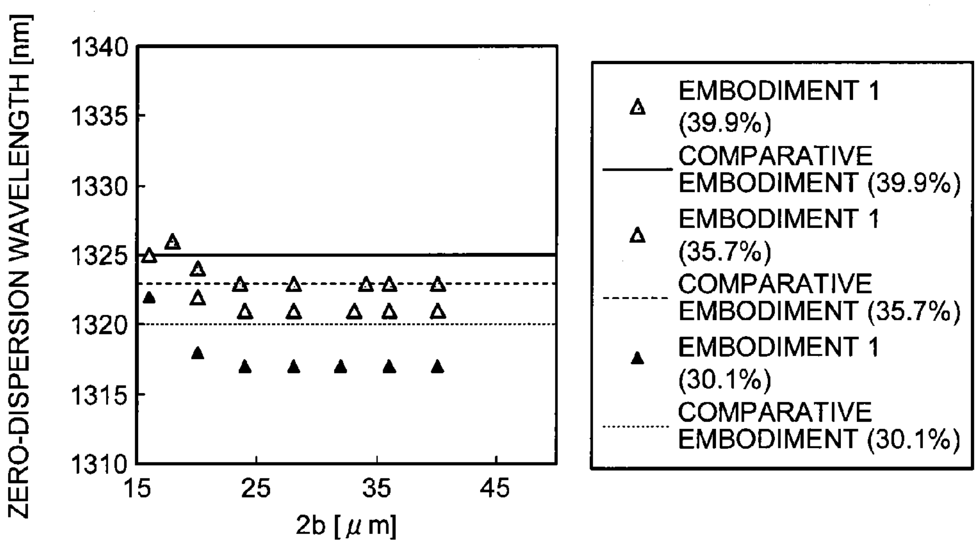

1340
1335
1330
1325
1320
1315
1310
ZERO-DISPERSION WAVELENGTH [nm]
15
25
35
45
2b [μ m]
EMBODIMENT 1 (39.9%)
COMPARATIVE EMBODIMENT (39.9%)
EMBODIMENT 1 (35.7%)
COMPARATIVE EMBODIMENT (35.7%)
EMBODIMENT 1 (30.1%)
COMPARATIVE EMBODIMENT (30.1%)

FIG.4E

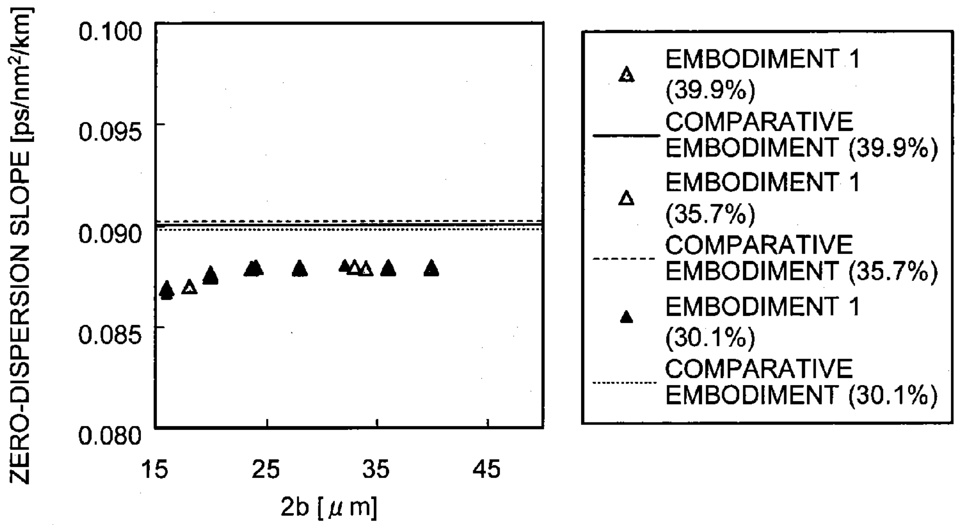
ZERO-DISPERSION SLOPE [ps/nm²/km]
0.100
0.095
0.090
0.085
0.080
15
25
35
45
2b [μm]
EMBODIMENT 1 (39.9%)
COMPARATIVE EMBODIMENT (39.9%)
EMBODIMENT 1 (35.7%)
COMPARATIVE EMBODIMENT (35.7%)
EMBODIMENT 1 (30.1%)
COMPARATIVE EMBODIMENT (30.1%)

FIG.5

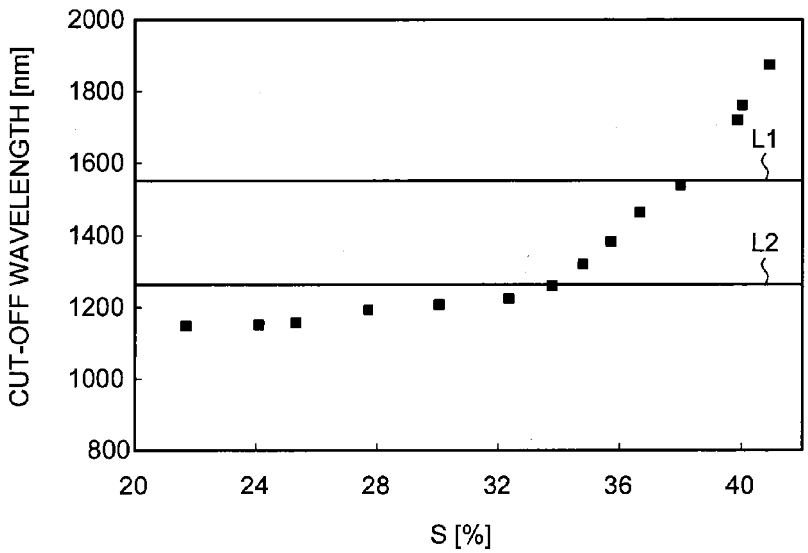
CUT-OFF WAVELENGTH [nm]
2000
1800
1600
1400
1200
1000
800
20
24
28
32
36
40
S [%]
L1
L2

FIG.6

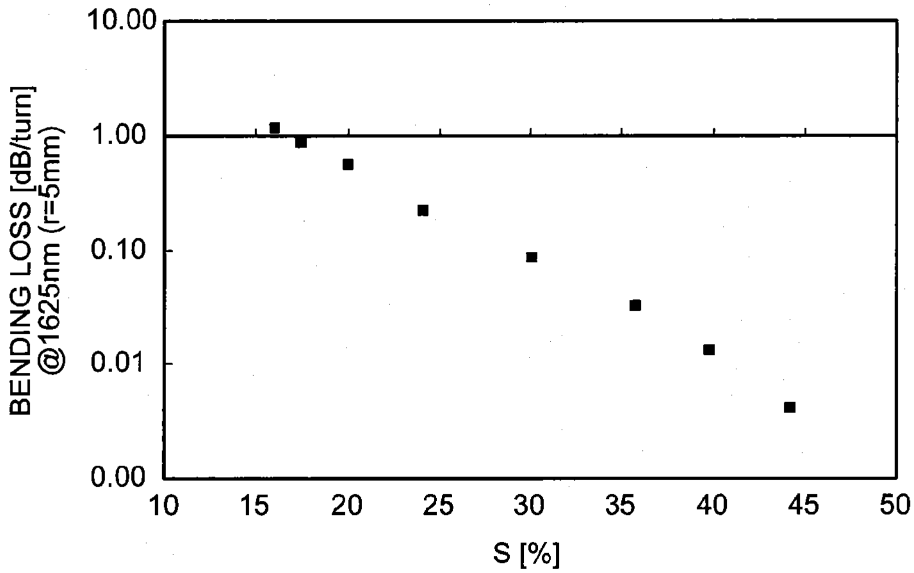
10.00
1.00
0.10
0.01
0.00
BENDING LOSS [dB/turn] @1625nm (r=5mm)
10
15
20
25
30
35
40
45
50
S [%]

FIG.7

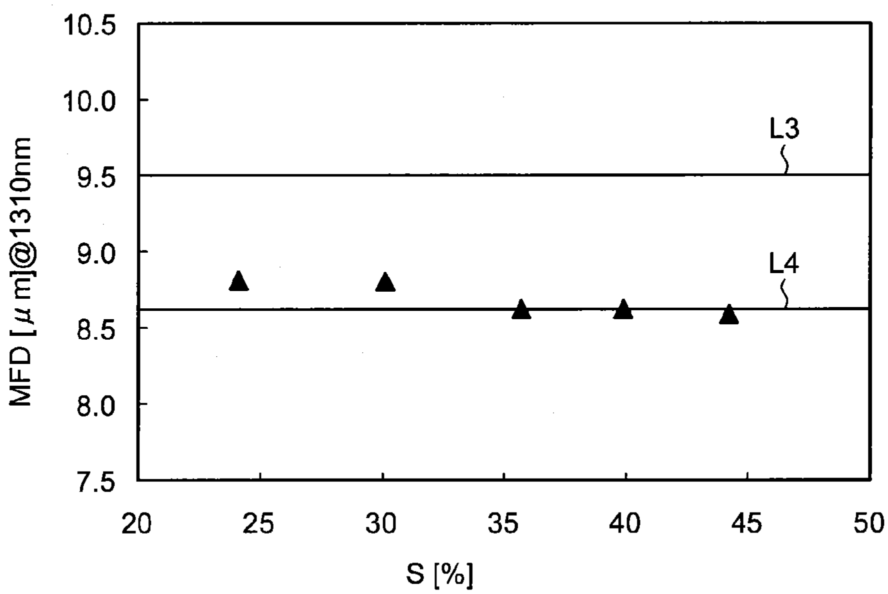
10.5
10.0
9.5
9.0
8.5
8.0
7.5
MFD [μm]@1310nm
L3
L4
20
25
30
35
40
45
50
S [%]

FIG.8

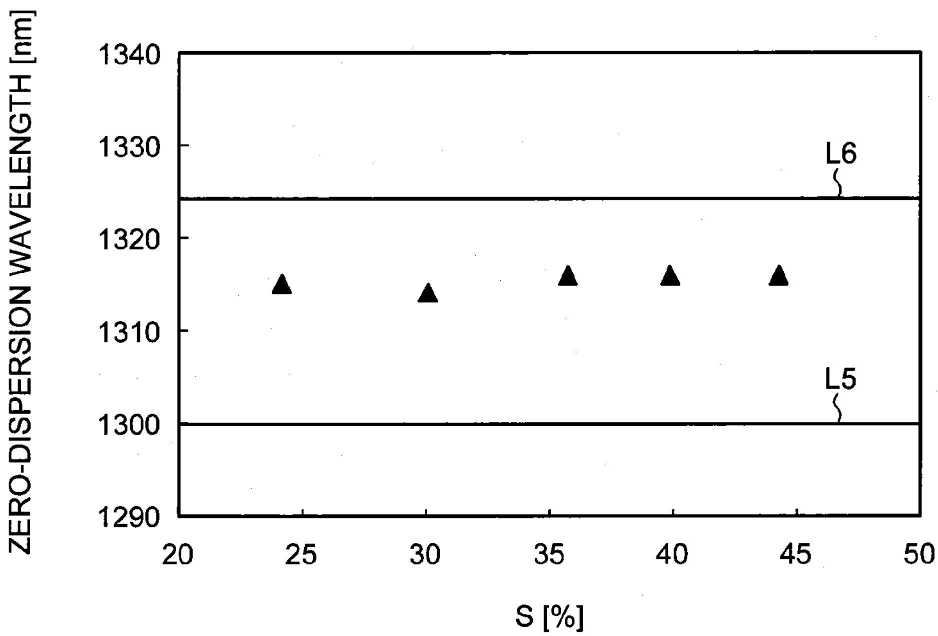
ZERO-DISPERSION WAVELENGTH [nm]
1340
1330
1320
1310
1300
1290
L6
L5
20
25
30
35
40
45
50
S [%]

FIG.9

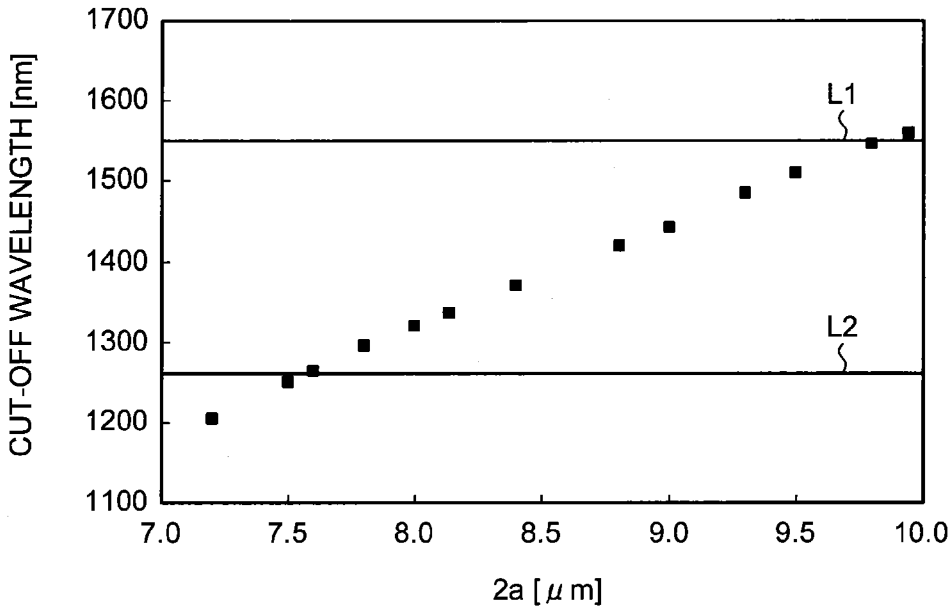
CUT-OFF WAVELENGTH [nm]
1700
1600
1500
1400
1300
1200
1100
L1
L2
7.0
7.5
8.0
8.5
9.0
9.5
10.0
2a [μm]

FIG.10

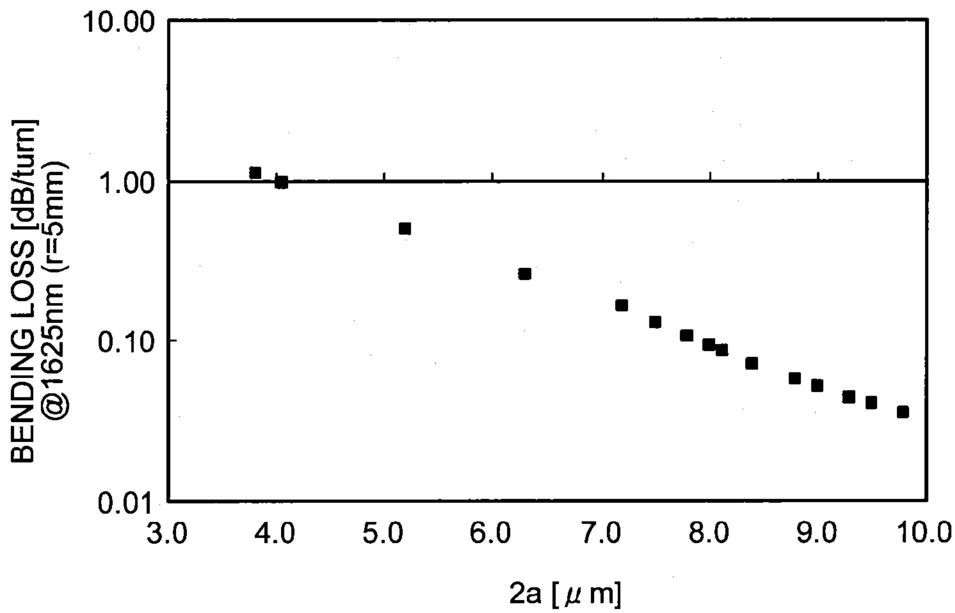

BENDING LOSS [dB/turn] @1625nm (r=5mm)
10.00
1.00
0.10
0.01
3.0
4.0
5.0
6.0
7.0
8.0
9.0
10.0
2a [μm]

FIG.11

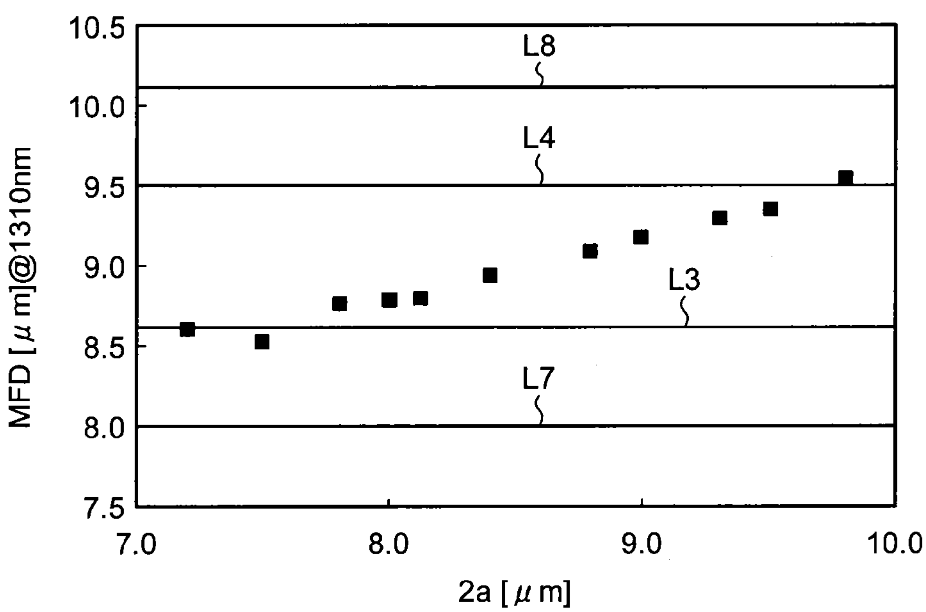

MFD [μm]@1310nm
10.5
10.0
9.5
9.0
8.5
8.0
7.5
L8
L4
L3
L7
7.0
8.0
9.0
10.0
2a [μm]

FIG.12

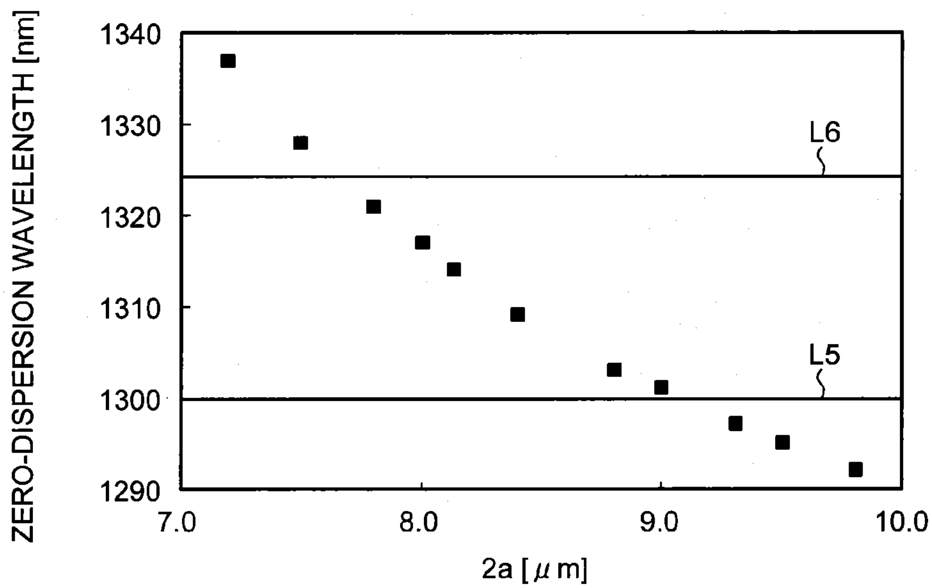
ZERO-DISPERSION WAVELENGTH [nm]
1340
1330
1320
1310
1300
1290
L6
L5
7.0
8.0
9.0
10.0
2a [μm]

FIG.13

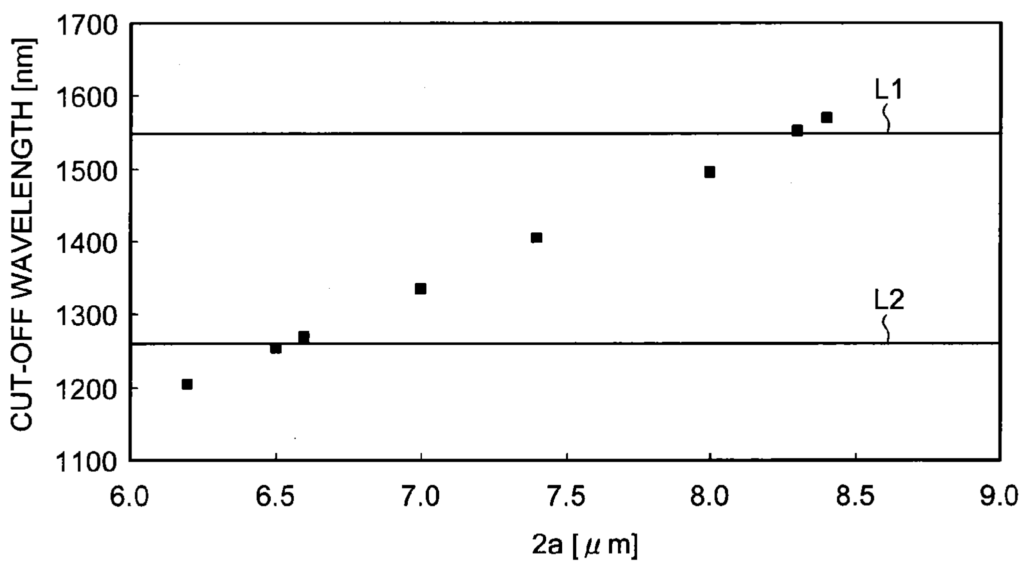
CUT-OFF WAVELENGTH [nm]
1700
1600
1500
1400
1300
1200
1100
L1
L2
6.0
6.5
7.0
7.5
8.0
8.5
9.0
2a [μm]

FIG.14

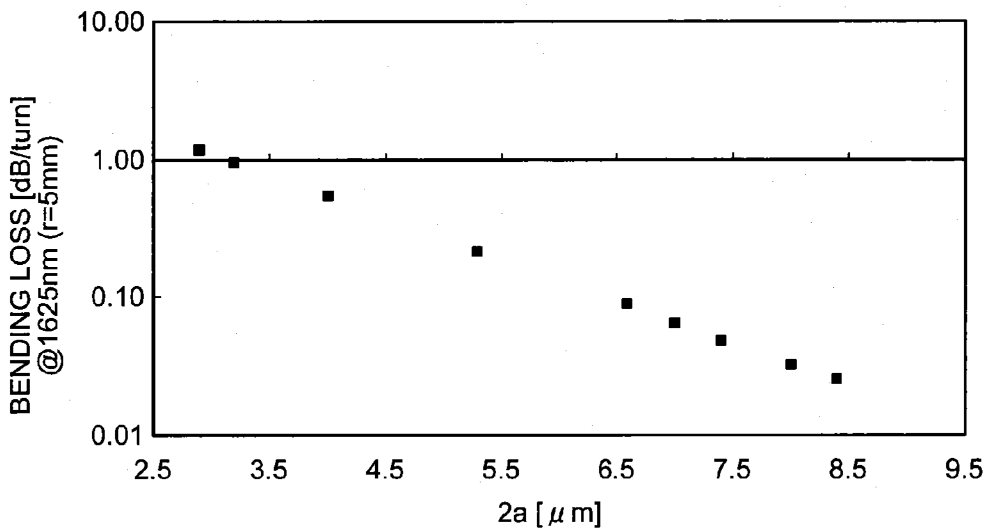
BENDING LOSS [dB/turn] @1625nm (r=5mm)
10.00
1.00
0.10
0.01
2.5
3.5
4.5
5.5
6.5
7.5
8.5
9.5
2a [μm]

FIG.15

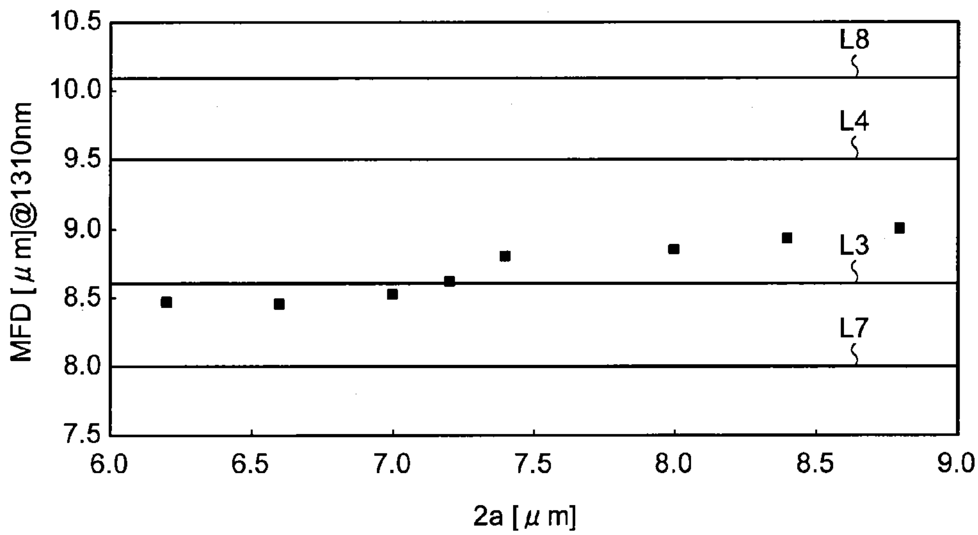
MFD [μm]@1310nm
10.5
10.0
9.5
9.0
8.5
8.0
7.5
L8
L4
L3
L7
6.0
6.5
7.0
7.5
8.0
8.5
9.0
2a [μm]

FIG.16

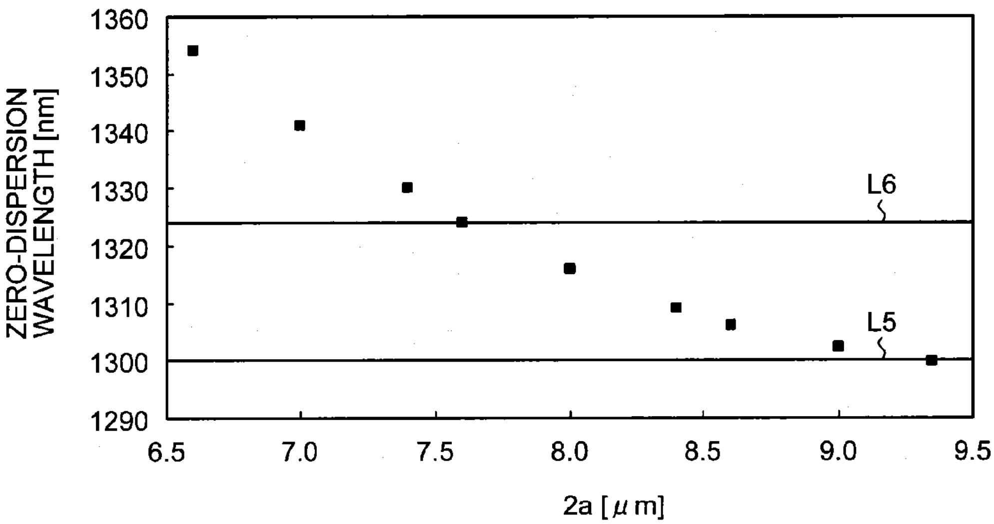
ZERO-DISPERSION WAVELENGTH [nm]
1360
1350
1340
1330
1320
1310
1300
1290
L6
L5
6.5
7.0
7.5
8.0
8.5
9.0
9.5
2a [μm]

FIG.17

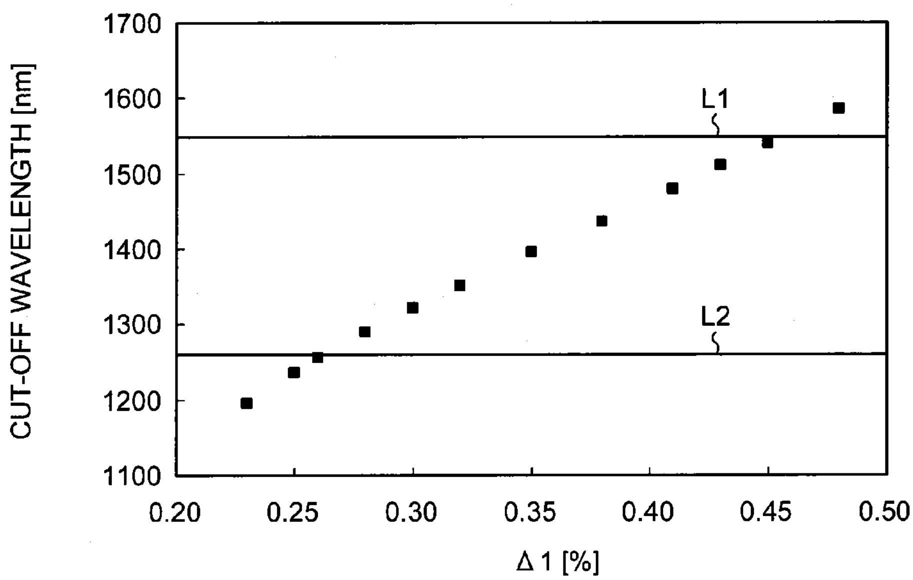
CUT-OFF WAVELENGTH [nm]
1700
1600
1500
1400
1300
1200
1100
L1
L2
0.20
0.25
0.30
0.35
0.40
0.45
0.50
Δ1 [%]

FIG.18

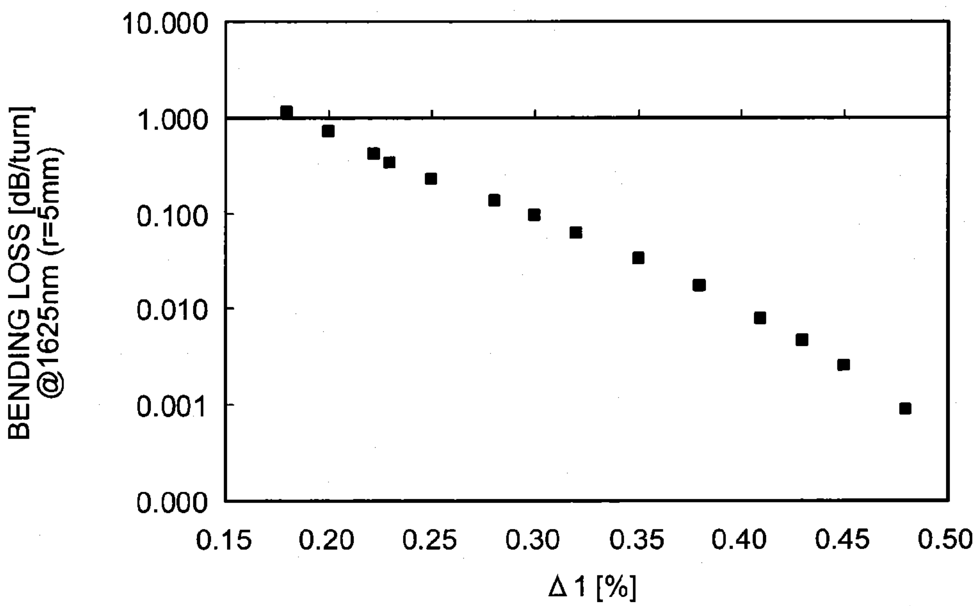
BENDING LOSS [dB/turn] @1625nm (r=5mm)
10.000
1.000
0.100
0.010
0.001
0.000
0.15
0.20
0.25
0.30
0.35
0.40
0.45
0.50
Δ1 [%]

FIG.19

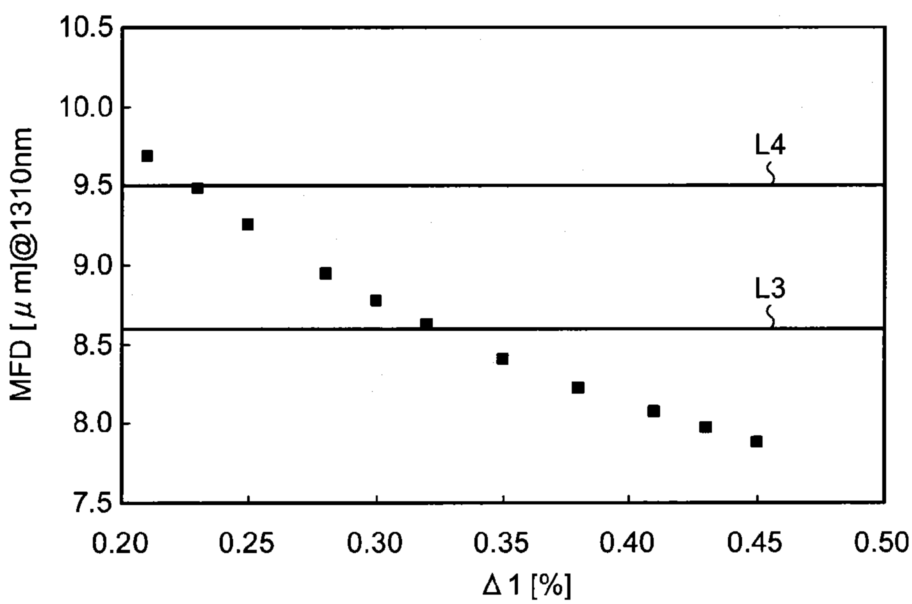
MFD [μm]@1310nm
10.5
10.0
9.5
9.0
8.5
8.0
7.5
0.20
0.25
0.30
0.35
0.40
0.45
0.50
Δ1 [%]
L4
L3

FIG.20

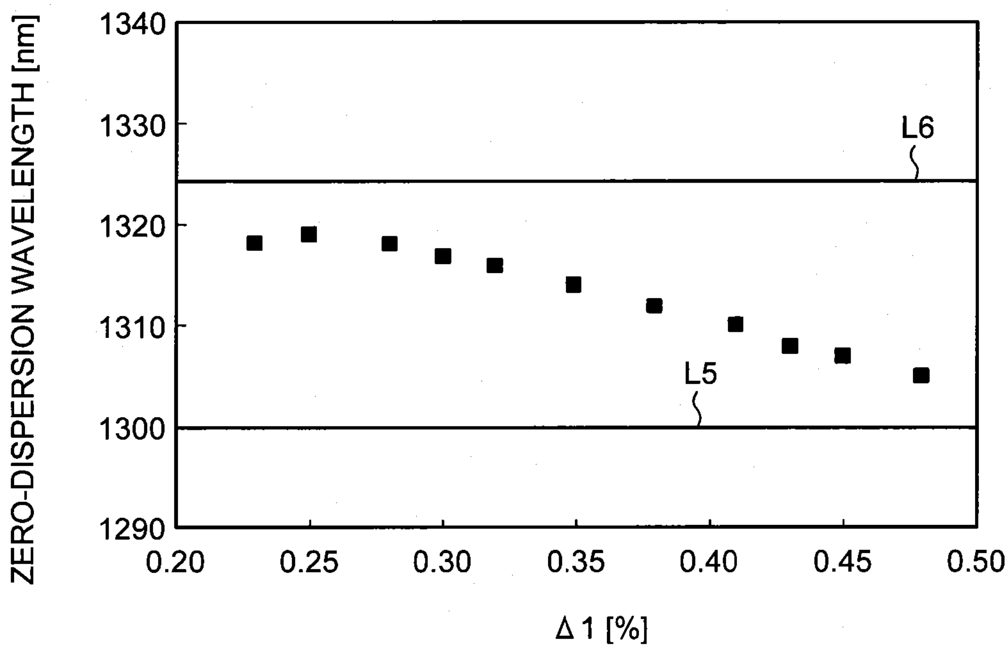
1340
1330
1320
1310
1300
1290
0.20
0.25
0.30
0.35
0.40
0.45
0.50
ZERO-DISPERSION WAVELENGTH [nm]
Δ1 [%]
L6
L5

FIG.21

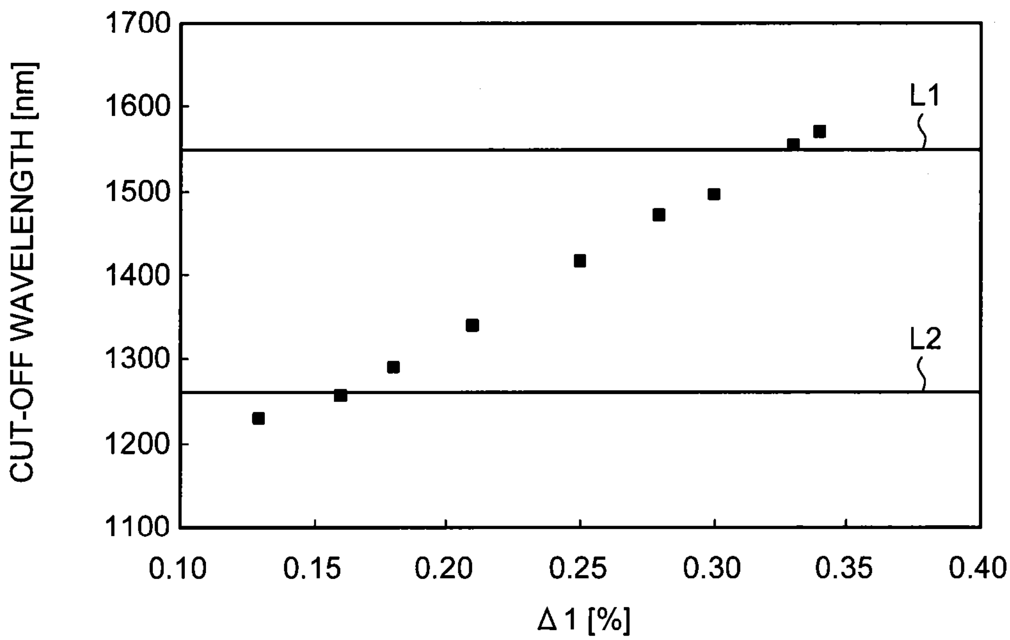
1700
1600
1500
1400
1300
1200
1100
0.10
0.15
0.20
0.25
0.30
0.35
0.40
CUT-OFF WAVELENGTH [nm]
Δ1 [%]
L1
L2

FIG.22

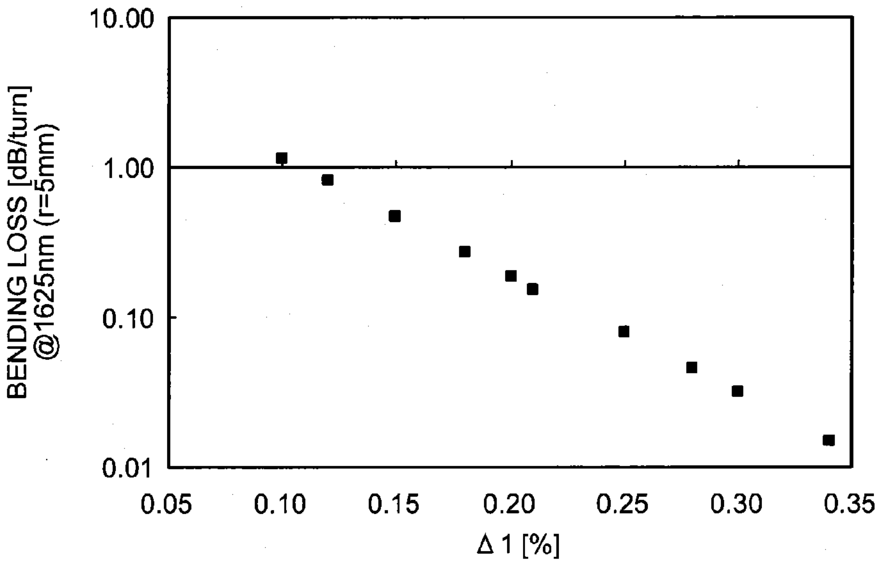

10.00
1.00
0.10
0.01
BENDING LOSS [dB/turn] @1625nm (r=5mm)
0.05
0.10
0.15
0.20
0.25
0.30
0.35
Δ 1 [%]

FIG.23

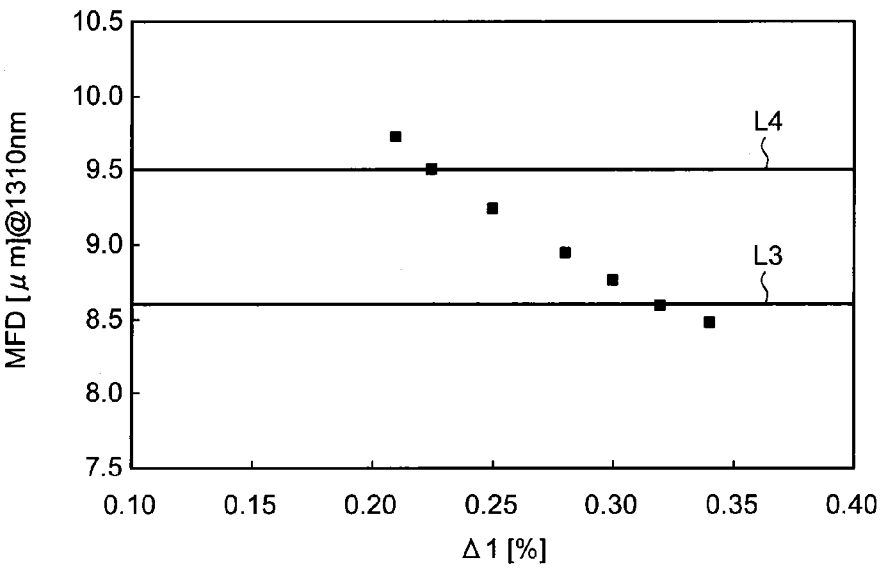

10.5
10.0
9.5
9.0
8.5
8.0
7.5
MFD [μ m]@1310nm
L4
L3
0.10
0.15
0.20
0.25
0.30
0.35
0.40
Δ 1 [%]

FIG.24

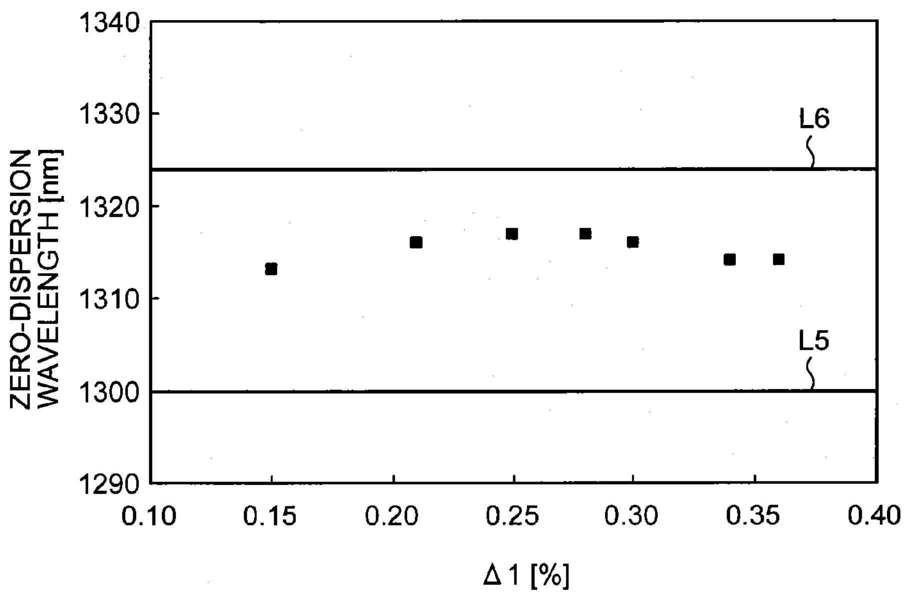
1340
1330
1320
1310
1300
1290
ZERO-DISPERSION WAVELENGTH [nm]
L6
L5
0.10
0.15
0.20
0.25
0.30
0.35
0.40
Δ1 [%]

FIG.25

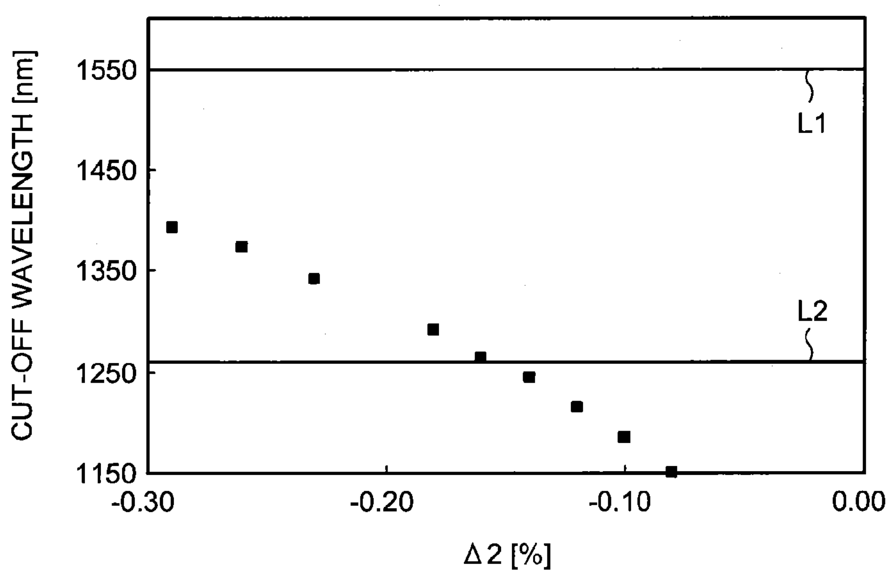
1550
1450
1350
1250
1150
CUT-OFF WAVELENGTH [nm]
L1
L2
-0.30
-0.20
-0.10
0.00
Δ2 [%]

FIG.26

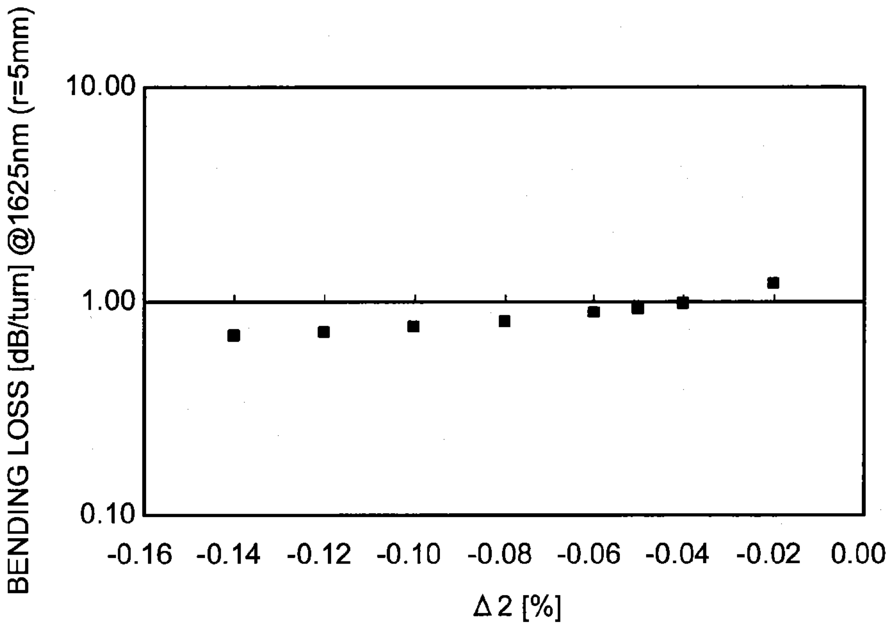
BENDING LOSS [dB/turn] @1625nm (r=5mm)
10.00
1.00
0.10
-0.16
-0.14
-0.12
-0.10
-0.08
-0.06
-0.04
-0.02
0.00
Δ2 [%]

FIG.27

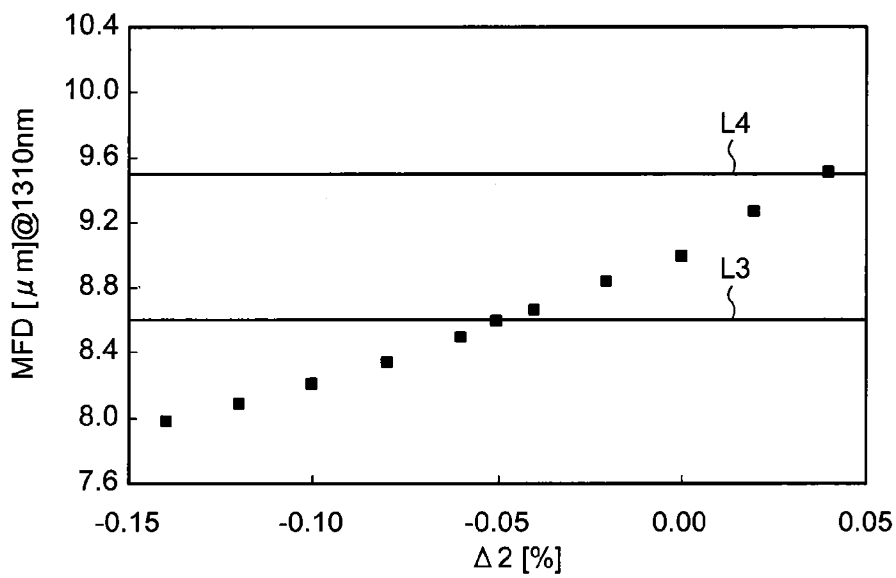
MFD [μm]@1310nm
10.4
10.0
9.6
9.2
8.8
8.4
8.0
7.6
L4
L3
-0.15
-0.10
-0.05
0.00
0.05
Δ2 [%]

FIG.28

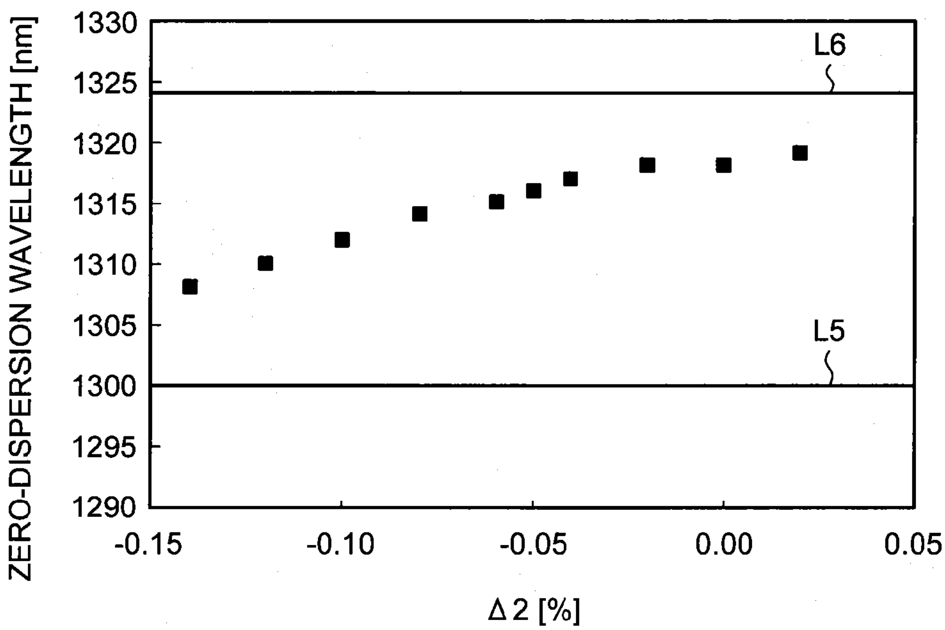
ZERO-DISPERSION WAVELENGTH [nm]
1330
1325
1320
1315
1310
1305
1300
1295
1290
L6
L5
-0.15
-0.10
-0.05
0.00
0.05
Δ2 [%]

FIG.29

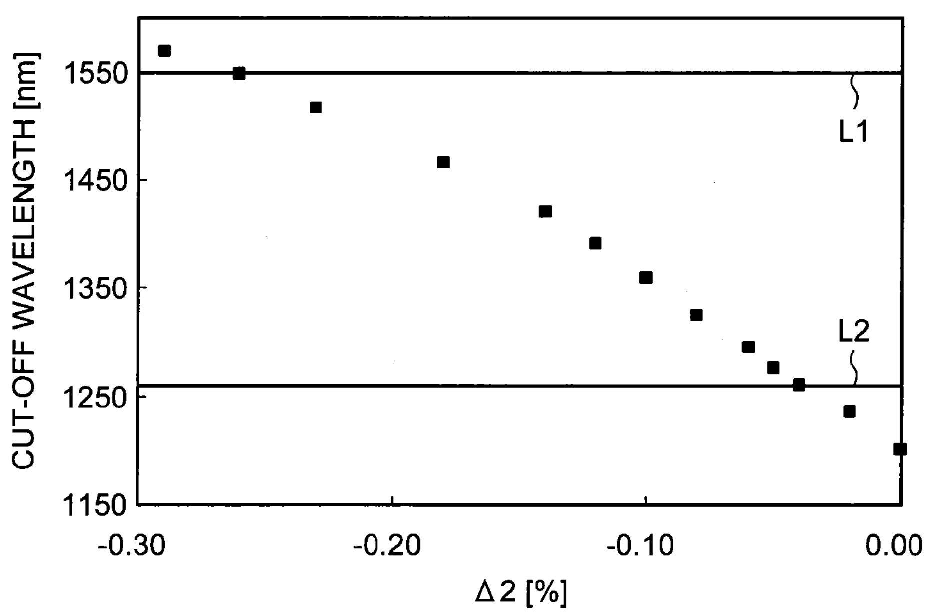
CUT-OFF WAVELENGTH [nm]
1550
1450
1350
1250
1150
L1
L2
-0.30
-0.20
-0.10
0.00
Δ2 [%]

FIG.30

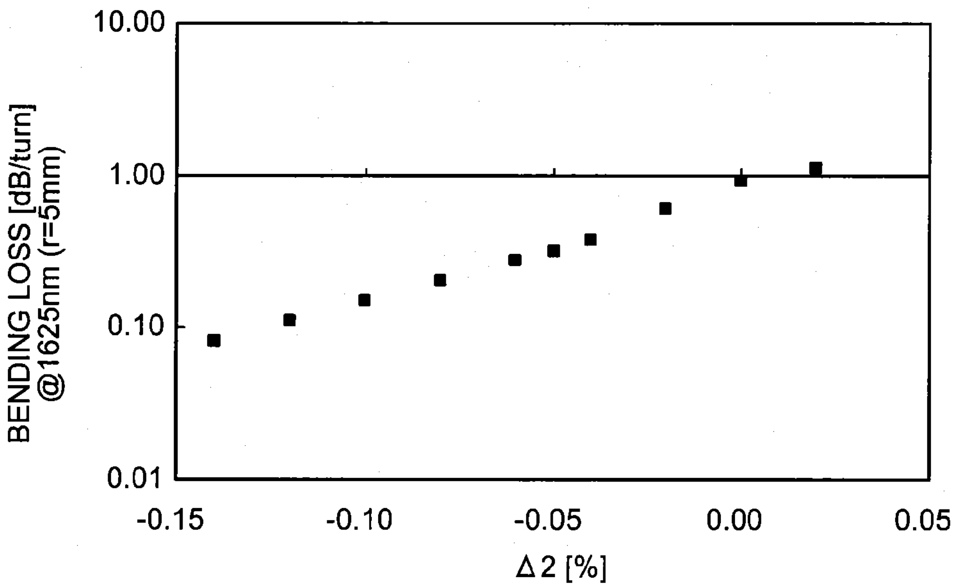
10.00
1.00
0.10
0.01
BENDING LOSS [dB/turn] @1625nm (r=5mm)
-0.15
-0.10
-0.05
0.00
0.05
Δ2 [%]

FIG.31

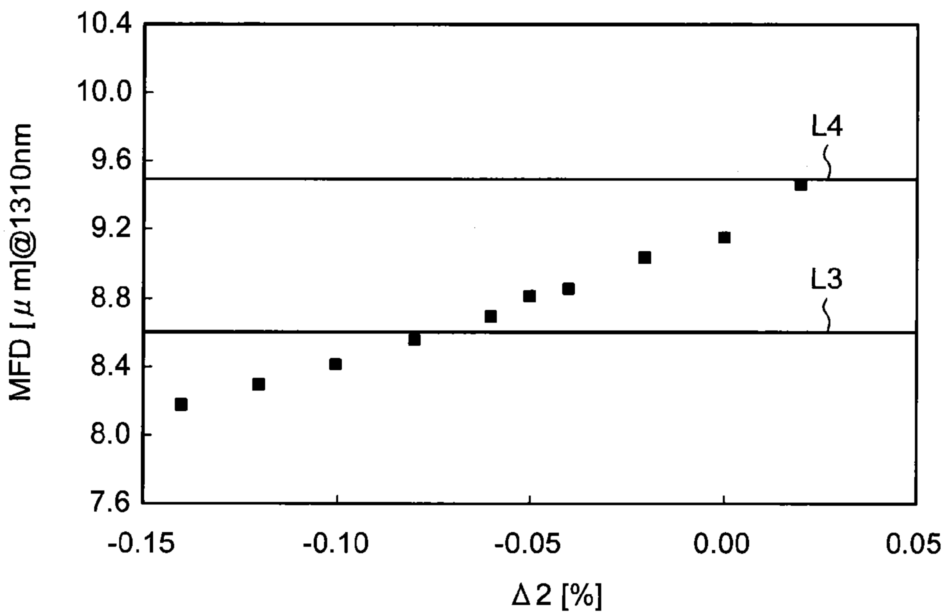
10.4
10.0
9.6
9.2
8.8
8.4
8.0
7.6
MFD [μm]@1310nm
L4
L3
-0.15
-0.10
-0.05
0.00
0.05
Δ2 [%]

FIG.32

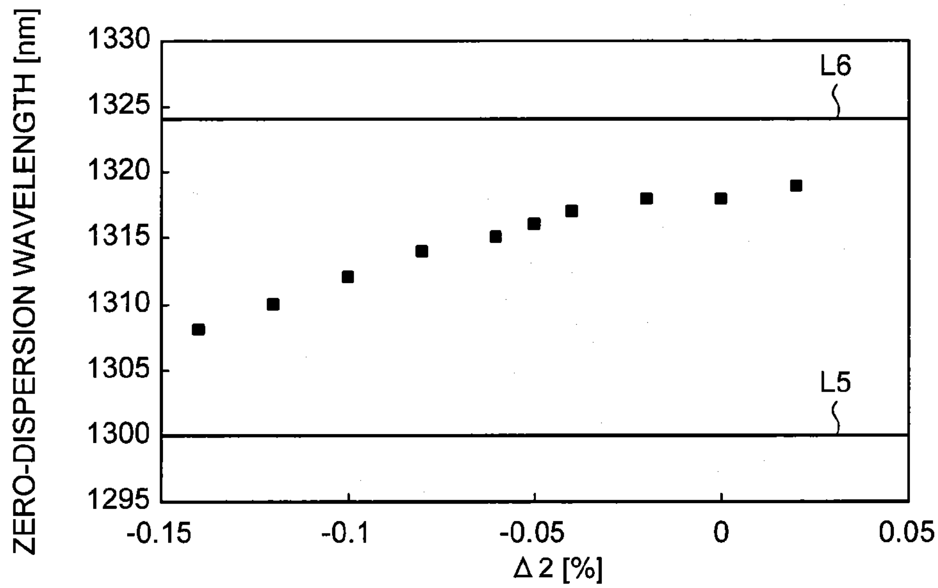

ZERO-DISPERSION WAVELENGTH [nm]
1330
1325
1320
1315
1310
1305
1300
1295
L6
L5
-0.15
-0.1
-0.05
0
0.05
Δ 2 [%]

FIG.33

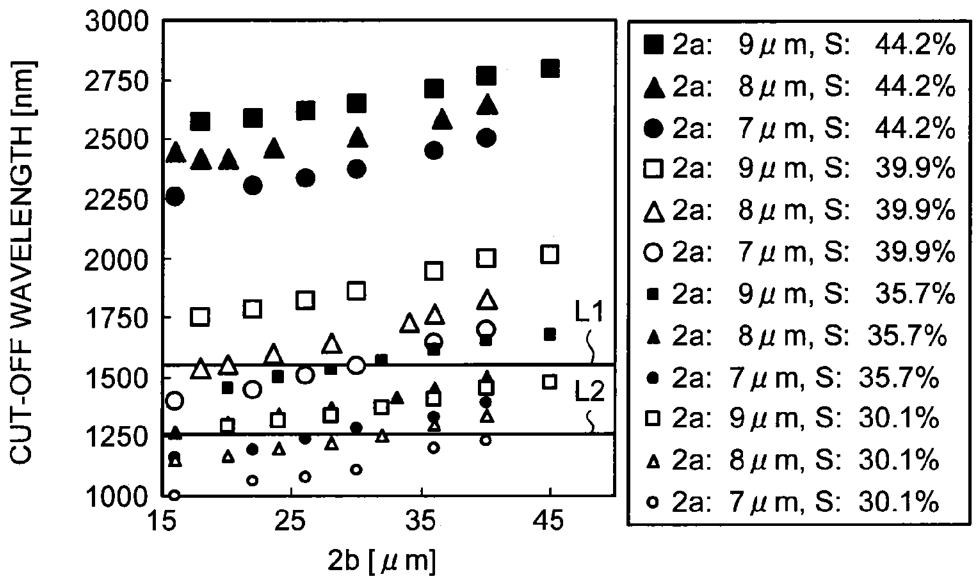

CUT-OFF WAVELENGTH [nm]
3000
2750
2500
2250
2000
1750
1500
1250
1000
15
25
35
45
2b [μm]
L1
L2
2a: 9μm, S: 44.2%
2a: 8μm, S: 44.2%
2a: 7μm, S: 44.2%
2a: 9μm, S: 39.9%
2a: 8μm, S: 39.9%
2a: 7μm, S: 39.9%
2a: 9μm, S: 35.7%
2a: 8μm, S: 35.7%
2a: 7μm, S: 35.7%
2a: 9μm, S: 30.1%
2a: 8μm, S: 30.1%
2a: 7μm, S: 30.1%

FIG.34

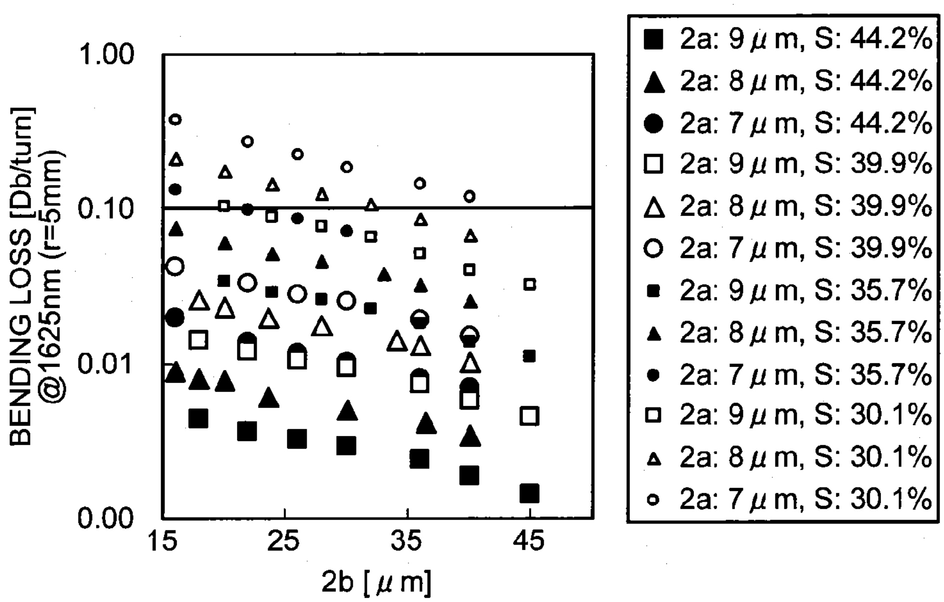

BENDING LOSS [Db/turn] @1625nm (r=5mm)
1.00
0.10
0.01
0.00
15
25
35
45
2b [μm]
2a: 9 μm, S: 44.2%
2a: 8 μm, S: 44.2%
2a: 7 μm, S: 44.2%
2a: 9 μm, S: 39.9%
2a: 8 μm, S: 39.9%
2a: 7 μm, S: 39.9%
2a: 9 μm, S: 35.7%
2a: 8 μm, S: 35.7%
2a: 7 μm, S: 35.7%
2a: 9 μm, S: 30.1%
2a: 8 μm, S: 30.1%
2a: 7 μm, S: 30.1%

FIG.35

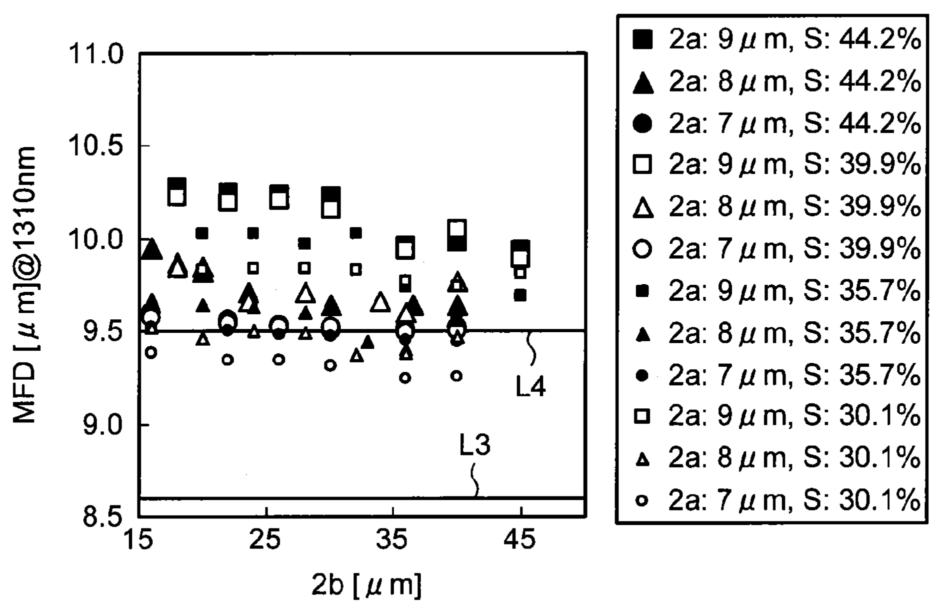

MFD [μm]@1310nm
11.0
10.5
10.0
9.5
9.0
8.5
15
25
35
45
2b [μm]
L4
L3
2a: 9 μm, S: 44.2%
2a: 8 μm, S: 44.2%
2a: 7 μm, S: 44.2%
2a: 9 μm, S: 39.9%
2a: 8 μm, S: 39.9%
2a: 7 μm, S: 39.9%
2a: 9 μm, S: 35.7%
2a: 8 μm, S: 35.7%
2a: 7 μm, S: 35.7%
2a: 9 μm, S: 30.1%
2a: 8 μm, S: 30.1%
2a: 7 μm, S: 30.1%

FIG.36

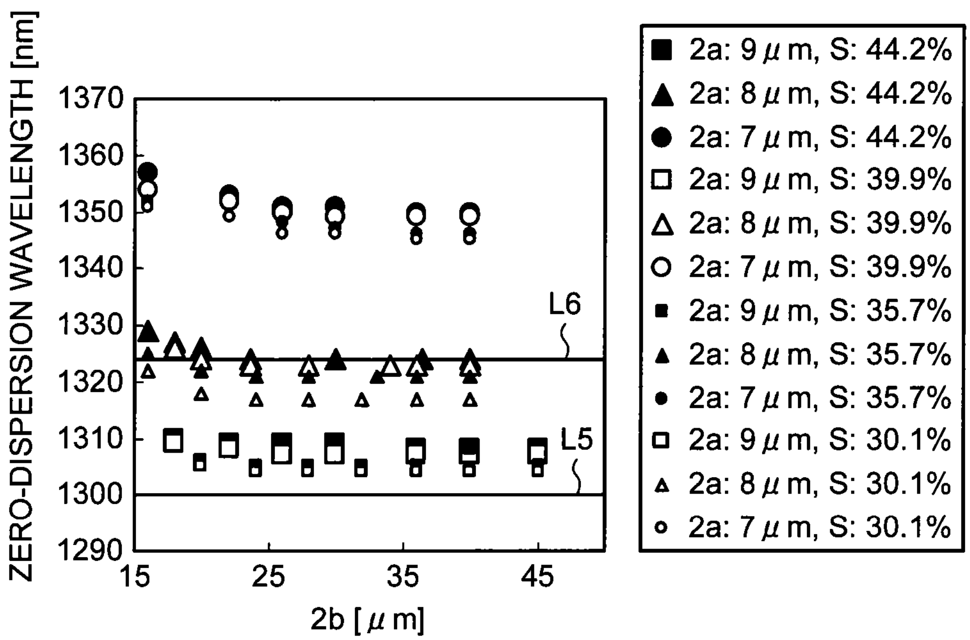
ZERO-DISPERSION WAVELENGTH [nm]
1370
1360
1350
1340
1330
1320
1310
1300
1290
15
25
35
45
2b [μm]
L6
L5
2a: 9 μm, S: 44.2%
2a: 8 μm, S: 44.2%
2a: 7 μm, S: 44.2%
2a: 9 μm, S: 39.9%
2a: 8 μm, S: 39.9%
2a: 7 μm, S: 39.9%
2a: 9 μm, S: 35.7%
2a: 8 μm, S: 35.7%
2a: 7 μm, S: 35.7%
2a: 9 μm, S: 30.1%
2a: 8 μm, S: 30.1%
2a: 7 μm, S: 30.1%

FIG.37A

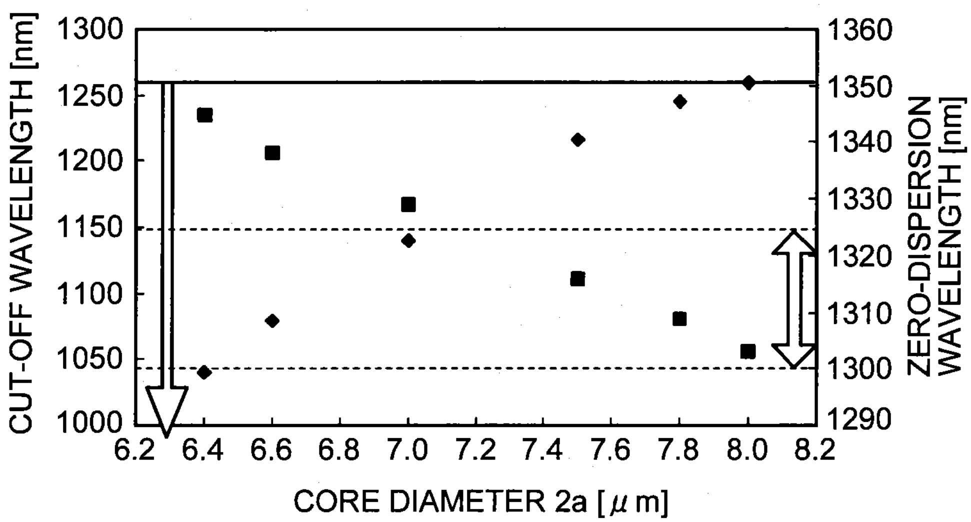

FIG.37B

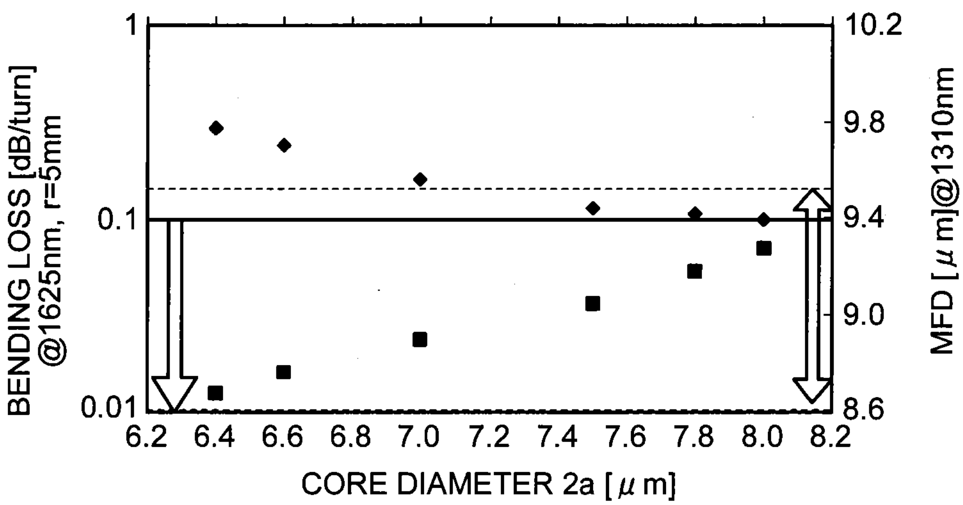

FIG.38A

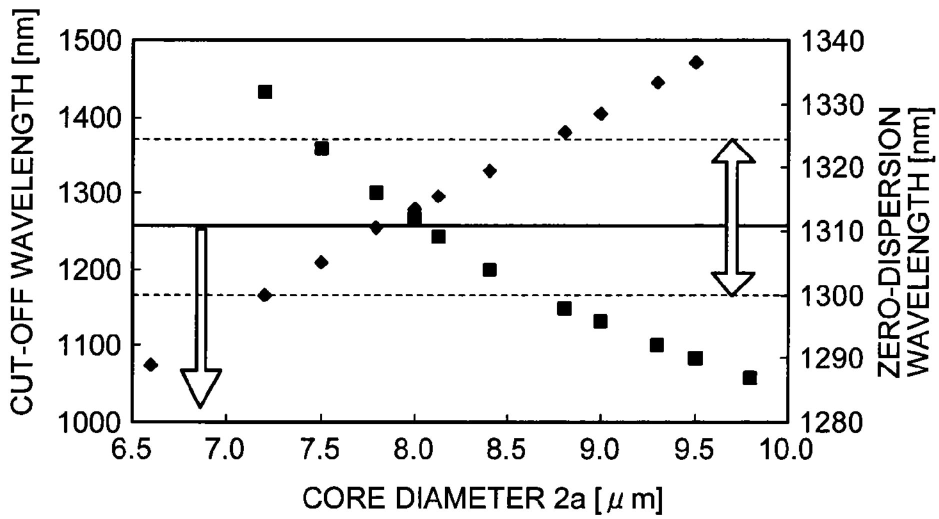

FIG.38B

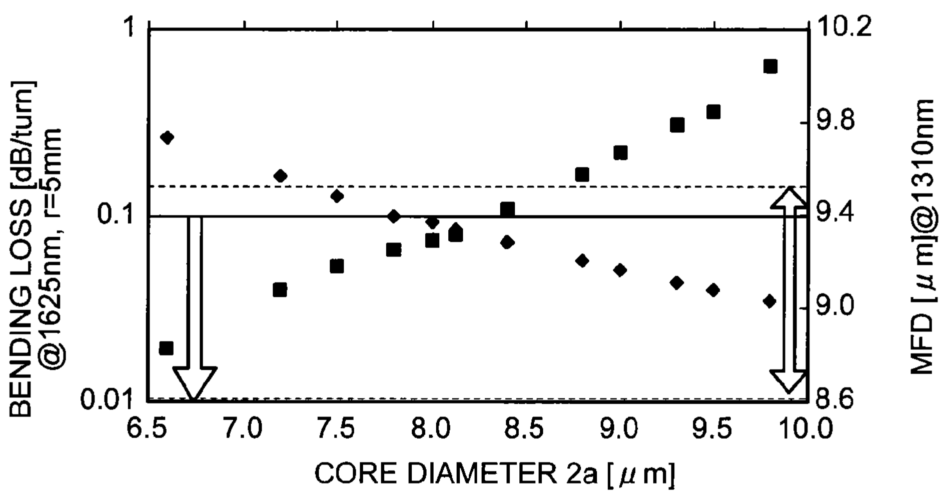

FIG.39A

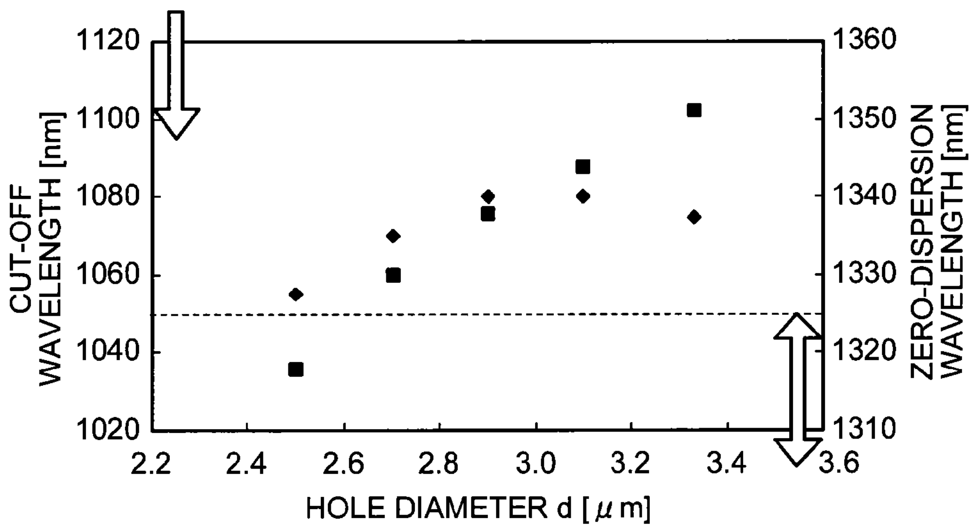

FIG.39B

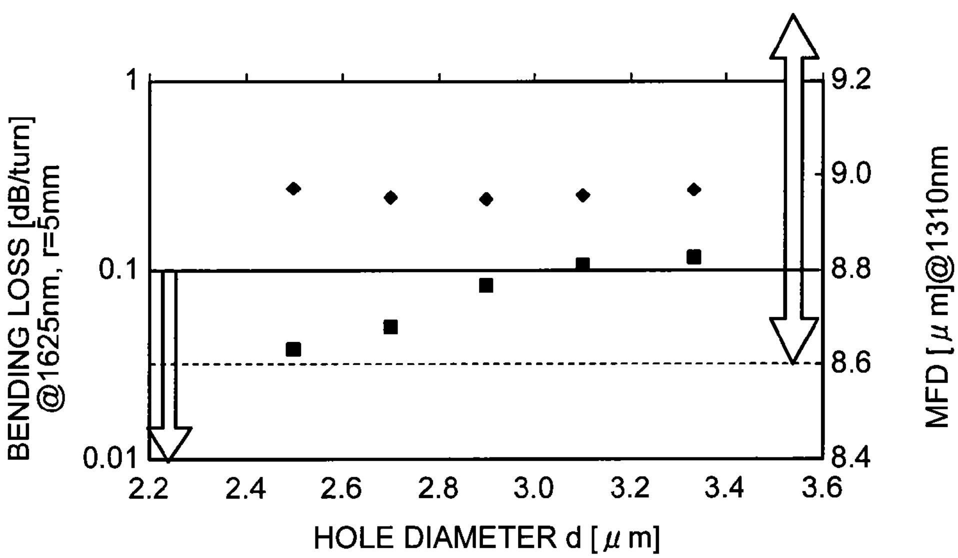

FIG.40A

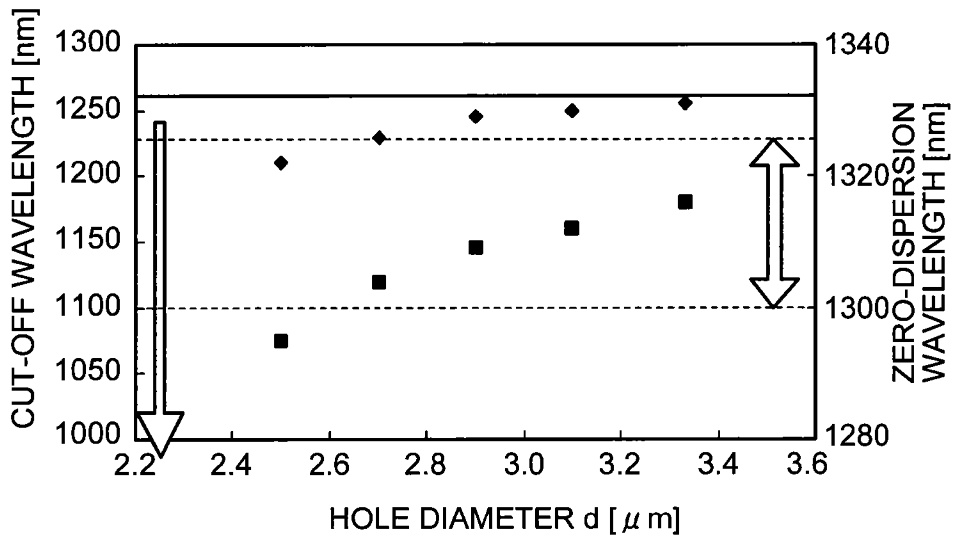

FIG.40B

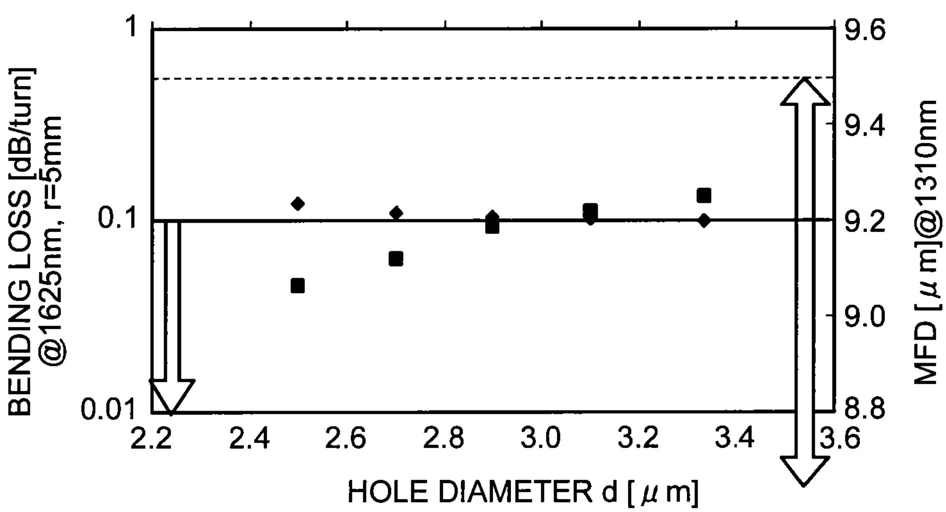

FIG.41A

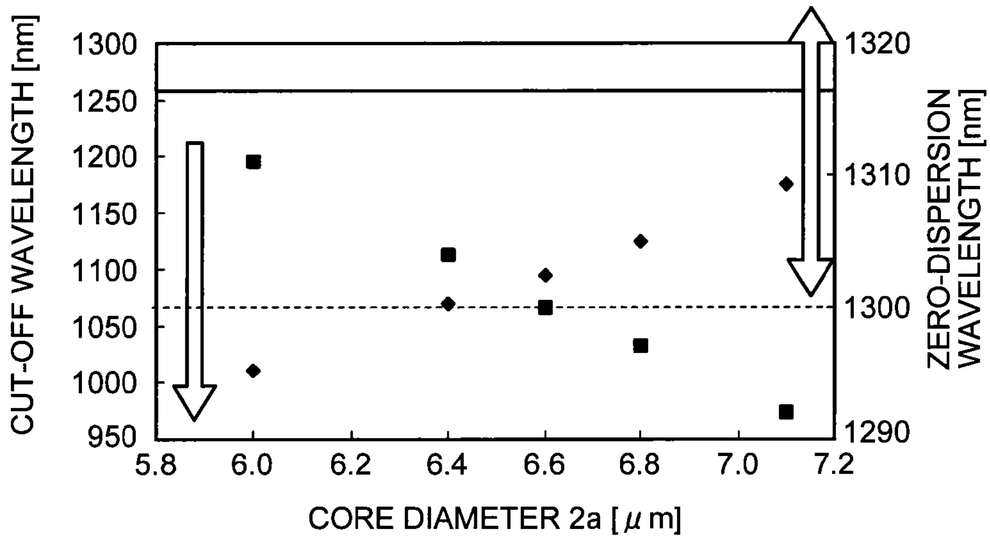

FIG.41B

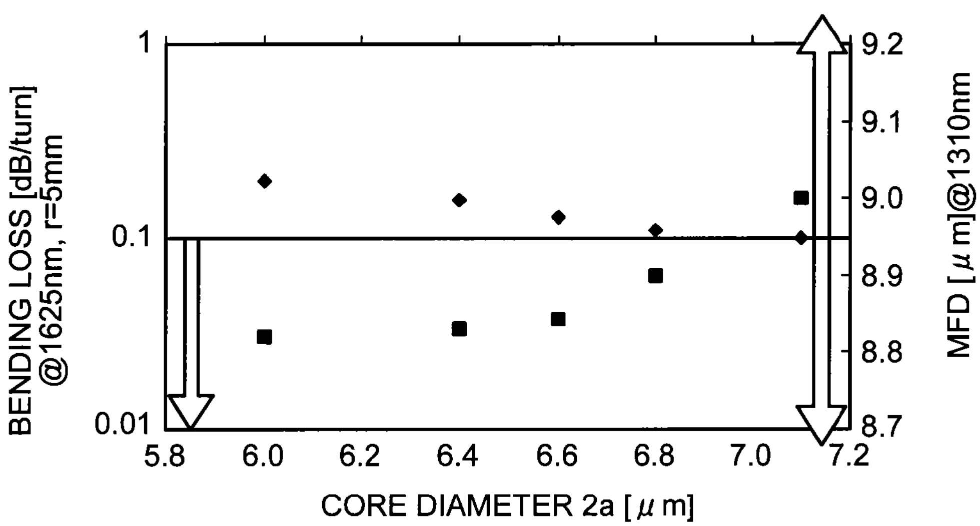

FIG.42A

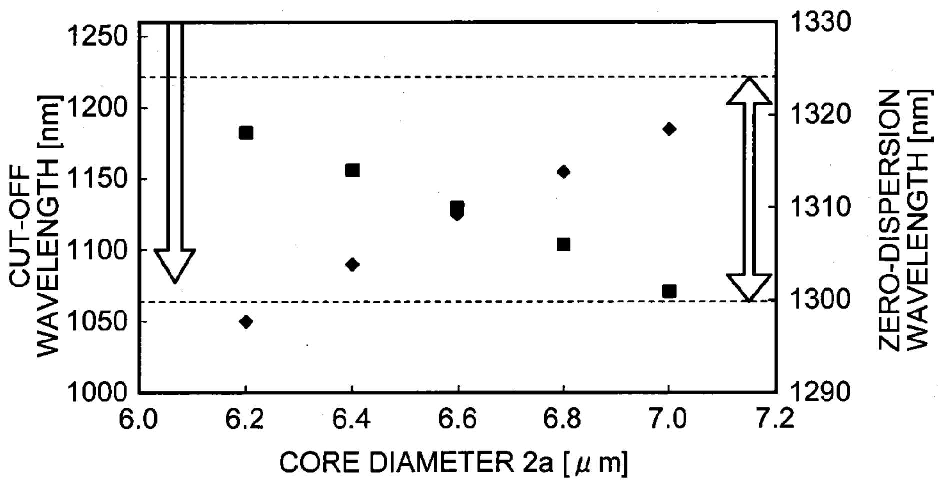

FIG.42B

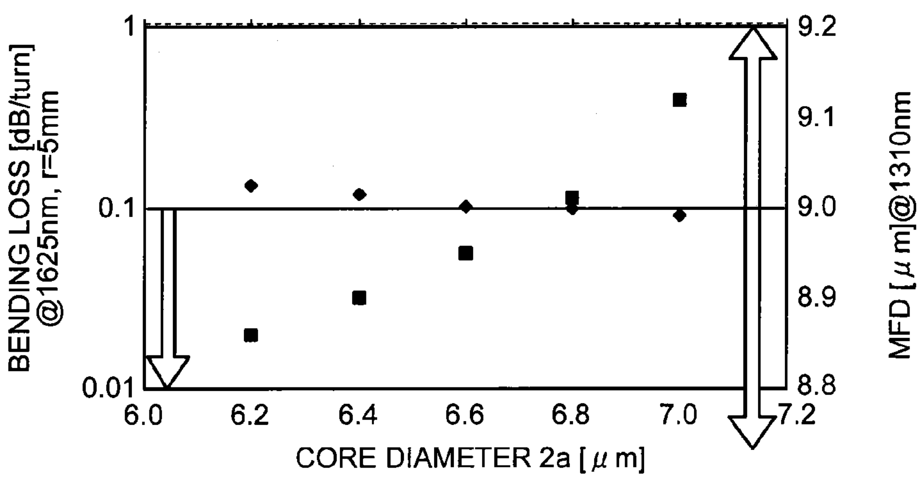

FIG.43A

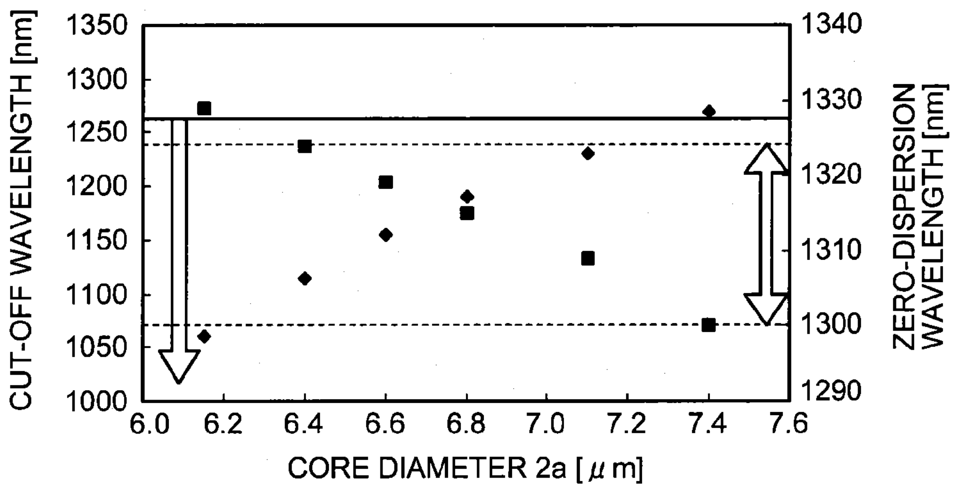

FIG.43B

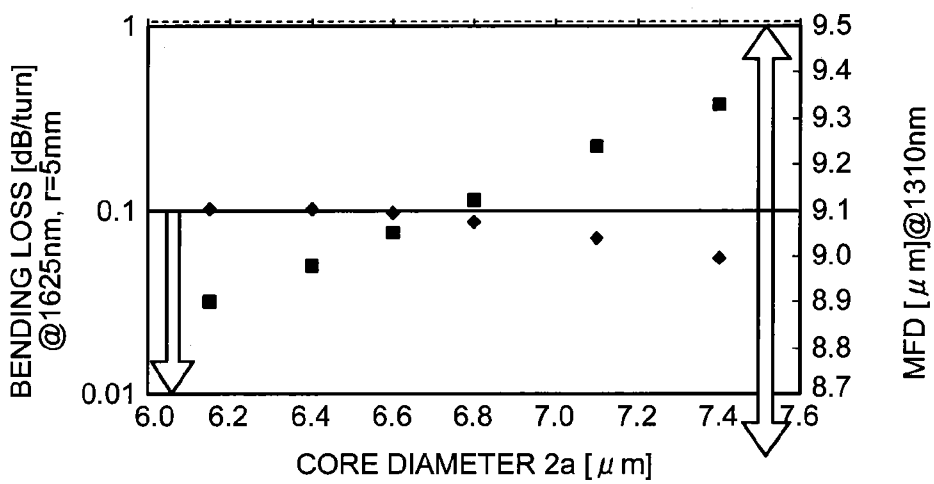

FIG.44A

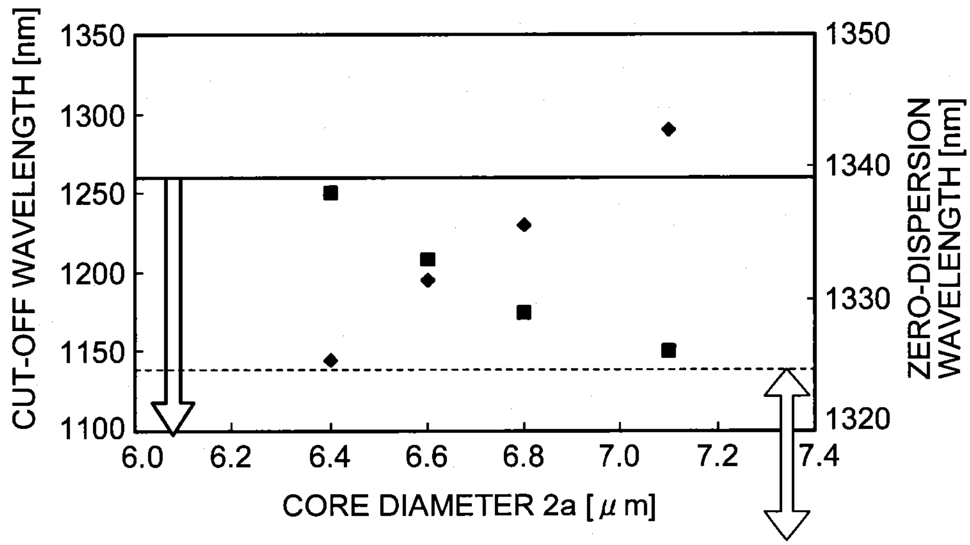

FIG.44B

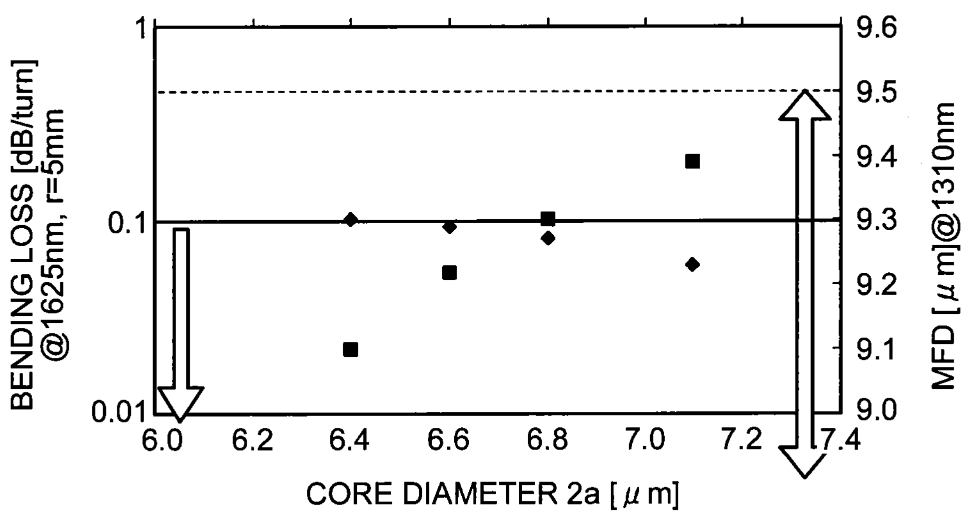

FIG.45A

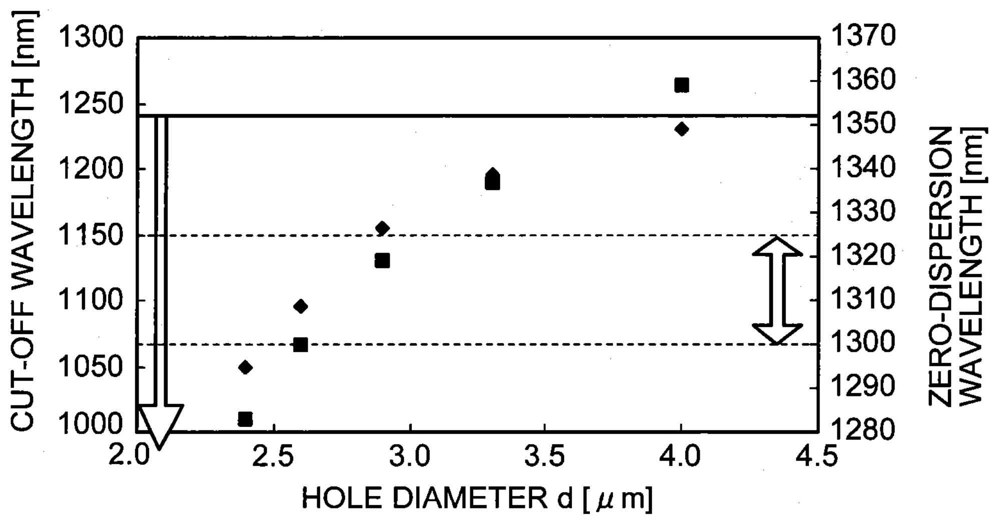

FIG.45B

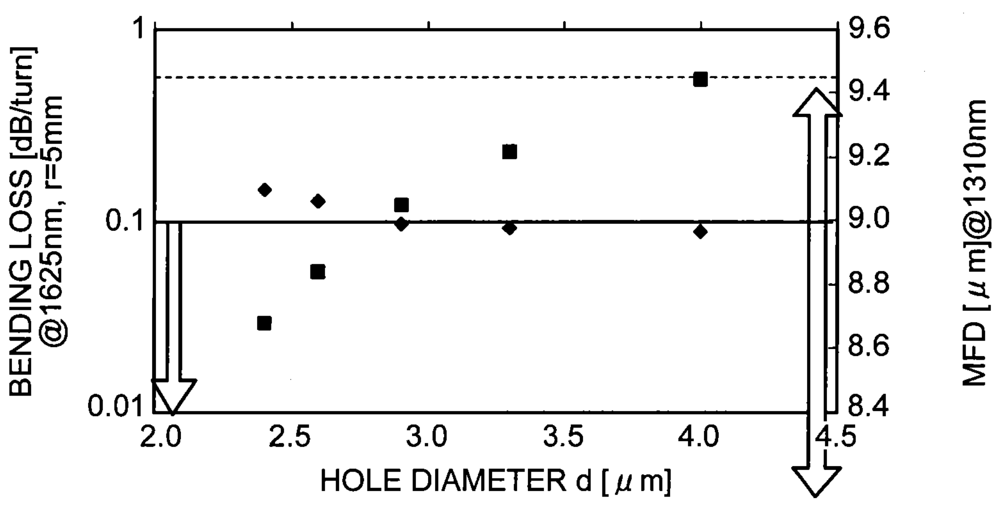

FIG.46A

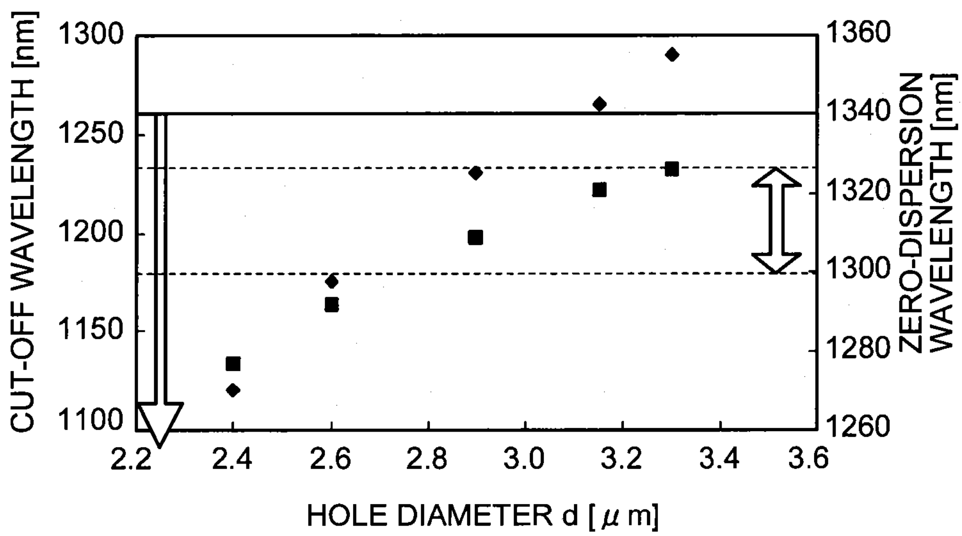

FIG.46B

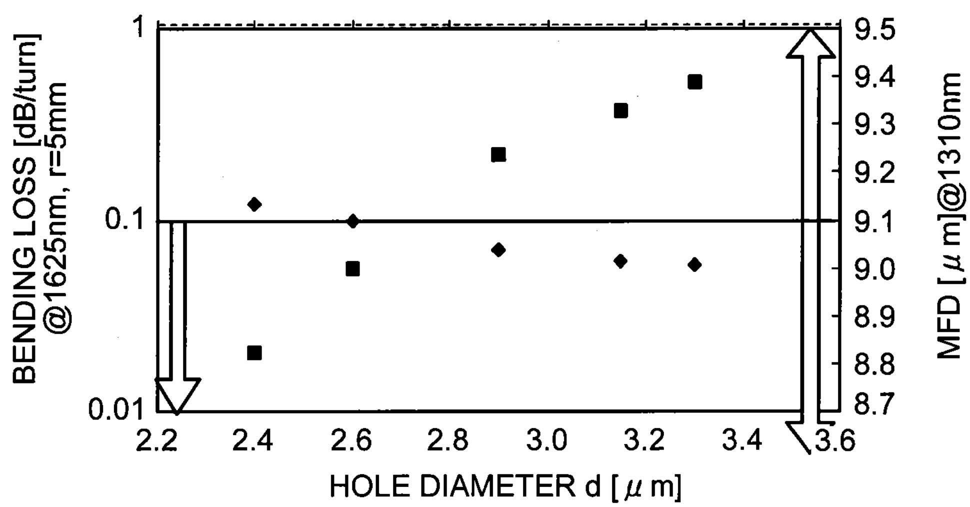

FIG.47A

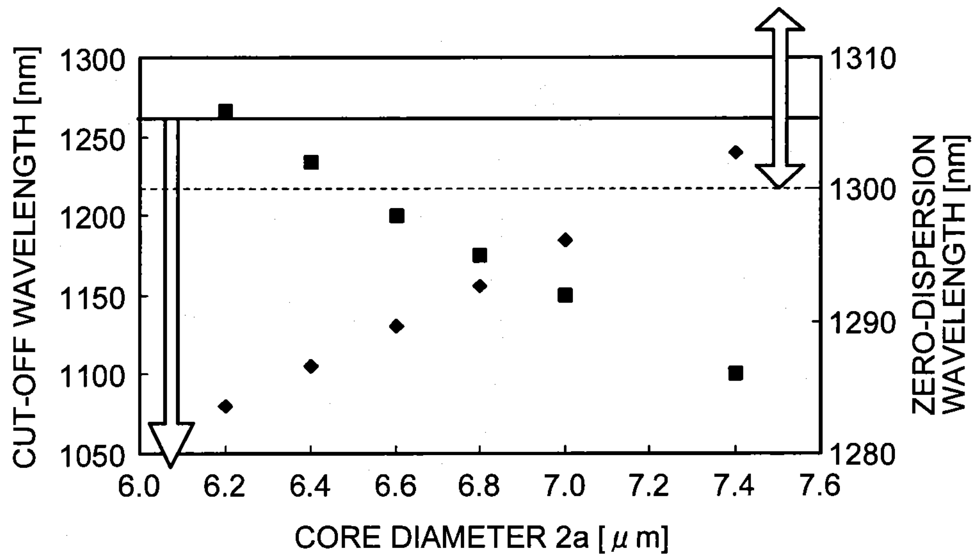

FIG.47B

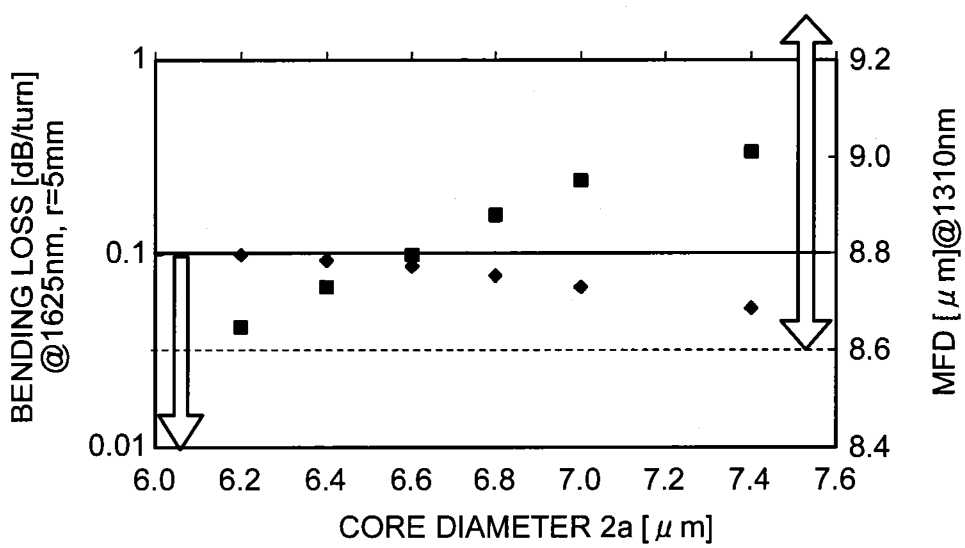

FIG.48A

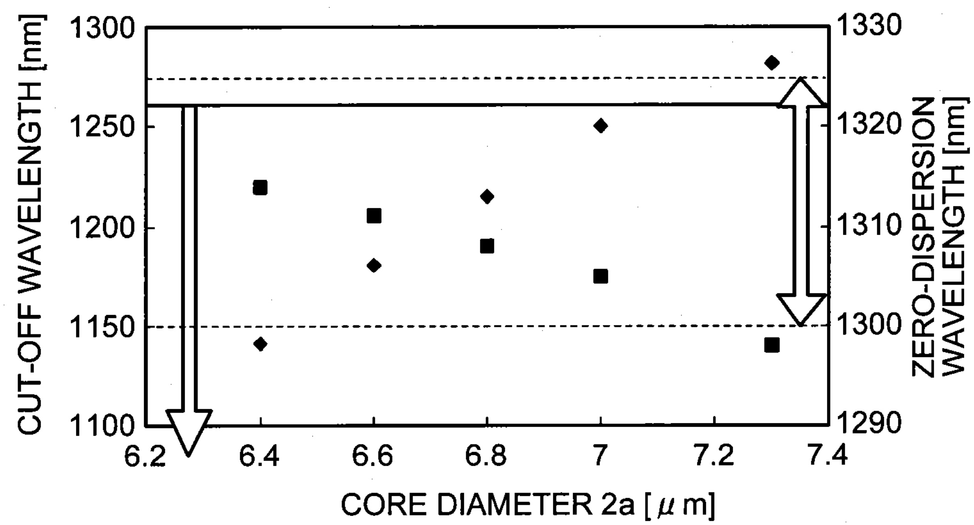

FIG.48B

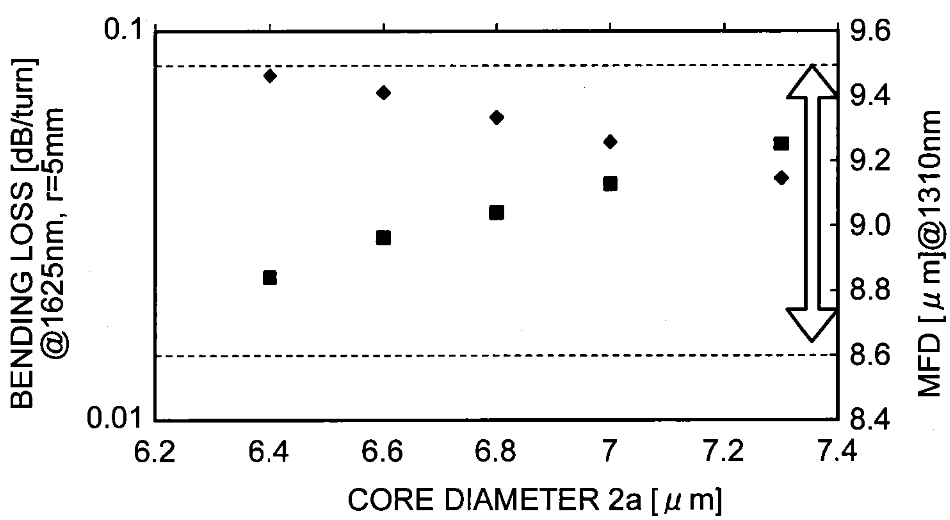

FIG.49A

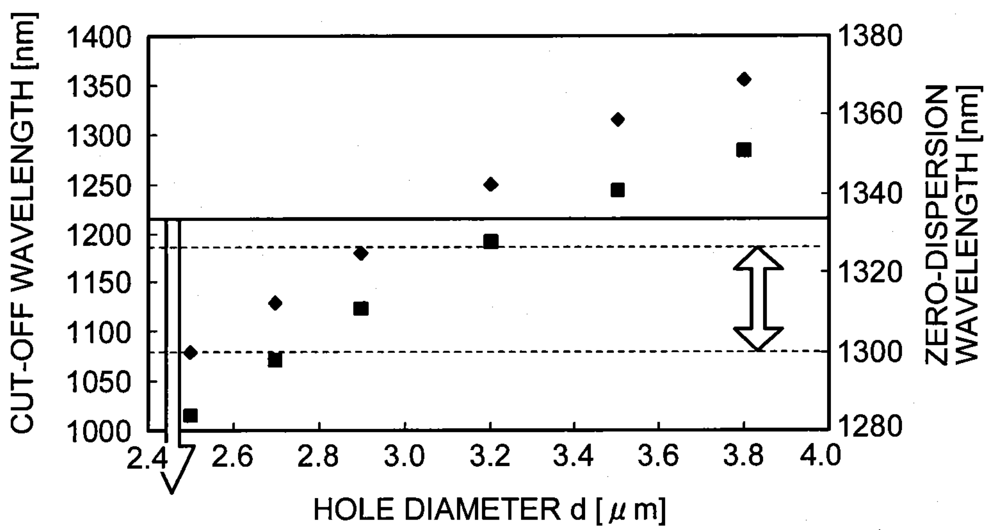

FIG.49B

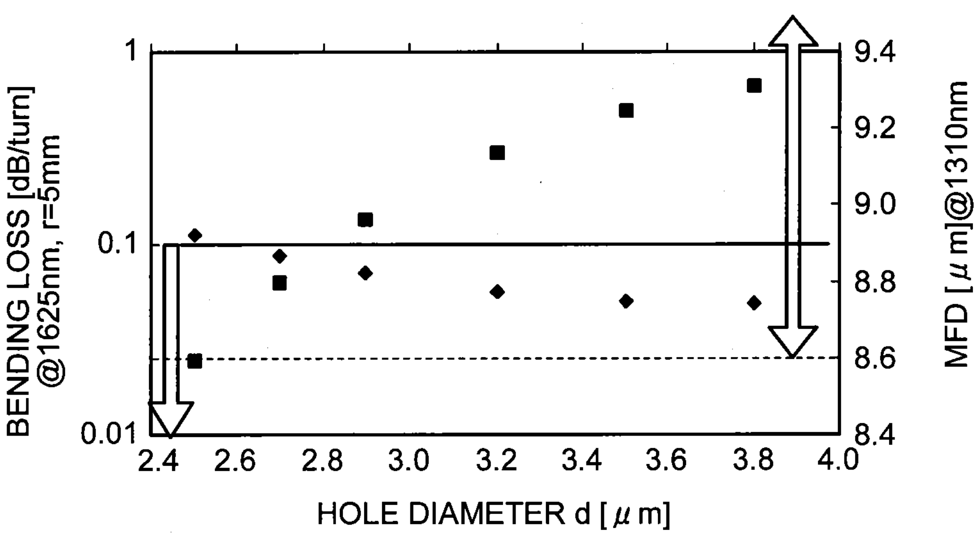

FIG.50A

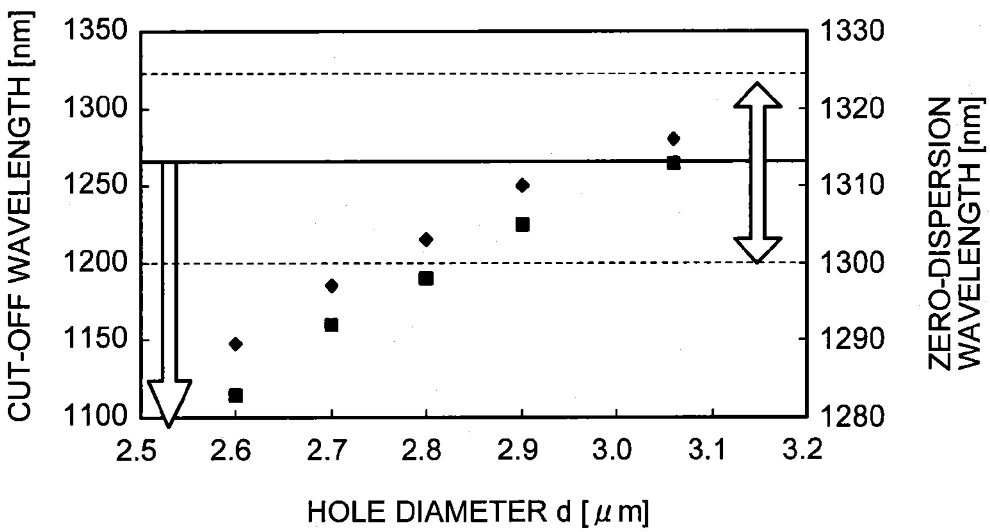

FIG.50B

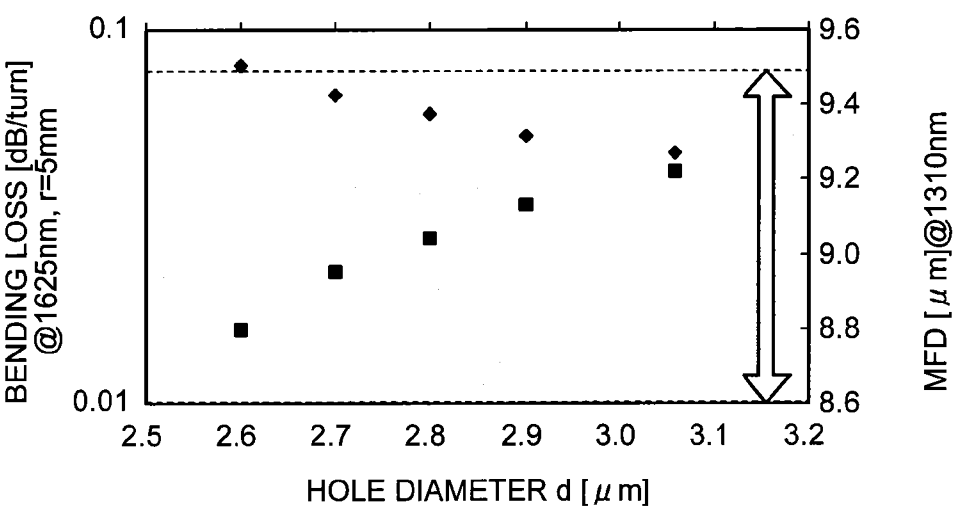

FIG.51A

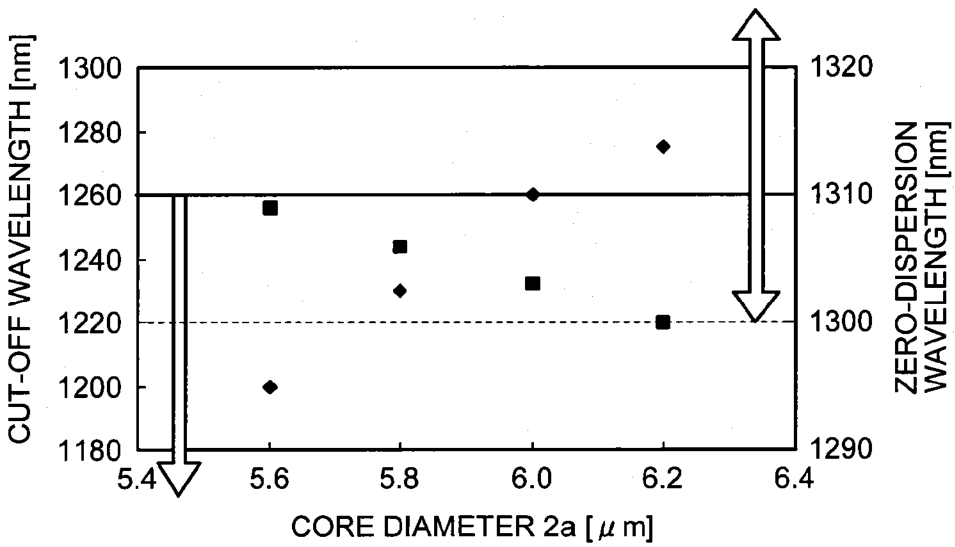

FIG.51B

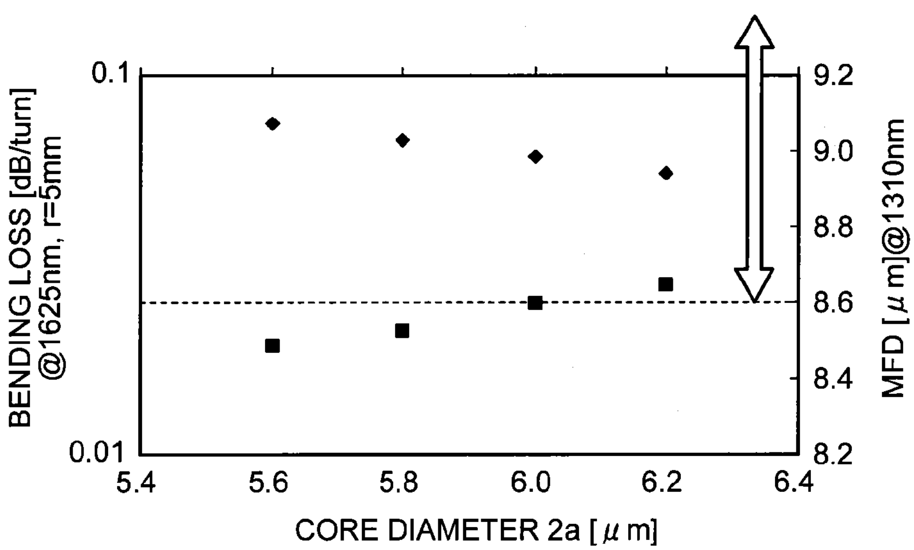

FIG.52A

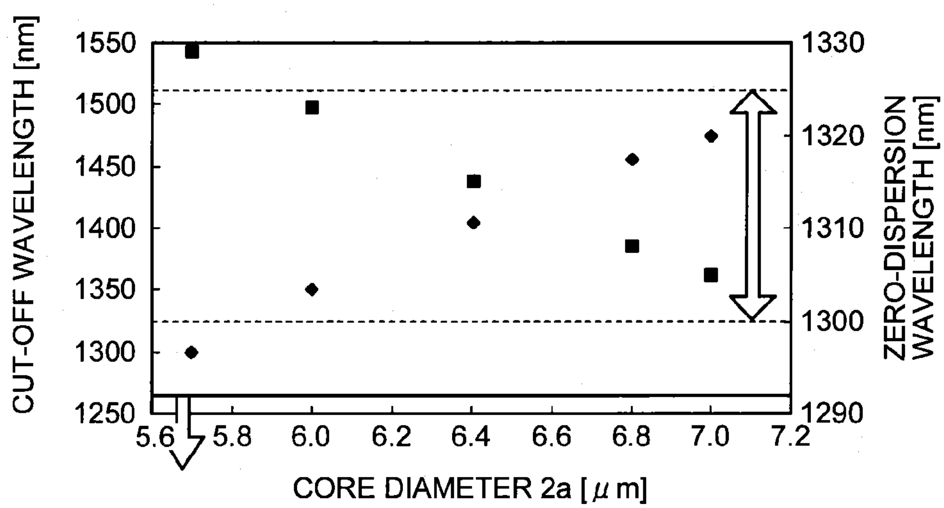

FIG.52B

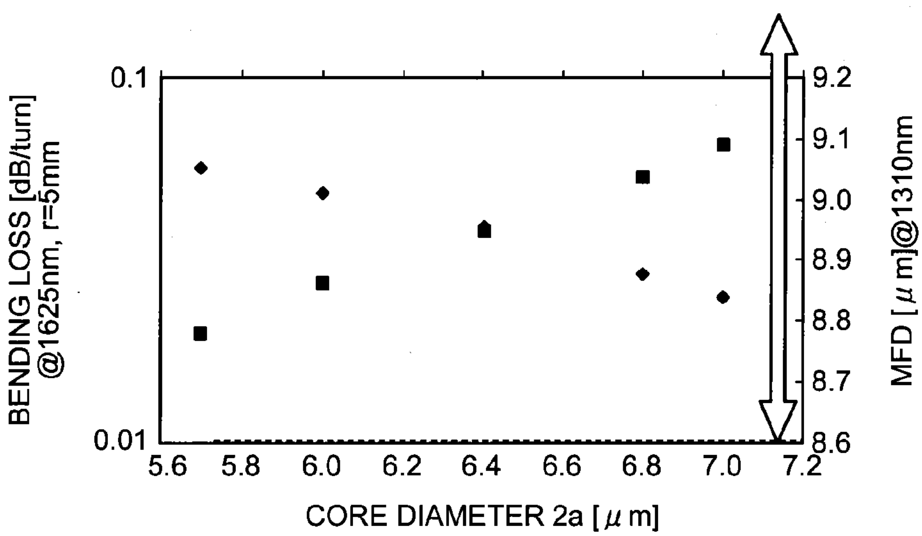

FIG.53A

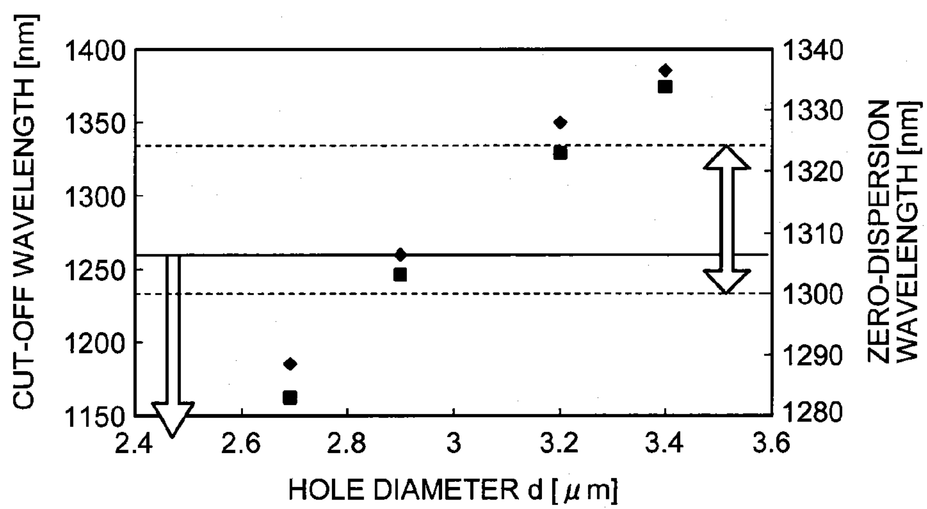

FIG.53B

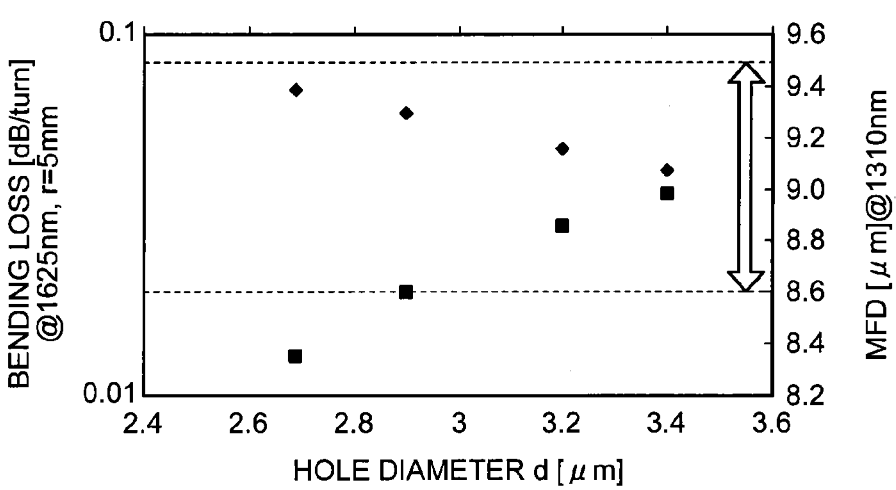

FIG.54A

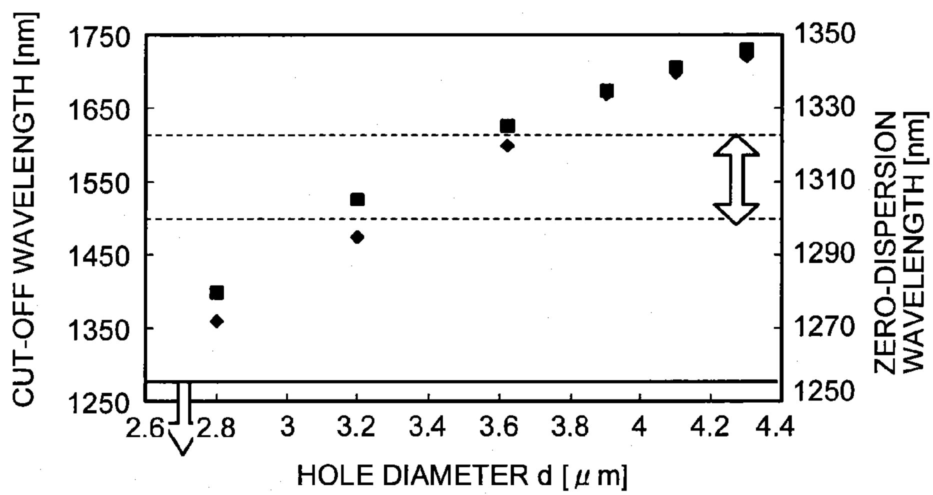

FIG.54B

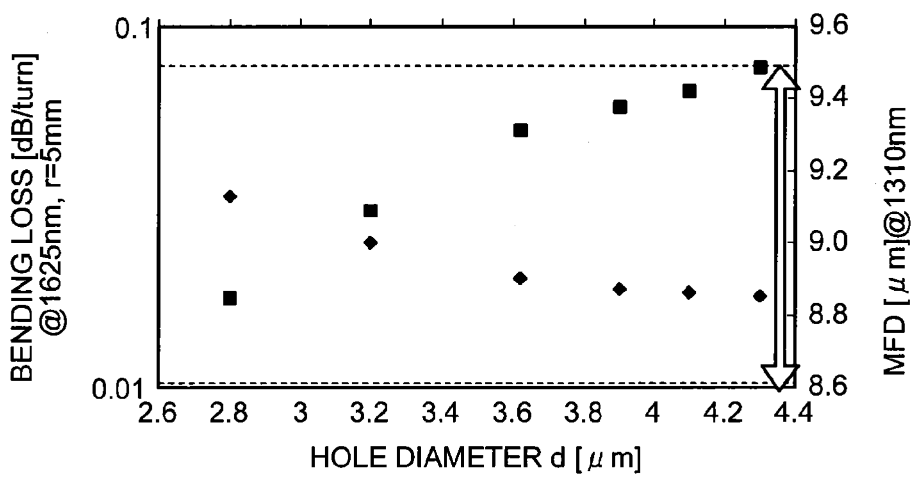

FIG.55A

Hole occupancy rate	S	%	30.1	30.1	30.1	30.1	30.1	30.0	30.1	30.1	30.1
Distance	L1	μm	10.40	11.23	12.06	12.89	13.86	10.40	11.23	12.06	12.9
Hole diameter	d	μm	2.50	2.70	2.90	3.10	3.33	2.50	2.70	2.90	3.10
Core diameter	2a	μm	6.6	6.6	6.6	6.6	6.6	7.8	7.8	7.8	7.8
Relative refractive index difference	Δ1	%	0.30	0.30	0.30	0.30	0.30	0.30	0.30	0.30	0.30
Inner cladding layer diameter	2b	μm	36	36	36	36	36	36	36	36	36
Relative refractive index difference	Δ2	%	-0.05	-0.05	-0.05	-0.05	-0.05	-0.05	-0.05	-0.05	-0.05
Chromatic dispersion	ps/nm/km	1310nm	-1.30	-2.14	-2.96	-3.41	-3.90	0.98	-0.18	-0.33	-0.65
		1550nm	18.69	17.51	16.32	15.44	14.56	20.26	19.24	18.20	17.55
Zero-dispersion wavelength	nm		1318	1330	1338	1344	1351	1295	1304	1309	1312
Zero-dispersion slope	ps/nm²/km		0.0952	0.0918	0.0883	0.0864	0.0829	0.0968	0.0939	0.0907	0.0887
MFD	μm	1310nm	8.63	8.68	8.77	8.81	8.83	9.07	9.12	9.19	9.22
		1550nm	9.05	9.27	9.42	9.76	10.14	9.37	9.46	9.69	9.79
Cut-off wavelength	nm		1055	1070	1080	1080	1075	1210	1230	1245	1250
Bending loss	dB/turn	1625nm r=5mm	0.3	0.2	0.2	0.3	0.3	0.1	0.1	0.1	0.1

Hole occupancy rate	S	%	30.1	30.1	30.1	30.1	30.1	30.1	30.1	30.1	30.1
Distance	L1	μm	13.9	12.06	12.06	12.06	12.06	12.06	12.06	13.86	13.9
Hole diameter	d	μm	3.33	2.90	2.90	2.90	2.90	2.90	2.90	3.33	3.33
Core diameter	2a	μm	7.8	6.4	6.6	7	7.5	7.8	8	6.6	7.2
Relative refractive index difference	Δ1	%	0.30	0.30	0.30	0.30	0.30	0.30	0.30	0.30	0.30
Inner cladding layer diameter	2b	μm	36	36	36	36	36	36	36	36	36
Relative refractive index difference	Δ2	%	-0.05	-0.05	-0.05	-0.05	-0.05	-0.05	-0.05	-0.05	-0.05
Chromatic dispersion	ps/nm/km	1310nm	-0.98		-2.96	-2.14	-1.32	-0.33		-3.90	-2.28
		1550nm	16.83	16.02	16.32	16.79	17.98	18.20	18.52	14.56	15.71
Zero-dispersion wavelength	nm		1316	1345	1338	1329	1316	1309	1303	1351	1332
Zero-dispersion slope	ps/nm²/km		0.0866	0.0880	0.0883	0.0889	0.0905	0.0907	0.0909	0.0829	0.0842
MFD	μm	1310nm	9.25	8.68	8.77	8.90	9.05	9.19	9.28	8.83	9.08
		1550nm	9.88	9.31	9.42	9.48	9.57	9.69	9.80	10.14	9.82
Cut-off wavelength	nm		1255	1040	1080	1140	1216	1245	1260	1075	1165
Bending loss	dB/turn	1625nm r=5mm	0.1	0.3	0.2	0.2	0.1	0.1	0.1	0.3	0.2

FIG.55B

Hole occupancy rate	S	%	30.1	30.1	30.1	30.1	30.1	30.0	30.1	30.1	30.1
Distance	L1	μm	13.9	13.9	13.9	13.9	13.9	13.9	13.9	13.9	13.9
Hole diameter	d	μm	3.33	3.33	3.33	3.33	3.33	3.33	3.33	3.33	3.33
Core diameter	2a	μm	7.5	7.8	8	8.13	8.4	8.8	9.0	9.3	9.5
Relative refractive index difference	Δ1	%	0.30	0.30	0.30	0.30	0.30	0.30	0.30	0.30	0.30
Inner cladding layer diameter	2b	μm	36	36	36	36	36	36	36	36	36
Relative refractive index difference	Δ2	%	-0.05	-0.05	-0.05	-0.05	-0.05	-0.05	-0.05	-0.05	-0.05
Chromatic dispersion	ps/nm/km	1310nm	-1.59	-0.98	-0.61	-0.38	0.05	0.60	0.84	1.17	1.36
		1550nm	16.28	16.83	17.17	17.39	17.81	18.39	18.65	19.02	19.25
Zero-dispersion wavelength	nm		1323	1316	1312	1309	1304	1298	1296	1292	1290
Zero-dispersion slope	ps/nm²/km		0.0854	0.0866	0.0874	0.0880	0.0892	0.0907	0.0913	0.0924	0.0931
MFD	μm	1310nm	9.18	9.25	9.29	9.32	9.43	9.58	9.67	9.79	9.85
		1550nm	9.62	9.88	9.86	9.84	9.97	10.07	10.13	10.22	10.25
Cut-off wavelength	nm		1210	1255	1280	1296	1330	1380	1403	1445	1470
Bending loss	dB/turn	1625nm r=5mm	0.1	0.1	0.1	0.1	0.1	0.1	0.1	0.0	0.0

Hole occupancy rate	S	%	30.1	30.1	30.1	30.1	30.1	30.1	30.1	30.1	30.1
Distance	L1	μm	13.9	13.9	13.9	13.9	13.9	13.9	13.9	13.9	13.9
Hole diameter	d	μm	3.33	3.3	3.3	3.3	3.3	3.3	3.3	3.3	3.3
Core diameter	2a	μm	9.8	9.0	8.0	8.0	8.0	8.0	9.0	8.0	9.8
Relative refractive index difference	Δ1	%	0.30	0.30	0.35	0.38	0.41	0.43	0.30	0.45	0.30
Inner cladding layer diameter	2b	μm	36	20	36	36	36	36	45	36	36
Relative refractive index difference	Δ2	%	-0.05	-0.05	-0.05	-0.05	-0.05	-0.05	-0.05	-0.05	-0.05
Chromatic dispersion	ps/nm/km	1310nm	1.63	0.77	-0.34	-0.16	0.02	0.14	0.84	0.25	1.63
		1550nm	19.56	18.55	17.08	17.12	17.21	17.28	18.66	17.37	19.56
Zero-dispersion wavelength	nm		1287	1297	1309	1307	1305	1303	1296	1302	1287
Zero-dispersion slope	ps/nm²/km		0.0940	0.091	0.087	0.087	0.088	0.088	0.091	0.088	0.094
MFD	μm	1310nm	10.04	9.73	8.91	8.73	8.57	8.47	9.71	8.38	10.04
		1550nm	10.44	11.23	10.39	10.15	9.94	9.81	11.19	9.69	11.44
Cut-off wavelength	nm		1505	1295	1355	1395	1440	1470	1475	1500	1505
Bending loss	dB/turn	1625nm r=5mm	0.0	0.1	0.0	0.0	0.0	0.0	0.0	0.0	0.0

FIG.55C

Hole occupancy rate	S	%	35.7	35.7	35.7	35.7	35.7	35.7	35.7	35.7	35.7
Distance	L1	μm	9.10	9.10	9.10	9.10	9.10	9.45	9.45	9.45	9.45
Hole diameter	d	μm	2.60	2.60	2.60	2.60	2.60	2.70	2.70	2.70	2.70
Core diameter	2a	μm	6.0	6.4	6.6	6.8	7.1	6.2	6.4	6.6	6.8
Relative refractive index difference	Δ1	%	0.30	0.30	0.30	0.30	0.30	0.30	0.30	0.30	0.30
Inner cladding layer diameter	2b	μm	36	36	36	36	36	36	36	36	36
Relative refractive index difference	Δ2	%	-0.05	-0.05	-0.05	-0.05	-0.05	-0.05	-0.05	-0.05	-0.05
Chromatic dispersion	ps/nm/km	1310nm	0.38	0.94	1.50	2.11	2.76	-0.76	-0.21	0.36	0.92
		1550nm	21.41	21.76	22.01	22.35	22.67	20.22	20.87	21.46	22.24
Zero-dispersion wavelength	nm		1311	1304	1300	1297	1292	1318	1314	1310	1306
Zero-dispersion slope	ps/nm²/km		0.1042	0.104	0.1038	0.1036	0.1034	0.0982	0.0979	0.0976	0.0973
MFD	μm	1310nm	8.82	8.83	8.84	8.90	9.00	8.86	8.90	8.95	9.01
		1550nm	9.53	9.50	9.47	9.61	9.81	9.57	9.61	9.69	9.67
Cut-off wavelength	nm		1010	1070	1095	1125	1175	1050	1090	1125	1155
Bending loss	dB/turn	1625nm r=5mm	0.2	0.2	0.1	0.1	0.1	0.1	0.1	0.1	0.1
Hole occupancy rate	S	%	35.7	35.7	35.7	35.7	35.7	35.7	35.7	35.7	35.7
Distance	L1	μm	9.45	10.15	10.15	10.15	10.15	10.15	10.15	9.45	9.45
Hole diameter	d	μm	2.70	2.90	2.90	2.90	2.90	2.90	2.90	2.40	2.60
Core diameter	2a	μm	7.0	6.15	6.4	6.6	6.8	7.1	7.4	6.6	6.6
Relative refractive index difference	Δ1	%	0.30	0.30	0.30	0.30	0.30	0.30	0.30	0.30	0.30
Inner cladding layer diameter	2b	μm	36	36	36	36	36	36	36	36	36
Relative refractive index difference	Δ2	%	-0.05	-0.05	-0.05	-0.05	-0.05	-0.05	-0.05	-0.05	-0.05
Chromatic dispersion	ps/nm/km	1310nm	1.48	-1.48	-0.92	-0.42	0.11	0.55	1.50	3.41	1.50
		1550nm	22.81	19.34	19.65	19.81	20.13	20.42	21.87	22.14	22.01
Zero-dispersion wavelength	nm		1301	1329	1324	1319	1315	1309	1300	1283	1300
Zero-dispersion slope	ps/nm²/km		0.0970	0.102	0.099	0.0982	0.098	0.0985	0.0984	0.109	0.1038
MFD	μm	1310nm	9.12	8.90	8.98	9.05	9.12	9.24	9.33	8.68	8.84
		1550nm	9.92	9.70	9.78	9.87	9.95	10.02	10.14	9.05	9.47
Cut-off wavelength	nm		1185	1060	1115	1155	1190	1230	1270	1050	1095
Bending loss	dB/turn	1625nm r=5mm	0.1	0.1	0.1	0.1	0.1	0.1	0.1	0.1	0.1

FIG.55D

Hole occupancy rate	S	%	35.7	35.7	35.7	35.7	35.7	35.7	35.7	35.7	35.7
Distance	L1	μm	10.15	11.55	14.0	11.55	11.55	11.55	11.55	14.0	14.0
Hole diameter	d	μm	2.90	3.30	4.00	3.30	3.30	3.30	3.30	4.0	4.0
Core diameter	2a	μm	6.6	6.6	6.6	6.4	6.6	6.8	7.1	6.6	7.0
Relative refractive index difference	Δ1	%	0.30	0.30	0.30	0.30	0.30	0.30	0.30	0.30	0.30
Inner cladding layer diameter	2b	μm	36	36	36	36	36	36	36	36	36
Relative refractive index difference	Δ2	%	-0.05	-0.05	-0.05	-0.05	-0.05	-0.05	-0.05	-0.05	-0.05
Chromatic dispersion	ps/nm/km	1310nm	-0.42	-1.64	-3.78	-3.88	-2.89	-2.02	-1.06	-3.78	-2.68
		1550nm	19.81	17.53	14.84	16.25	16.88	17.51	18.23	14.84	15.57
Zero-dispersion wavelength	nm		1319	1337	1359	1338	1333	1329	1326	1359	1346
Zero-dispersion slope	$ps/nm^2/km$		0.0982	0.092	0.084	0.091	0.092	0.0922	0.0923	0.084	0.084
MFD	μm	1310nm	9.05	9.22	9.44	9.10	9.22	9.30	9.39	9.44	9.52
		1550nm	9.87	10.26	10.73	10.25	10.30	10.34	10.38	10.73	10.78
Cut-off wavelength	nm		1155	1195	1230	1145	1195	1230	1290	1230	1295
Bending loss	dB/turn	1625nm r=5mm	0.1	0.1	0.1	0.1	0.1	0.1	0.1	0.1	0.1

Hole occupancy rate	S	%	35.7	35.7	35.7	35.7	35.7	35.7	35.7	35.7
Distance	L1	μm	14.0	14.0	14.0	8.40	9.10	10.15	11.03	11.55
Hole diameter	d	μm	4.0	4.0	4.0	2.40	2.60	2.90	3.15	3.30
Core diameter	2a	μm	7.4	8.0	8.4	7.1	7.1	7.1	7.1	7.1
Relative refractive index difference	Δ1	%	0.30	0.30	0.30	0.30	0.30	0.30	0.30	0.30
Inner cladding layer diameter	2b	μm	36	36	36	36	36	36	36	36
Relative refractive index difference	Δ2	%	-0.05	-0.05	-0.05	-0.05	-0.05	-0.05	-0.05	-0.05
Chromatic dispersion	ps/nm/km	1310nm	-1.73	-0.54	0.11	3.93	2.26	0.55	-0.26	-1.06
		1550nm	16.31	17.39	17.99	24.29	22.35	20.42	19.36	18.23
Zero-dispersion wavelength	nm		1335	1321	1314	1277	1292	1309	1321	1326
Zero-dispersion slope	$ps/nm^2/km$		0.086	0.088	0.090	0.1087	0.0996	0.0985	0.0944	0.0923
MFD	μm	1310nm	9.60	9.75	9.93	8.82	9.00	9.24	9.33	9.39
		1550nm	10.64	10.61	10.95	9.29	9.63	10.02	10.21	10.38
Cut-off wavelength	nm		1365	1455	1530	1120	1175	1230	1265	1290
Bending loss	dB/turn	1625nm r=5mm	0.0	0.0	0.0	0.1	0.1	0.1	0.1	0.1

FIG.55E

Hole occupancy rate	S	%	38.0	38.0	38.0	38.0	38.0	38.0
Distance	L1	μm	8.88	8.88	8.88	8.88	8.88	8.88
Hole diameter	d	μm	2.7	2.7	2.7	2.7	2.7	2.7
Core diameter	2a	μm	6.2	6.4	6.6	6.8	7.0	7.4
Relative refractive index difference	Δ1	%	0.30	0.30	0.30	0.30	0.30	0.30
Inner cladding layer diameter	2b	μm	36	36	36	36	36	36
Relative refractive index difference	Δ2	%	-0.05	-0.05	-0.05	-0.05	-0.05	-0.05
Chromatic dispersion	ps/nm/km	1310nm	1.62	1.98	2.27	2.56	2.93	3.54
		1550nm	22.23	22.56	22.87	23.14	23.30	23.72
Zero-dispersion wavelength	nm		1306	1302	1298	1295	1292	1286
Zero-dispersion slope	ps/nm²/km		0.105	0.105	0.106	0.106	0.106	0.107
MFD	μm	1310nm	8.65	8.73	8.80	8.88	8.95	9.01
		1550nm	9.21	9.30	9.38	9.46	9.51	9.46
Cut-off wavelength	nm		1080	1105	1130	1156	1185	1240
Bending loss	dB/turn	1625nm r=5mm	0.1	0.1	0.1	0.1	0.1	0.1

Hole occupancy rate	S	%	38.0	38.0	38.0	38.0	38.0	38.0
Distance	L1	μm	8.55	8.88	9.21	9.52	10.065	8.22
Hole diameter	d	μm	2.6	2.7	2.8	2.9	3.06	2.50
Core diameter	2a	μm	7.0	7.0	7.0	7.0	7.0	6.6
Relative refractive index difference	Δ1	%	0.30	0.30	0.30	0.30	0.30	0.30
Inner cladding layer diameter	2b	μm	36	36	36	36	36	36
Relative refractive index difference	Δ2	%	-0.05	-0.05	-0.05	-0.05	-0.05	-0.05
Chromatic dispersion	ps/nm/km	1310nm	3.61	2.93	2.23	1.48	0.70	3.45
		1550nm	24.10	23.30	22.51	21.80	20.73	24.21
Zero-dispersion wavelength	nm		1283	1292	1298	1305	1313	1284
Zero-dispersion slope	ps/nm²/km		0.107	0.106	0.104	0.102	0.099	0.110
MFD	μm	1310nm	8.80	8.95	9.04	9.13	9.22	8.60
		1550nm	9.43	9.51	9.66	9.82	9.99	9.12
Cut-off wavelength	nm		1148	1185	1215	1250	1280	1080
Bending loss	dB/turn	1625nm r=5mm	0.1	0.1	0.1	0.1	0.0	0.1

FIG.55F

Hole occupancy rate	S	%	38.0	38.0	38.0	38.0	38.0	38.0
Distance	L1	μm	8.88	9.54	10.52	11.5	12.50	9.54
Hole diameter	d	μm	2.7	2.9	3.2	3.5	3.8	2.9
Core diameter	2a	μm	6.6	6.6	6.6	6.6	6.6	6.4
Relative refractive index difference	Δ1	%	0.30	0.30	0.30	0.30	0.30	0.30
Inner cladding layer diameter	2b	μm	36	36	36	36	36	36
Relative refractive index difference	Δ2	%	-0.05	-0.05	-0.05	-0.05	-0.05	-0.05
Chromatic dispersion	ps/nm/km	1310nm	2.27	0.87	-0.76	-1.97	-2.86	1.98
		1550nm	22.87	21.33	19.41	17.84	16.51	22.56
Zero-dispersion wavelength	nm		1298	1311	1328	1341	1351	1314
Zero-dispersion slope	ps/nm^2/km		0.106	0.102	0.097	0.093	0.089	0.102
MFD	μm	1310nm	8.80	8.96	9.13	9.24	9.31	8.84
		1550nm	9.38	9.67	10.01	10.27	10.47	9.54
Cut-off wavelength	nm		1130	1180	1250	1315	1355	1141
Bending loss	dB/turn	1625nm r=5mm	0.1	0.1	0.1	0.0	0.0	0.1

Hole occupancy rate	S	%	38.0	38.0	38.0	38.0
Distance	L1	μm	9.54	9.54	9.54	9.54
Hole diameter	d	μm	2.9	2.9	2.9	2.9
Core diameter	2a	μm	6.6	6.8	7.0	7.3
Relative refractive index difference	Δ1	%	0.30	0.30	0.30	0.30
Inner cladding layer diameter	2b	μm	36	36	36	36
Relative refractive index difference	Δ2	%	-0.05	-0.05	-0.05	-0.05
Chromatic dispersion	ps/nm/km	1310nm	0.87	-0.14	-1.20	-2.31
		1550nm	21.33	20.18	18.97	17.73
Zero-dispersion wavelength	nm		1311	1308	1305	1298
Zero-dispersion slope	ps/nm^2/km		0.102	0.103	0.103	0.104
MFD	μm	1310nm	8.96	9.04	9.13	9.25
		1550nm	9.67	9.75	9.86	9.99
Cut-off wavelength	nm		1180	1215	1250	1282
Bending loss	dB/turn	1625nm r=5mm	0.1	0.1	0.1	0.0

FIG.55G

Hole occupancy rate	S	%	42.0	42.0	42.0	42.0	42.0	42.0	42.0
Distance	L1	μm	8.63	8.63	8.63	8.63	9.52	9.52	9.52
Hole diameter	d	μm	2.9	2.9	2.9	2.9	3.2	3.2	3.2
Core diameter	2a	μm	5.6	5.8	6.0	6.2	5.7	6.0	6.4
Relative refractive index difference	Δ1	%	0.30	0.30	0.30	0.30	0.30	0.30	0.30
Inner cladding layer diameter	2b	μm	28.8	28.8	28.8	28.8	28.8	28.8	28.8
Relative refractive index difference	Δ2	%	-0.05	-0.05	-0.05	-0.05	-0.05	-0.05	-0.05
Chromatic dispersion	ps/nm/km	1310nm	1.73	2.06	2.39	2.82	-0.38	0.24	1.00
		1550nm	-	22.90	23.35	23.84	21.01	21.32	21.70
Zero-dispersion wavelength	nm		1309	1306	1303	1300	1329	1323	1315
Zero-dispersion slope	$ps/nm^2/km$		0.110	0.109	0.109	0.108	0.104	0.104	0.104
MFD	μm	1310nm	8.49	8.53	8.60	8.65	8.78	8.86	8.95
		1550nm	9.05	9.18	9.15	9.18	9.53	9.58	9.63
Cut-off wavelength	nm		1200	1230	1260	1275	1300	1350	1405
Bending loss	dB/turn	1625nm r=5mm	0.1	0.1	0.1	0.1	0.1	0.0	0.0

Hole occupancy rate	S	%	42.0	42.0	42.0	42.0	42.0	42.0	42.0
Distance	L1	μm	9.52	9.52	9.52	8.33	9.52	9.52	10.77
Hole diameter	d	μm	3.2	3.2	3.2	2.8	3.2	3.2	3.62
Core diameter	2a	μm	6.4	6.8	6.8	5.7	7.0	7.0	7.0
Relative refractive index difference	Δ1	%	0.33	0.30	0.33	0.30	0.30	0.33	0.30
Inner cladding layer diameter	2b	μm	28.8	30.6	30.6	28.8	31.5	31.5	31.5
Relative refractive index difference	Δ2	%	-0.05	-0.05	-0.05	-0.05	-0.05	-0.05	-0.05
Chromatic dispersion	ps/nm/km	1310nm	0.47	1.72	1.29	3.09	2.06	1.67	0.04
		1550nm	21.04	22.12	21.56	23.84	22.35	21.82	19.92
Zero-dispersion wavelength	nm		1320	1308	1312	1280	1305	1308	1325
Zero-dispersion slope	$ps/nm^2/km$		0.102	0.104	0.102	0.089	0.097	0.102	0.097
MFD	μm	1310nm	8.77	9.04	8.87	8.85	9.09	8.93	9.32
		1550nm	9.47	9.68	9.53	9.57	9.71	9.57	10.15
Cut-off wavelength	nm		1440	1455	1490	1360	1475	1510	1600
Bending loss	dB/turn	1625nm r=5mm	0.0	0.0	0.0	0.0	0.0	0.0	0.0

FIG.55H

Hole occupancy rate	S	%	42.0	42.0	42.0	42.0	42.0	42.0	42.0
Distance	L1	μm	10.77	11.6	11.6	12.2	12.2	12.79	12.79
Hole diameter	d	μm	3.62	3.9	3.9	4..1	4.1	4.3	4.3
Core diameter	2a	μm	7.0	7.0	7.0	7.0	7.0	7.0	7.0
Relative refractive index difference	Δ1	%	0.33	0.30	0.33	0.30	0.33	0.30	0.33
Inner cladding layer diameter	2b	μm	31.5	31.5	31.5	31.5	31.5	31.5	31.5
Relative refractive index difference	Δ2	%	-0.05	-0.05	-0.05	-0.05	-0.05	-0.05	-0.05
Chromatic dispersion	ps/nm/km	1310nm	-0.24	-0.91	-1.11	-1.45	-1.58	-1.88	-1.94
		1550nm	19.38	18.63	18.10	17.83	17.33	17.14	16.67
Zero-dispersion wavelength	nm		1328	1335	1337	1341	1342	1346	1346
Zero-dispersion slope	$ps/nm^2/km$		0.095	0.094	0.092	0.091	0.089	0.089	0.087
MFD	μm	1310nm	9.11	9.38	9.18	9.42	9.19	9.48	9.24
		1550nm	9.95	10.33	10.12	10.44	10.18	10.59	10.30
Cut-off wavelength	nm		1630	1670	1700	1700	1730	1720	1755
Bending loss	dB/turn	1625nm r=5mm	0.0	0.0	0.0	0.0	0.0	0.0	0.0

Hole occupancy rate	S	%	42.0	42.0	42.0	42.0
Distance	L1	μm	8	8.63	9.52	10.12
Hole diameter	d	μm	2.69	2.9	3.2	3.4
Core diameter	2a	μm	6.0	6.0	6.0	6.0
Relative refractive index difference	Δ1	%	0.30	0.30	0.30	0.30
Inner cladding layer diameter	2b	μm	28.8	28.8	28.8	28.8
Relative refractive index difference	Δ2	%	-0.05	-0.05	-0.05	-0.05
Chromatic dispersion	ps/nm/km	1310nm	4.12	2.39	0.24	-1.87
		1550nm	25.10	23.35	21.32	19.34
Zero-dispersion wavelength	nm		1283	1303	1323	1334
Zero-dispersion slope	$ps/nm^2/km$		0.113	0.109	0.104	0.102
MFD	μm	1310nm	8.35	8.60	8.86	8.98
		1550nm	8.73	9.15	9.58	9.97
Cut-off wavelength	nm		1185	1260	1350	1385
Bending loss	dB/turn	1625nm r=5mm	0.1	0.1	0.0	0.0

FIG.56

Hole occupancy rate	S	%	35.7	35.7	35.7	30.1	35.7	30.1	35.7	30.1
Distance	L1	μm	14.0	14.0	14.0	13.9	14.0	13.9	14.0	13.9
Hole diameter	d	μm	4.0	4.0	4.0	3.3	4.0	3.3	4.0	3.3
Core diameter	2a	μm	6.6	8.0	7.0	9.0	8.0	8.0	8.0	8.0
Relative refractive index difference	Δ1	%	0.30	0.30	0.30	0.30	0.21	0.35	0.25	0.38
Inner cladding layer diameter	2b	μm	36	16	36	20	36	36	36	36
Relative refractive index difference	Δ2	%	-0.05	-0.05	-0.05	-0.05	-0.05	-0.05	-0.05	-0.05
Chromatic dispersion	ps/nm/km	1310nm	-3.78	-0.91	-2.68	0.77	-0.55	-0.34	-0.65	-0.16
		1550nm	14.84	17.01	15.57	18.55	18.41	17.08	17.79	17.12
Zero-dispersion wavelength	nm		1354	1320	1341	1302	1316	1314	1317	1312
Zero-dispersion slope	ps/nm^2/km		0.084	0.087	0.084	0.091	0.092	0.087	0.090	0.087
MFD	μm	1310nm	8.44	8.87	8.52	9.23	9.72	8.41	9.24	8.23
		1550nm	9.73	10.01	9.78	10.23	10.97	9.39	10.41	9.15
Cut-off wavelength	nm		1270	1310	1335	1335	1340	1395	1415	1435
Bending loss	dB/turn	1625nm r=5mm	0.1	0.1	0.1	0.1	0.2	0.0	0.1	0.0

Hole occupancy rate	S	%	35.7	30.1	35.7	30.1	30.1	30.1	30.1
Distance	L1	μm	14.0	13.9	14.0	13.9	13.9	13.9	13.9
Hole diameter	d	μm	4.0	3.3	4.0	3.3	3.3	3.3	3.3
Core diameter	2a	μm	8.0	8.0	9.0	8.0	9.0	8.0	9.8
Relative refractive index difference	Δ1	%	0.28	0.41	0.30	0.43	0.30	0.45	0.30
Inner cladding layer diameter	2b	μm	36	36	20	36	45	36	36
Relative refractive index difference	Δ2	%	-0.05	-0.05	-0.05	-0.05	-0.05	-0.05	-0.05
Chromatic dispersion	ps/nm/km	1310nm	-0.60	0.02	0.83	0.14	0.84	0.25	1.63
		1550nm	17.49	17.21	18.72	17.28	18.66	17.37	19.56
Zero-dispersion wavelength	nm		1317	1310	1301	1308	1301	1307	1292
Zero-dispersion slope	ps/nm^2/km		0.088	0.088	0.091	0.088	0.091	0.088	0.094
MFD	μm	1310nm	8.94	8.07	9.23	7.97	9.21	7.88	9.54
		1550nm	10.05	8.94	10.21	8.81	10.19	8.69	10.44
Cut-off wavelength	nm		1470	1480	1495	1510	1515	1540	1545
Bending loss	dB/turn	1625nm r=5mm	0.1	0.0	0.0	0.0	0.0	0.0	0.0

FIG.57

Hole occupancy rate	S	%	30.1	30.1	30.1	30.3	24.1
Distance	L1	μm	13.86	13.86	13.86	13.19	13.50
Hole diameter	d	μm	3.33	3.33	3.33	3.19	2.60
Core diameter	2a	μm	8.1	8.0	8.1	7.6	8.1
Relative refractive index difference	Δ1	%	0.30	0.23	0.30	0.30	0.30
Inner cladding layer diameter	2b	μm	16	36	20	33	36
Relative refractive index difference	Δ2	%	-0.05	-0.05	-0.05	-0.05	-0.05
Chromatic dispersion	ps/nm/km	1310nm	-0.77	-0.76	-0.48	-1.18	-0.41
		1550nm	17.00	17.81	17.26	16.93	17.31
Zero-dispersion wavelength	nm		1319	1318	1315	1323	1315
Zero-dispersion slope	ps/nm^2/km		0.0867	0.0900	0.0876	0.0872	0.0877
MFD	μm	1310nm	8.92	9.48	8.86	8.63	8.79
		1550nm	10.07	10.73	9.95	9.73	9.84
Cut-off wavelength	nm		1195	1195	1210	1235	1235
Bending loss	dB/turn	1625nm r=5mm	0.2	0.3	0.2	0.1	0.2

Hole occupancy rate	S	%	30.1	30.1	26.0	30.1	29.8
Distance	L1	μm	13.86	13.86	13.22	13.86	13.86
Hole diameter	d	μm	3.33	3.33	2.75	3.33	3.30
Core diameter	2a	μm	8.0	8.1	8.2	8.1	7.8
Relative refractive index difference	Δ1	%	0.25	0.30	0.30	0.30	0.30
Inner cladding layer diameter	2b	μm	36	24	35	28	34
Relative refractive index difference	Δ2	%	-0.05	-0.05	-0.05	-0.05	-0.05
Chromatic dispersion	ps/nm/km	1310nm	-0.76	-0.39	-0.23	-0.39	-0.98
		1550nm	17.55	17.37	17.64	17.38	16.81
Zero-dispersion wavelength	nm		1319	1314	1313	1314	1321
Zero-dispersion slope	ps/nm^2/km		0.0888	0.0880	0.0886	0.0880	0.0866
MFD	μm	1310nm	9.25	8.90	8.80	8.89	8.70
		1550nm	10.45	10.00	9.84	9.99	9.81
Cut-off wavelength	nm		1235	1236	1255	1260	1260
Bending loss	dB/turn	1625nm r=5mm	0.2	0.1	0.2	0.1	0.1

HOLE-ASSISTED OPTICAL FIBER

CROSS-REFERENCE TO RELATED APPLICATIONS

This application is a continuation of PCT International Application No. PCT/JP2011/068073 filed on Aug. 8, 2011 which claims the benefit of priority from Japanese Patent Application No. 2010-179058 filed on Aug. 9, 2010, the entire contents of which are incorporated herein by reference.

BACKGROUND

1. Technical Field

The disclosure relates to a hole-assisted optical fiber.

2. Related Art

Conventionally, an optical fiber compliant with ITU-T G.652 (made by International Telecommunication Union) has been used for optical communications. In the ITU-T G.652, as optical fiber characteristics, a mode field diameter at a wavelength of 1310 nm is specified as in a range of 8.6 to 9.5 (±0.6) μm, a cut-off wavelength by a 22 m method defined in ITU-T G.650 is specified as equal to or less than 1260 nm, and a zero-dispersion wavelength is specified as in a range of 1300 to 1324 nm.

A hole-assisted optical fiber (HAF) is an optical fiber having a constitution such that holes are provided in a cladding portion formed around a core portion to which germanium or the like is added, the core being high in refraction index (see Japanese Patent No. 3854627 and Japanese Patent Application Laid-open No. 2004-226540). The hole-assisted optical fiber is provided with the holes to intensify the confinement of light to the core portion thus being characterized by a decrease in bending loss. Therefore, bending loss characteristics further more excellent than that specified in the ITU-T G.657B can be realized and hence, the hole-assisted optical fiber has come to attention as an optical fiber used in place of the above-mentioned conventional optical fiber compliant with the ITU-T G.652.

In addition, in the ITU-T G.652, the value of the bending loss when bent at a radius of 7.5 mm is specified as equal to or less than 1 dB/turn for a wavelength of 1625 nm and equal to or less than 0.5 dB/turn for a wavelength of 1550 nm. Here, "dB/turn" is a unit expressing the increase in transmission loss per one turn in decibels when an optical fiber is wound by one around (one turn) at a predetermined radius.

Here, when the hole-assisted optical fiber is used as an optical communications-use optical fiber compliant with ITU-T G.652, it is necessary to realize single-mode transmission at a wavelength (1556 nm, for example) used for optical communications. Furthermore, at the same time, in order to improve productivity, the hole-assisted optical fiber preferably has a large design margin for achieving desired properties thereof.

SUMMARY

In accordance with some embodiments, a hole-assisted optical fiber includes a core portion and a cladding portion. The cladding portion includes an inner cladding layer formed around an outer periphery of the core portion and having a refractive index lower than that of the core portion, an outer cladding layer formed around an outer periphery of the inner cladding layer and having a refractive index higher than that of the inner cladding layer and lower than that of the core portion, and a plurality of holes formed around the core portion. A diameter of the core portion is in a range of 3 μm to 9.8 μm. A relative refractive index difference of the core portion relative to the outer cladding layer is in a range of 0.11% to 0.45%. An outside diameter of the inner cladding layer is equal to or less than 53 μm. A relative refractive index difference of the inner cladding layer relative to the outer cladding layer is a negative value equal to or more than −0.30%. A diameter of each of the plurality of holes is in a range of 2.4 μm to 4.0 μm. A hole occupancy rate is in a range of 17% to 48%. A bending loss at a wavelength of 1625 nm when bent at a radius of 5 mm is equal to or less than 1 dB/turn. A cut-off wavelength is equal to or less than 1550 nm. The hole occupancy rate S (%) is defined by the following expression (1):

$$S=N\pi(d/2)^2/[\pi(R+d)^2-\pi R^2] \tag{1}$$

where N is the number of the plurality of holes, d (μm) is the diameter of each of the plurality of holes, and R (μm) is a radius of an inscribed circle which is brought into internal contact with each of the plurality of holes.

The above and other objects, features, advantages and technical and industrial significance of this invention will be better understood by reading the following detailed description of presently preferred embodiments of the invention, when considered in connection with the accompanying drawings.

BRIEF DESCRIPTION OF THE DRAWINGS

FIG. **1** is a view illustrating a schematic cross section of a hole-assisted optical fiber according to a first embodiment and a refractive index profile corresponding thereto;

FIG. **2** is an explanatory view for explaining structural parameters of the hole-assisted optical fiber illustrated in FIG. **1**;

FIG. **3**A is a view illustrating a relationship between a hole occupancy rate S and a cut-off wavelength for the hole-assisted optical fiber according to the first embodiment and a hole-assisted optical fiber according to a comparative embodiment;

FIG. **3**B is a view illustrating a relationship between the hole occupancy rate S and a bending loss for the hole-assisted optical fiber according to the first embodiment and the hole-assisted optical fiber according to the comparative embodiment;

FIG. **4**A is a view illustrating a relationship between an inner cladding layer outside diameter **2***b* and a cut-off wavelength for a hole-assisted optical fiber **10** according to the first embodiment and the hole-assisted optical fiber according to the comparative embodiment;

FIG. **4**B is a view illustrating a relationship between the inner cladding layer outside diameter **2***b* and the bending loss for the hole-assisted optical fiber according to the first embodiment and the hole-assisted optical fiber according to the comparative embodiment;

FIG. **4**C is a view illustrating a relationship between the inner cladding layer outside diameter **2***b* and an MFD for the hole-assisted optical fiber according to the first embodiment and the hole-assisted optical fiber according to the comparative embodiment;

FIG. **4**D is a view illustrating a relationship between the inner cladding layer outside diameter **2***b* and a zero-dispersion wavelength for the hole-assisted optical fiber according to the first embodiment and the hole-assisted optical fiber according to the comparative embodiment;

FIG. **4**E is a view illustrating a relationship between the inner cladding layer outside diameter **2***b* and a zero-dispersion slope for the hole-assisted optical fiber according to the first embodiment and the hole-assisted optical fiber according to the comparative embodiment;

FIG. **5** is a view illustrating a relationship between the hole occupancy rate S and the cut-off wavelength;

FIG. **6** is a view illustrating a relationship between the hole occupancy rate S and the bending loss;

FIG. **7** is a view illustrating a relationship between the hole occupancy rate S and a MFD;

FIG. **8** is a view illustrating a relationship between the hole occupancy rate S and the zero-dispersion wavelength;

FIG. **9** is a view illustrating a relationship between a core diameter **2***a* and the cut-off wavelength;

FIG. **10** is a view illustrating a relationship between the core diameter **2***a* and the bending loss;

FIG. **11** is a view illustrating a relationship between the core diameter **2***a* and the MFD;

FIG. **12** is a view illustrating a relationship between the core diameter **2***a* and the zero-dispersion wavelength;

FIG. **13** is a view illustrating a relationship between the core diameter **2***a* and the cut-off wavelength;

FIG. **14** is a view illustrating a relationship between the core diameter **2***a* and the macrobendng loss;

FIG. **15** is a view illustrating a relationship between the core diameter **2***a* and the MFD;

FIG. **16** is a view illustrating a relationship between the core diameter **2***a* and the zero-dispersion wavelength;

FIG. **17** is a view illustrating a relationship between a relative refractive index difference Δ**1** and the cut-off wavelength;

FIG. **18** is a view illustrating a relationship between the relative refractive index difference Δ**1** and the bending loss;

FIG. **19** is a view illustrating a relationship between the relative refractive index difference Δ**1** and the MFD;

FIG. **20** is a view illustrating a relationship between the relative refractive index difference Δ**1** and the zero-dispersion wavelength;

FIG. **21** is a view illustrating a relationship between the relative refractive index difference Δ**1** and the cut-off wavelength;

FIG. **22** is a view illustrating a relationship between the relative refractive index difference Δ**1** and the bending loss;

FIG. **23** is a view illustrating a relationship between the relative refractive index difference Δ**1** and the MFD;

FIG. **24** is a view illustrating a relationship between the relative refractive index difference Δ**1** and the zero-dispersion wavelength;

FIG. **25** is a view illustrating a relationship between a relative refractive index difference Δ**2** and the cut-off wavelength;

FIG. **26** is a view illustrating a relationship between the relative refractive index difference Δ**2** and the bending loss;

FIG. **27** is a view illustrating a relationship between the relative refractive index difference Δ**2** and the MFD;

FIG. **28** is a view illustrating a relationship between the relative refractive index difference Δ**2** and the zero-dispersion wavelength;

FIG. **29** is a view illustrating a relationship between the relative refractive index difference Δ**2** and the cut-off wavelength;

FIG. **30** is a view illustrating a relationship between the relative refractive index difference Δ**2** and the bending loss;

FIG. **31** is a view illustrating a relationship between the relative refractive index difference Δ**2** and the MFD;

FIG. **32** is a view illustrating a relationship between the relative refractive index difference Δ**2** and the zero-dispersion wavelength;

FIG. **33** is a view illustrating a relationship between the inner cladding layer outside diameter **2***b* and the cut-off wavelength;

FIG. **34** is a view illustrating a relationship between the inner cladding layer outside diameter **2***b* and the bending loss;

FIG. **35** is a view illustrating a relationship between the inner cladding layer outside diameter **2***b* and the MFD;

FIG. **36** is a view illustrating a relationship between the inner cladding layer outside diameter **2***b* and the zero-dispersion wavelength;

FIG. **37**A is a view illustrating a relationship between the core diameter **2***a* and optical properties when the hole occupancy rate S is 30.1% and a hole diameter d is 2.9 μm;

FIG. **37**B is a view illustrating a relationship between the core diameter **2***a* and optical properties when the hole occupancy rate S is 30.1% and the hole diameter d is 2.9 μm;

FIG. **38**A is a view illustrating a relationship between the core diameter **2***a* and optical the properties when the hole occupancy rate S is 30.1% and the hole diameter d is 3.3 μm;

FIG. **38**B is a view illustrating a relationship between the core diameter **2***a* and the optical properties when the hole occupancy rate S is 30.1% and the hole diameter d is 3.3 μm;

FIG. **39**A is a view illustrating a relationship between the hole diameter d and the optical properties when the hole occupancy rate S is 30.1% and the core diameter **2***a* is 6.6 μm;

FIG. **39**B is a view illustrating a relationship between the hole diameter d and the optical properties when the hole occupancy rate S is 30.1% and the core diameter **2***a* is 6.6 μm;

FIG. **40**A is a view illustrating a relationship between the hole diameter d and the optical properties when the hole occupancy rate S is 30.1% and the core diameter **2***a* is 7.8 μm;

FIG. **40**B is a view illustrating a relationship between the hole diameter d and the optical properties when the hole occupancy rate S is 30.1% and the core diameter **2***a* is 7.8 μm;

FIG. **41**A is a view illustrating a relationship between the core diameter **2***a* and the optical properties when the hole occupancy rate S is 35.7% and the hole diameter d is 2.6 μm;

FIG. **41**B is a view illustrating a relationship between the core diameter **2***a* and the optical properties when the hole occupancy rate S is 35.7% and the hole diameter d is 2.6 μm;

FIG. **42**A is a view illustrating a relationship between the core diameter **2***a* and the optical properties when the hole occupancy rate S is 35.7% and the hole diameter d is 2.7 μm;

FIG. **42**B is a view illustrating a relationship between the core diameter **2***a* and the optical properties when the hole occupancy rate S is 35.7% and the hole diameter d is 2.7 μm;

FIG. **43**A is a view illustrating a relationship between the core diameter **2***a* and the optical properties when the hole occupancy rate S is 35.7% and the hole diameter d is 2.9 μm;

FIG. **43**B is a view illustrating a relationship between the core diameter **2***a* and the optical properties when the hole occupancy rate S is 35.7% and the hole diameter d is 2.9 μm;

FIG. **44**A is a view illustrating a relationship between the core diameter **2***a* and the optical properties when the hole occupancy rate S is 35.7% and the hole diameter d is 3.3 μm;

FIG. **44**B is a view illustrating a relationship between the core diameter **2***a* and the optical properties when the hole occupancy rate S is 35.7% and the hole diameter d is 3.3 μm;

FIG. **45**A is a view illustrating a relationship between the hole diameter d and the optical properties when the hole occupancy rate S is 35.7% and the core diameter **2***a* is 6.6 μm;

FIG. **45**B is a view illustrating a relationship between the hole diameter d and the optical properties when the hole occupancy rate S is 35.7% and the core diameter **2***a* is 6.6 μm;

FIG. **46**A is a view illustrating a relationship between the hole diameter d and the optical properties when the hole occupancy rate S is 35.7% and the core diameter **2***a* is 7.1 μm;

FIG. **46**B is a view illustrating a relationship between the hole diameter d and the optical properties when the hole occupancy rate S is 35.7% and the core diameter **2**a is 7.1 μm;

FIG. **47**A is a view illustrating a relationship between the core diameter **2**a and the optical properties when the hole occupancy rate S is 38.0% and the hole diameter d is 2.7 μm;

FIG. **47**B is a view illustrating a relationship between the core diameter **2**a and the optical properties when the hole occupancy rate S is 38.0% and the hole diameter d is 2.7 μm;

FIG. **48**A is a view illustrating a relationship between the core diameter **2**a and the optical properties when the hole occupancy rate S is 38.0% and the hole diameter d is 2.9 μm;

FIG. **48**B is a view illustrating a relationship between the core diameter **2**a and the optical properties when the hole occupancy rate S is 38.0% and the hole diameter d is 2.9 μm;

FIG. **49**A is a view illustrating a relationship between the hole diameter d and the optical properties when the hole occupancy rate S is 38.0% and the core diameter **2**a is 6.6 μm;

FIG. **49**B is a view illustrating a relationship between the hole diameter d and the optical properties when the hole occupancy rate S is 38.0% and the core diameter **2**a is 6.6 μm;

FIG. **50**A is a view illustrating a relationship between the hole diameter d and the optical properties when the hole occupancy rate S is 38.0% and the core diameter **2**a is 7.0 μm;

FIG. **50**B is a view illustrating a relationship between the hole diameter d and the optical properties when the hole occupancy rate S is 38.0% and the core diameter **2**a is 7.0 μm;

FIG. **51**A is a view illustrating a relationship between the core diameter **2**a and the optical properties when the hole occupancy rate S is 42.0% and the hole diameter d is 2.9 μm;

FIG. **51**B is a view illustrating a relationship between the core diameter **2**a and the optical properties when the hole occupancy rate S is 42.0% and the hole diameter d is 2.9 μm;

FIG. **52**A is a view illustrating a relationship between the core diameter **2**a and the optical properties when the hole occupancy rate S is 42.0% and the hole diameter d is 3.2 μm;

FIG. **52**B is a view illustrating a relationship between the core diameter **2**a and the optical properties when the hole occupancy rate S is 42.0% and the hole diameter d is 3.2 μm;

FIG. **53**A is a view illustrating a relationship between the hole diameter d and the optical properties when the hole occupancy rate S is 42.0% and the core diameter **2**a is 6.0 μm;

FIG. **53**B is a view illustrating a relationship between the hole diameter d and the optical properties when the hole occupancy rate S is 42.0% and the core diameter **2**a is 6.0 μm;

FIG. **54**A is a view illustrating a relationship between the hole diameter d and the optical properties when the hole occupancy rate S is 42.0% and the core diameter **2**a is 7.0 μm;

FIG. **54**B is a view illustrating a relationship between the hole diameter d and the optical properties when the hole occupancy rate S is 42.0% and the core diameter **2**a is 7.0 μm;

FIG. **55**A is a view illustrating a relationship between the combination of the structural parameters and optical properties when the hole occupancy rate S is 30.1%;

FIG. **55**B is a view illustrating a relationship between the combination of the structural parameters and optical properties when the hole occupancy rate S is 30.1%;

FIG. **55**C is a view illustrating a relationship between the combination of the structural parameters and the optical properties when the hole occupancy rate S is 35.7%;

FIG. **55**D is a view illustrating a relationship between the combination of the structural parameters and the optical properties when the hole occupancy rate S is 35.7%;

FIG. **55**E is a view illustrating a relationship between the combination of the structural parameters and the optical properties when the hole occupancy rate S is 38.0%;

FIG. **55**F is a view illustrating a relationship between the combination of the structural parameters and the optical properties when the hole occupancy rate S is 38.0%;

FIG. **55**G is a view illustrating a relationship between the combination of the structural parameters and the optical properties when the hole occupancy rate S is 42.0%;

FIG. **55**H is a view illustrating a relationship between the combination of the structural parameters and the optical properties when the hole occupancy rate S is 42.0%;

FIG. **56** is a view illustrating a relationship between the combination of the hole occupancy rate and other design parameters, and the optical properties; and

FIG. **57** is a view illustrating a relationship between another combination of the hole occupancy rate and other design parameters, and the optical properties.

DETAILED DESCRIPTION

Hereinafter, with reference to the drawings, embodiments of a hole-assisted optical fiber according to the present invention are explained in detail. Here, the present invention is not limited to the embodiments. Furthermore, in the drawings, identical parts or parts corresponding to each other are properly given same numerals. Furthermore, unless otherwise specified, the value of a bending loss is specified at a wavelength of 1625 nm when bent at a radius of 5 mm, and the value of a mode field diameter (MFD) is specified at a wavelength of 1310 nm. In addition, terms that are not defined in this specification conform to definitions or measurement methods described in ITU-T G.650.1.

First Embodiment

FIG. **1** is a view illustrating a schematic cross section of a hole-assisted optical fiber **10** according to a first embodiment of the present invention and a refractive index profile corresponding thereto. As illustrated in FIG. **1**, the hole-assisted optical fiber **10** includes a core portion **11** and a cladding portion having an inner cladding layer **12**a formed around an outer periphery of the core portion **11**, an outer cladding layer **12**b formed around an outer periphery of the inner cladding layer **12**a, and ten holes **12**c formed around the core portion **11**. The holes **12**c are arranged so that the distances between the holes **12**c and the center of the core portion **11** are equal to each other and central angles are equal to each other.

The core portion **11** is made of silica based glass to which dopant for improving a refraction index, such as germanium (Ge), is added. The inner cladding layer **12**a is, for example, made of silica based glass to which dopant for lowering the refractive index, such as fluorine (F), is added. The outer cladding layer **12**b is, for example, made of pure silica glass in which dopant for adjusting the refractive index is not contained. Therefore, as illustrated by the refraction index profile P, the inner cladding layer **12**a has a refractive index lower than that of the core portion **11**. Furthermore, the outer cladding layer **12**b has a refractive index higher than that of the inner cladding layer **12**a and lower than that of the core portion **11**. Here, a broken line H indicates the positions of the holes **12**c.

The design parameters of the hole-assisted optical fiber **10** are specified. First of all, as a parameter for the refractive index out of the design parameters, as illustrated in FIG. **1**, the relative refractive index difference of the core portion **11** to the outer cladding layer **12**b is Δ**1**, and the relative refractive index difference of the inner cladding layer **12**a to the outer cladding layer **12**b is Δ**2**.

Next, structural parameters out of the design parameters of the hole-assisted optical fiber **10** are explained. FIG. **2** is an explanatory view for explaining structural parameters of the hole-assisted optical fiber **10** illustrated in FIG. **1**. As illustrated in FIG. **2**, the diameter of the core portion **11** (a core diameter) is expressed as 2a [μm], the outside diameter of the inner cladding layer **12***a* (an inner cladding layer outside diameter) is expressed as 2b [μm], the diameter of the hole **12***c* (a hole diameter) is expressed as d [μm], the distance from the center of the core portion **11** to the center of the hole **12***c* is expressed as L**1** [μm], and the minimum distance from the center of the core portion **11** to the outer edge of the hole **12***c*; that is, the radius of an inscribed circle C**1** brought into internal contact with each hole **12***c* with the center of the core portion **11** as the center is expressed as R [μm].

Here, a core diameter **2***a* is defined as a diameter at a position where the relative refractive index difference Δ**1** becomes 0% on the border between the core portion **11** and the inner cladding layer **12***a*. Furthermore, an inner cladding layer outside diameter **2***b* is defined as a diameter at a position where a relative refractive index difference becomes one-half of the relative refractive index difference Δ**2** on the border between the inner cladding layer **12***a* and the outer cladding layer **12***b*.

Furthermore, the number of the holes **12***c* is expressed as N, and the following expression (1) defines a hole occupancy rate S [%].

$$S=N\pi(d/2)^2/[\pi(R+d)^2-\pi R^2] \quad (1)$$

The hole occupancy rate S indicates a ratio of an area occupied by the holes **12***c* to the area of an annular region whose radius is (R+d), the annular region being formed between a circumscribed circle C**2** and the inscribed circle C**1** of each hole **12***c*.

Furthermore, in FIGS. **1** and **2**, the holes **12***c* are positioned in the inner cladding layer **12***a*. However, the position of each hole **12***c* is not limited in particular. That is, a large and small relationship between the distance L**1** and the inner cladding layer outside diameter **2***b* is arbitrarily changed. Therefore, the holes **12***c* may be positioned in the outer cladding layer **12***b*, and may be positioned so that the holes **12***c* are arranged in an area extending over the inner cladding layer **12***a* and the outer cladding layer **12***b*.

Next, in the hole-assisted optical fiber **10** according to the present embodiment, the characteristics of the cut-off wavelength and the bending loss with respect to the hole occupancy rate S are explained. Hereinafter, the core diameter **2***a* is set to 8 μm, the inner cladding layer outside diameter **2***b* is set to 36 μl, the relative refractive index difference Δ**1** is set to 0.3%, and the relative refractive index difference Δ**2** is set to −0.05%. Furthermore, as a comparative embodiment, in the structure of the hole-assisted optical fiber **10** illustrated in FIG. **1**, the core diameter **2***a* is set to 8 μm, the inner cladding layer outside diameter **2***b* is set to 36 and the relative refractive index difference Δ**1** is set to 0.3%. Here, the relative refractive index difference Δ**2** is 0%, and the characteristics of a hole assisted optical fiber substantially having a structure with no inner cladding layer are explained.

FIG. **3**A is a view illustrating a relationship between the hole occupancy rate S and the cut-off wavelength for the hole-assisted optical fiber **10** according to the first embodiment and the hole-assisted optical fiber according to the comparative embodiment. Furthermore, FIG. **3**B is a view illustrating a relationship between the hole occupancy rate S and the bending loss for the hole-assisted optical fiber according to the first embodiment and the hole-assisted optical fiber according to the comparative embodiment.

As illustrated in FIG. **3**A, the hole-assisted optical fiber **10** according to the first embodiment and the hole-assisted optical fiber according to the comparative embodiment each has a cut-off wavelength in the similar range with respect to the same hole occupancy rate S. For example, when the cut-off wavelength is set to equal to or less than 1550 nm, the hole occupancy rate S in both the first embodiment and the comparative embodiment may be set to equal to or less than 37.5%.

On the other hand, as illustrated in FIG. **3**B, with respect to the bending loss, the hole-assisted optical fiber **10** according to the first embodiment is further excellent in bending loss characteristics with respect to the same hole occupancy rate S thus realizing further small bending loss. For example, the bending loss when the cut-off wavelength is 1260 nm is 0.196 dB/turn in the comparative embodiment, and as small as 0.085 dB/turn in the first embodiment. Furthermore, when the bending loss is set to equal to or less than 0.1 dB/turn, it is necessary to set the hole occupancy rate S to equal to or more than 33% in the comparative embodiment. On the other hand, in the first embodiment, the hole occupancy rate S may be set to equal to or more than 28.5% thus realizing a bending loss of equal to or less than 0.1 dB/turn with respect to the hole occupancy rate S in a wider range.

Furthermore, the hole-assisted optical fiber **10** according to the first embodiment is further excellent in bending loss characteristics and hence, when a hole-assisted optical fiber with bending loss characteristics equivalent to that of the hole-assisted optical fiber according to the comparative embodiment is designed, the cut-off wavelength can be set shorter. As a result, a wavelength bandwidth in which a single-mode transmission can be realized becomes wider. For example, a cut-off wavelength when the bending loss is 0.1 dB/turn is 1270 nm in the comparative embodiment and 1170 nm in the first embodiment.

Next, in the hole-assisted optical fiber **10** according to the first embodiment and the hole-assisted optical fiber according to the comparative embodiment, a cut-off wavelength, a bending loss, a mode field diameter (MFD), a zero-dispersion wavelength, and a zero-dispersion slope when the hole occupancy rate S is 30.1%, 35.7%, or 39.9%, and the inner cladding layer outside diameter **2***b* is changed are explained. Here, the zero-dispersion slope means the gradient of chromatic dispersion at the zero-dispersion wavelength. Hereinafter, the core diameter **2***a* is 8 μm, the relative refractive index difference Δ**1** is 0.3%, and the relative refractive index difference Δ**2** is −0.05%.

FIG. **4**A is a view illustrating a relationship between the inner cladding layer outside diameter **2***b* and the cut-off wavelength for the hole-assisted optical fiber **10** according to the first embodiment and the hole-assisted optical fiber according to the comparative embodiment. FIG. **4**B is a view illustrating a relationship between the inner cladding layer outside diameter **2***b* and the bending loss for the hole-assisted optical fiber according to the first embodiment and the hole-assisted optical fiber according to the comparative embodiment. FIG. **4**C is a view illustrating a relationship between the inner cladding layer outside diameter **2***b* and an MFD for the hole-assisted optical fiber according to the first embodiment and the hole-assisted optical fiber according to the comparative embodiment. FIG. **4**D is a view illustrating a relationship between the inner cladding layer outside diameter **2***b* and the zero-dispersion wavelength for the hole-assisted optical fiber according to the first embodiment and the hole-assisted optical fiber according to the comparative embodiment. Furthermore, FIG. **4**E is a view illustrating a relationship between the inner cladding layer outside diameter **2***b* and the zero-dispersion slope for the hole-assisted optical fiber according to the first embodiment and the hole-assisted optical fiber according to the comparative embodiment.

As illustrated in FIGS. **4**A to **4**E, in the hole-assisted optical fiber according to the comparative embodiment, the inner cladding layer **12***a* does not exist and hence, the characteristics thereof; that is, the cut-off wavelength, the bending loss, the MFD, the zero-dispersion wavelength, and the zero-dispersion slope have constant values. On the other hand, the hole-assisted optical fiber **10** according to the first embodiment is provided with the inner cladding layer **12***a* and the inner cladding layer outside diameter **2***b* is adjusted thus adjusting the above-mentioned characteristics over the wide range. That is, in the hole-assisted optical fiber **10** according to the first embodiment, the combination of the other design parameters and the inner cladding layer outside diameter **2***b* can further increase the degree of freedom in the setting of the design parameter.

Here, as illustrated in FIG. **4**A, the cut-off wavelength of the hole-assisted optical fiber **10** according to the first embodiment turns into a long wavelength along with the increase of the hole occupancy rate S or the increase of the inner cladding layer outside diameter **2***b*. For example, if the hole occupancy rate S is 39.9%, when the inner cladding layer outside diameter **2***b* is larger than approximately 35 μm, the cut-off wavelength of the first embodiment becomes longer than that of the comparative embodiment. In the same manner as above, if the hole occupancy rate S is 35.7%, when the inner cladding layer outside diameter **2***b* is larger than approximately 28 μm, the cut-off wavelength of the first embodiment becomes longer than that of the comparative embodiment. If the hole occupancy rate S is 30.1%, when the inner cladding layer outside diameter **2***b* is larger than approximately 27 μm, the cut-off wavelength of the first embodiment becomes longer than that of the comparative embodiment.

Furthermore, as illustrated in FIG. **4**B, the bending loss of the hole-assisted optical fiber **10** according to the first embodiment turns into a low loss along with the increase of the hole occupancy rate S and the increase of the inner cladding layer outside diameter **2***b*. Furthermore, to consider also any case out of the cases where the hole occupancy rate S is 39.9%, 35.7%, and 30.1%, when the inner cladding layer outside diameter **2***b* is larger than approximately 15 μm to 16 μm, the bending loss of the first embodiment becomes lower than that of the comparative embodiment.

Furthermore, as illustrated in FIGS. **4**C to **4**E, the MFD, the zero-dispersion wavelength, and the zero-dispersion slope are less dependent on the inner cladding layer outside diameter **2***b*. Particularly, the zero-dispersion slope is also less dependent on the hole occupancy rate S. However, in the hole-assisted optical fiber **10** according to the first embodiment, any characteristics of the MFD, the zero-dispersion wavelength, and the zero-dispersion slope thereof can also be made smaller than those of the hole-assisted optical fiber according to the comparative embodiment.

That is, the hole-assisted optical fiber **10** according to the first embodiment is provided with the inner cladding layer **12***a* whereby the degree of freedom in design margin and design for realizing desired characteristics is large compared with the case of the hole-assisted optical fiber according to the comparative embodiment. As a result, a load in designing is reduced and the permissible amount of a manufacture error becomes large thus further improving productivity.

Furthermore, the hole-assisted optical fiber **10** according to the first embodiment has the core diameter **2***a* set in a range of 3 μm to 9.8 a relative refractive index difference Δ**1** set in a range of 0.11% to 0.45%, the inner cladding layer outside diameter **2***b* set to a value larger than a core diameter **2***a* of equal to or less than 53 a relative refractive index difference Δ**2** set to a negative value of equal to or more than −0.30%, a hole diameter d set in a range of 2.7 μm to 4.0 μm, and a hole occupancy rate S set in a range of 17% to 48% thus realizing characteristics such that the bending loss is equal to or less than 1 dB/turn being smaller than a value specified in ITU-T G.657B and the cut-off wavelength is equal to or less than 1550 nm.

Furthermore, the core diameter **2***a* is set in a range of 6.0 μm to 8.4 μm, the relative refractive index difference Δ**1** is set in a range of 0.23% to 0.32%, the inner cladding layer outside diameter **2***b* is set to a value larger than a core diameter **2***a* of equal to or less than 50 μm, the relative refractive index difference Δ**2** is set to a negative value of equal to or more than −0.15%, the hole diameter d is set in a range of 2.2 μm to 3.4 μm, and the hole occupancy rate S is set to equal to or less than 42% thus realizing characteristics such that the bending loss is equal to or less than 1 dB/turn, the cut-off wavelength is equal to or less than 1260 nm, the mode field diameter is in a range of 8.6 μm to 9.5 μm, and the zero-dispersion wavelength is in a range of 1300 nm to 1324 nm, the characteristics, which is compliant with the ITU-T G.652.

In addition, the core diameter **2***a* is set in a range of 6.0 μm to 8.4 μm, the relative refractive index difference Δ**1** is set in a range of 0.23% to 0.32%, the inner cladding layer outside diameter **2***b* is set to a value larger than a core diameter **2***a* of equal to or less than 50 μm, the relative refractive index difference Δ**2** is set to a negative value of equal to or more than −0.15%, the hole diameter d is set in a range of 2.7 μm to 3.4 μm, and the hole occupancy rate S is set to equal to or less than 42% thus realizing characteristics that is compliant with the ITU-T G.652 and the bending loss is as small as equal to or less than 0.1 dB/turn.

Hereinafter, based on the results of simulation calculations, in the hole-assisted optical fiber **10** according to the first embodiment, a relationship between the preferable ranges of design parameters such as the above-mentioned hole occupancy rate S, the core diameter **2***a*, relative refractive index differences Δ**1** and Δ**2**, the inner cladding layer outside diameter **2***b*, and hole diameter d and optical properties realized by the design parameters, such as the cut-off wavelength, the bending loss, the mode field diameter (MFD), and the zero-dispersion wavelength is explained.

Relationship between hole occupancy rate and optical properties

First of all, relationships between the hole occupancy rate S and optical properties are explained. Here, with respect to the other design parameters, the core diameter **2***a* is fixedly set to 8 μm, the inner cladding layer outside diameter **2***b* is fixedly set to 36 μm, the relative refractive index difference Δ**1** is fixedly set to 0.30%, and the relative refractive index difference Δ**2** is fixedly set to −0.05%.

FIG. **5** is a view illustrating a relationship between the hole occupancy rate S and the cut-off wavelength. Here, lines L**1** and L**2** indicate positions at which the cut-off wavelengths are 1550 nm and 1260 nm, respectively. As illustrated in FIG. **5**, when the hole occupancy rate S is equal to or less than 38%, the cut-off wavelength can be set to equal to or less than 1550 nm. When the hole occupancy rate S is equal to or less than 34%, the cut-off wavelength can be set to equal to or less than 1260 nm, which is compliant with the ITU-T G.652.

FIG. **6** is a view illustrating a relationship between the hole occupancy rate S and the bending loss. As illustrated in FIG. **6**, when the hole occupancy rate S is 17%, the bending loss is

1 dB/turn. Therefore, when the hole occupancy rate S is set to equal to or more than 17%, the bending loss can be set to equal to or less than 1 dB/turn.

FIG. **7** is a view illustrating a relationship between the hole occupancy rate S and the MFD. Here, lines L**3** and L**4** indicate positions at which the MFDs are 8.6 μm and 9.5 μm, respectively. As illustrated in FIG. **7**, when the hole occupancy rate S is equal to or less than 45%, the MFD can be set in a range of 8.6 μm to 9.5 μm, which is compliant with the ITU-T G.652. For example, when the hole occupancy rate S is equal to or less than 33%, the MFD can be set to equal to or more than 8.7 μm.

FIG. **8** is a view illustrating a relationship between the hole occupancy rate S and the zero-dispersion wavelength. Here, lines L**5** and L**6** indicate positions at which the zero-dispersion wavelengths are 1300 nm and 1324 nm, respectively. As illustrated in FIG. **8**, the zero-dispersion wavelength hardly depends on the hole occupancy rate S and hence, the hole occupancy rate S is set to equal to or less than 45% and the zero-dispersion wavelength can be set in a range of 1300 nm to 1324 nm, which is compliant with the ITU-T G.652.

Relationship between core diameter and optical properties

Next, relationships between the core diameter **2***a* and optical properties are explained. Here, with respect to the other design parameters, the hole occupancy rate S is fixedly set to 30.1%, the inner cladding layer outside diameter **2***b* is fixedly set to 36 μm, the relative refractive index difference Δ**1** is fixedly set to 0.30%, and the relative refractive index difference Δ**2** is fixedly set to −0.05%.

FIG. **9** is a view illustrating a relationship between the core diameter **2***a* and the cut-off wavelength. Here, lines L**1** and L**2** indicate positions at which the cut-off wavelengths are 1550 nm and 1260 nm, respectively. As illustrated in FIG. **9**, when the core diameter **2***a* is equal to or less than 9.8 μm, the cut-off wavelength can be set to equal to or less than 1550 nm. When the core diameter **2***a* is equal to or less than 7.5 μm, it is possible to confirm that the cut-off wavelength can be set to equal to or less than 1260 nm compliant with the ITU-T G.652.

FIG. **10** is a view illustrating a relationship between the core diameter **2***a* and the bending loss. As illustrated in FIG. **10**, when the core diameter **2***a* is 4 μm, the bending loss is 1 dB/turn. Therefore, when the core diameter **2***a* is set to equal to or more than 4 μm, the bending loss can be set to equal to or less than 1 dB/turn.

FIG. **11** is a view illustrating a relationship between the core diameter **2***a* and the MFD. Here, lines L**3** and L**4** indicate positions at which the MFDs are 8.6 μm and 9.5 μm, respectively. Furthermore, lines L**7** and L**8** indicate positions such that the MFDs are 8.0 μm and 10.1 μm, respectively. When data points illustrated in FIG. **11** are linearly approximated, it is possible to confirm that, when the core diameter **2***a* is in a range of 7.4 μm to 9.8 μm, the MFD can be set in a range of 8.6 μm to 9.5 μm, which is compliant with the ITU-T G.652.

FIG. **12** is a view illustrating a relationship between the core diameter **2***a* and the zero-dispersion wavelength. Here, lines L**5** and L**6** indicate positions at which the zero-dispersion wavelengths are 1300 nm and 1324 nm, respectively. When data points illustrated in FIG. **12** are approximated by a quaternary polynomial, it is possible to confirm that, when the core diameter **2***a* is in a range of 7.4 μm to 9 μm, the zero-dispersion wavelength can be set in a range of 1300 nm to 1324 nm, which is compliant with the ITU-T G.652.

Next, the case that only the hole occupancy rate S is changed to 35.7%, and the other design parameters are as follows without change; that is, the inner cladding layer outside diameter **2***b*, the relative refractive index difference Δ**1**, and the relative refractive index difference Δ**2** are fixedly set to 36 μm, 0.30%, and −0.05%, respectively, is explained.

FIG. **13** is a view illustrating a relationship between the core diameter **2***a* and the cut-off wavelength. Here, lines L**1** and L**2** indicate positions at which the cut-off wavelengths are 1550 nm and 1260 nm, respectively. As illustrated in FIG. **13**, it is possible to confirm that, when the core diameter **2***a* is equal to or less than 8.3 μm, the cut-off wavelength can be set to equal to or less than 1550 nm, and When the core diameter **2***a* is equal to or less than 6.5 μm, the cut-off wavelength can be set to equal to or less than 1260 nm, which is compliant with the ITU-T G.652.

FIG. **14** is a view illustrating a relationship between the core diameter **2***a* and the macrobendng loss. As illustrated in FIG. **14**, when the core diameter **2***a* is 3 μm, the bending loss is 1 dB/turn. Therefore, when the core diameter **2***a* is set to equal to or more than 3 μm, the bending loss can be set to equal to or less than 1 dB/turn.

FIG. **15** is a view illustrating a relationship between the core diameter **2***a* and the MFD. Here, lines L**3** and L**4** indicate positions at which the MFDs are 8.6 μm and 9.5 μm, respectively. Furthermore, lines L**7** and L**8** indicate positions such that the MFDs are 8.0 μm and 10.1 μm, respectively. When data points illustrated in FIG. **15** are linearly approximated to be extrapolated, it is possible to confirm that, when the core diameter **2***a* is equal to or more than 7.2 μm, the MFD can be set in a range of 8.6 μm to 9.5 μm, which is compliant with the ITU-T G.652.

FIG. **16** is a view illustrating a relationship between the core diameter **2***a* and the zero-dispersion wavelength. Here, lines L**5** and L**6** indicate positions at which the zero-dispersion wavelengths are 1300 nm and 1324 nm, respectively. As illustrated in FIG. **16**, it is possible to confirm that, when the core diameter **2***a* is in a range of 7.6 μm to 9.0 μm, the zero-dispersion wavelength can be set in a range of 1300 nm to 1324 nm, which is compliant with the ITU-T G.652.

Relationship between relative refractive index difference Δ**1** and optical properties

Next, relationships between the relative refractive index difference Δ**1** and optical properties are explained. Here, with respect to the other design parameters, the hole occupancy rate S is fixedly set to 30.1%, the core diameter **2***a* is fixedly set to 8 μm, the inner cladding layer outside diameter **2***b* is fixedly set to 36 μm, and the relative refractive index difference Δ**2** is fixedly set to −0.05%.

FIG. **17** is a view illustrating a relationship between the relative refractive index difference Δ**1** and the cut-off wavelength. Here, lines L**1** and L**2** indicate positions at which the cut-off wavelengths are 1550 nm and 1260 nm, respectively. As illustrated in FIG. **17**, it is possible to confirm that, when the relative refractive index difference Δ**1** is equal to or less than 0.45%, the cut-off wavelength can be set to equal to or less than 1550 nm, and when the relative refractive index difference Δ**1** is equal to or less than 0.26%, the cut-off wavelength can be set to equal to or less than 1260 nm, which is compliant with the ITU-T G.652.

FIG. **18** is a view illustrating a relationship between the relative refractive index difference Δ**1** and the bending loss. As illustrated in FIG. **18**, when the relative refractive index difference Δ**1** is 0.19%, the bending loss becomes 1 dB/turn. Therefore, when the relative refractive index difference Δ**1** is set to equal to or more than 0.19%, the bending loss can be set to equal to or less than 1 dB/turn.

FIG. **19** is a view illustrating a relationship between the relative refractive index difference Δ**1** and the MFD. Here, lines L**3** and L**4** indicate positions at which the MFDs are 8.6 μm and 9.5 μm, respectively. As illustrated in FIG. **19**, it is possible to confirm that, when the relative refractive index difference **Δ1** is in a range of 0.23% to 0.32%, the MFD can be set in a range of 8.6 μm to 9.5 μm, which is compliant with the ITU-T G.652.

FIG. **20** is a view illustrating a relationship between the relative refractive index difference **Δ1** and the zero-dispersion wavelength. Here, lines L**5** and L**6** indicate positions at which the zero-dispersion wavelengths are 1300 nm and 1324 nm, respectively. When data points illustrated in FIG. **20** are approximated by a quaternary polynomial, it is possible to confirm that, when the relative refractive index difference **Δ1** is equal to or less than 0.6%, the zero-dispersion wavelength can be set in a range of 1300 nm to 1324 nm, which is compliant with the ITU-T G.652.

Next, the case that only the hole occupancy rate S is changed to 35.7% and the other design parameters, which are the core diameter **2**a, the inner cladding layer outside diameter **2**b, and the relative refractive index difference **Δ2**, are fixedly set to 8 μm, 36 μm, and −0.05%, respectively, without change is explained.

FIG. **21** is a view illustrating a relationship between the relative refractive index difference **Δ1** and the cut-off wavelength. Here, lines L**1** and L**2** indicate positions at which the cut-off wavelengths are 1550 nm and 1260 nm, respectively. As illustrated in FIG. **21**, it is possible to confirm that, when the relative refractive index difference **Δ1** is equal to or less than 0.33%, the cut-off wavelength can be set to equal to or less than 1550 nm, and when the relative refractive index difference **Δ1** is equal to or less than 0.16%, the cut-off wavelength can be set to equal to or less than 1260 nm, which is compliant with the ITU-T G.652.

FIG. **22** is a view illustrating a relationship between the relative refractive index difference **Δ1** and the bending loss. As illustrated in FIG. **22**, when the relative refractive index difference **Δ1** is 0.11%, the bending loss is 1 dB/turn. Therefore, when the relative refractive index difference **Δ1** is set to equal to or more than 0.11%, the bending loss can be set to equal to or less than 1 dB/turn.

FIG. **23** is a view illustrating a relationship between the relative refractive index difference **Δ1** and the MFD. Here, lines L**3** and L**4** indicate positions at which the MFDs are 8.6 μm and 9.5 μm, respectively. When data points illustrated in FIG. **23** are linearly approximated, it is possible to confirm that, when the relative refractive index difference **Δ1** is in a range of 0.23% to 0.32%, the MFD can be set in a range of 8.6 μm to 9.5 μm, which is compliant with the ITU-T G.652.

FIG. **24** is a view illustrating a relationship between the relative refractive index difference **Δ1** and the zero-dispersion wavelength. Here, lines L**5** and L**6** indicate positions at which the zero-dispersion wavelengths are 1300 nm and 1324 nm, respectively. As illustrated in FIG. **24**, the zero-dispersion wavelength hardly depends on the relative refractive index difference **Δ1** and hence, for example, the relative refractive index difference **Δ1** is set to equal to or less than 45% and the zero-dispersion wavelength can be set in a range of 1300 nm to 1324 nm, which is compliant with the ITU-T G.652.

Relationship between relative refractive index difference **Δ2** and optical properties

Next, relationships between the relative refractive index difference **Δ2** and optical properties are explained. Here, with respect to the other design parameters, the hole occupancy rate S is fixedly set to 35.7%, the core diameter **2**a is fixedly set to 8 μm, the inner cladding layer outside diameter **2**b is fixedly set to 36 μm, and the relative refractive index difference **Δ1** is fixedly set to 0.30%.

FIG. **25** is a view illustrating a relationship between the relative refractive index difference **Δ2** and the cut-off wavelength. Here, lines L**1** and L**2** indicate positions at which the cut-off wavelengths are 1550 nm and 1260 nm, respectively. As illustrated in FIG. **25**, it is possible to confirm that, when the relative refractive index difference A**2** is equal to or more than −0.3%, the cut-off wavelength can be set to equal to or less than 1550 nm, and when the relative refractive index difference **Δ2** is equal to or more than −0.15%, the cut-off wavelength can be set to equal to or less than 1260 nm, which is compliant with the ITU-T G.652.

FIG. **26** is a view illustrating a relationship between the relative refractive index difference **Δ2** and the bending loss. As illustrated in FIG. **26**, it is possible to confirm that, when the relative refractive index difference **Δ2** is equal to or less than −0.04%, the bending loss can be set to equal to or less than 1 dB/turn.

FIG. **27** is a view illustrating a relationship between the relative refractive index difference **Δ2** and the MFD. Here, lines L**3** and L**4** indicate positions at which the MFDs are 8.6 μm and 9.5 μm, respectively. As illustrated in FIG. **27**, it is possible to confirm that, when the relative refractive index difference **Δ2** is in a range of −0.05% to 0.04%, the MFD can be set in a range of 8.6 μm to 9.5 μm, which is compliant with the ITU-T G.652.

FIG. **28** is a view illustrating a relationship between the relative refractive index difference **Δ2** and the zero-dispersion wavelength. Here, lines L**5** and L**6** indicate positions at which the zero-dispersion wavelengths are 1300 nm and 1324 nm, respectively. As illustrated in FIG. **28**, it is possible to confirm that, when the relative refractive index difference **Δ2** has a negative value equal to or more than −0.15%, the zero-dispersion wavelength can be set in a range of 1300 nm to 1324 nm, which is compliant with the ITU-T G.652.

Next, the case that only the hole occupancy rate S is changed to 35.7%, and the other design parameters are as follows without change; that is, the core diameter **2**a, the inner cladding layer outside diameter **2**b, and the relative refractive index difference **Δ1** are fixedly set to 8 μm, 36 μm, and 0.30% respectively is explained.

FIG. **29** is a view illustrating a relationship between the relative refractive index difference **Δ2** and the cut-off wavelength. Here, lines L**1** and L**2** indicate positions at which the cut-off wavelengths are 1550 nm and 1260 nm, respectively. As illustrated in FIG. **29**, it is possible to confirm that, when the relative refractive index difference **Δ2** is equal to or more than −0.26%, the cut-off wavelength can be set to equal to or less than 1550 nm, and when the relative refractive index difference **Δ2** is equal to or more than −0.04%, the cut-off wavelength can be set to equal to or less than 1260 nm, which is compliant with the ITU-T G.652.

FIG. **30** is a view illustrating a relationship between the relative refractive index difference **Δ2** and the bending loss. As illustrated in FIG. **30**, it is possible to confirm that, when the relative refractive index difference **Δ2** is equal to or less than 0%, the bending loss can be set to equal to or less than 1 dB/turn.

FIG. **31** is a view illustrating a relationship between the relative refractive index difference **Δ2** and the MFD. Here, lines L**3** and L**4** indicate positions at which the MFDs are 8.6 μm and 9.5 μm, respectively. As illustrated in FIG. **31**, it is possible to confirm that, when the relative refractive index difference **Δ2** is in a range of −0.07% 0.02%, the MFD can be set in a range of 8.6 μm to 9.5 μm, which is compliant with the ITU-T G.652.

FIG. **32** is a view illustrating a relationship between the relative refractive index difference **Δ2** and the zero-dispersion wavelength. Here, lines L**5** and L**6** indicate positions at which the zero-dispersion wavelengths are 1300 nm and 1324 nm, respectively. As illustrated in FIG. **32**, it is possible to confirm that, when the relative refractive index difference Δ**2** has a negative value equal to or more than −0.15%, the zero-dispersion wavelength can be set in a range of 1300 nm to 1324 nm, which is compliant with the ITU-T G.652.

Relationship between inner cladding layer outside diameter **2***b* and optical properties

Next, relationships between the inner cladding layer outside diameter **2***b* and optical properties are explained. Here, with respect to the other design parameters, the hole occupancy rate S is set to 30.1%, 35.7%, 39.9%, or 44.2%, the core diameter **2***a* is set to 7 μm, 8 μm, or 9 μm, the relative refractive index difference Δ**1** is set to 0.30%, and the relative refractive index difference Δ**2** is set to −0.05%.

FIG. **33** is a view illustrating a relationship between the inner cladding layer outside diameter **2***b* and the cut-off wavelength. Here, lines L**1** and L**2** indicate positions at which the cut-off wavelengths are 1550 nm and 1260 nm, respectively. As illustrated in FIG. **33**, the cut-off wavelength becomes larger along with the increases of the hole occupancy rate S, the core diameter **2***a*, and the inner cladding layer outside diameter **2***b*. Furthermore, if data points illustrated in FIG. **33** are approximated by a quadratic polynomial to be extrapolated, when the hole occupancy rate S is 30.1% and the core diameter **2***a* is 8 μm, it is possible to confirm that, when the inner cladding layer outside diameter **2***b* is in a range of 8 μm that is the core diameter **2***a* to 50 μm, the cut-off wavelength can be set to equal to or less than 1550 nm, and when the inner cladding layer outside diameter **2***b* is equal to or less than 32 μm, the cut-off wavelength can be set to equal to or less than 1260 nm, which is compliant with the ITU-T G.652. Furthermore, when the hole occupancy rate S is 35.7% and the core diameter **2***a* is 8 μm, it is possible to confirm that, when the inner cladding layer outside diameter **2***b* is in a range of 8 μm to 42 μm, the cut-off wavelength can be set to equal to or less than 1550 nm, and when the inner cladding layer outside diameter **2***b* is equal to or less than 10 μm, the cut-off wavelength can be set to equal to or less than 1260 nm.

FIG. **34** is a view illustrating a relationship between the inner cladding layer outside diameter **2***b* and the bending loss. As illustrated in FIG. **34**, the bending loss becomes lower along with the increases of the hole occupancy rate S, the core diameter **2***a*, and the inner cladding layer outside diameter **2***b*. Furthermore, when data points illustrated in FIG. **34** are approximated by an exponential curve to be extrapolated, in each case where the hole occupancy rate S is 30.1% or 35.7%, it is possible to confirm that, when the inner cladding layer outside diameter **2***b* is equal to or more than 8 μm, the bending loss can be set to equal to or less than 1 dB/turn.

FIG. **35** is a view illustrating a relationship between the inner cladding layer outside diameter **2***b* and the MFD. Here, lines L**3** and L**4** indicate positions at which the MFDs are 8.6 μm and 9.5 μm. As illustrated in FIG. **35**, the MFD hardly depends on the inner cladding layer outside diameter **2***b*. Furthermore, for example, when the hole occupancy rate S is 30.1%, it is possible to confirm that, when the inner cladding layer outside diameter **2***b* has a value ranging from 20 μm to 40 μm, the MFD can be set in a range of 8.6 μm to 9.5 μm, which is compliant with the ITU-T G.652.

FIG. **36** is a view illustrating a relationship between the inner cladding layer outside diameter **2***b* and the zero-dispersion wavelength. Here, lines L**5** and L**6** indicate positions at which the zero-dispersion wavelengths are 1300 nm and 1324 nm, respectively. As illustrated in FIG. **36**, the zero-dispersion wavelength hardly depends on the inner cladding layer outside diameter **2***b*. For example, when the hole occupancy rate S is 39.9% and the core diameter **2***a* is 9 μm, it is possible to confirm that, when the inner cladding layer outside diameter **2***b* is larger than 9 μm and not more than 50 μm, the zero-dispersion wavelength can be set in a range of 1300 nm to 1324 nm, which is compliant with the ITU-T G.652.

Relationship among hole diameter d, core diameter **2***a*, and optical properties

Next, a relationship between a hole diameter d, a core diameter **2***a*, and optical properties is explained. Hereinafter, first, under the condition that a hole occupancy rate S and the hole diameter d are fixedly set to specific values, the range of the core diameter **2***a* that satisfies desired optical properties is explained. Next, under the condition that the hole occupancy rate S and the core diameter **2***a* are fixedly set to specific values, the range of the hole diameter d that satisfies desired optical properties is explained. Here, with respect to the other design parameters, the core diameter **2***a*, the inner cladding layer outside diameter **2***b*, the relative refractive index difference Δ**1**, and the relative refractive index difference Δ**2** are fixedly set to 8 μm, 36 μm, 0.30%, and −0.05%, respectively.

First of all, the hole occupancy rate S is set to 30.1%. FIGS. **37**A and **37**B are views each illustrating a relationship between the core diameter **2***a* and the optical properties when the hole occupancy rate S is 30.1% and the hole diameter d is 2.9 μm. Here, FIG. **37**A illustrates a cut-off wavelength and a zero-dispersion wavelength, a square symbol and a diamond symbol in the drawing indicate the zero-dispersion wavelength and the cut-off wavelength, respectively, and a continuous line and a dashed line in the drawing indicate a position at which the cut-off wavelength is 1260 nm and positions at which the zero-dispersion wavelengths are 1300 nm and 1324 nm, respectively. Furthermore, FIG. **37**B illustrates a bending loss and an MFD, a black square symbol and a black diamond symbol in the drawing indicate the MFD and the bending loss, respectively, and a continuous line and a dashed line in the drawing indicate a position at which the bending loss is 0.1 dB/turn and positions at which the MFDs are 8.6 μm and 9.5 μm, respectively. Here, in FIG. **38**A to FIG. **54**A and FIG. **38**B to FIG. **54**B explained below also, a square symbol, a diamond symbol, a continuous line, and a dashed line each has the same meaning as above. As illustrated in FIGS. **37**A and **37**B, if the hole diameter d is 2.9 μm, when the core diameter **2***a* is in a range of 7.8 μm to 8.0 μm, a bending loss of equal to or less than 0.1 dB/turn, a cut-off wavelength of equal to or less than 1260 nm, an MFD of in a range of 8.6 μm to 9.5 μm at a wavelength of 1310 nm, and a zero-dispersion wavelength of in a range of 1300 nm to 1324 nm can be realized.

FIGS. **38**A and **38**B are views each illustrating a relationship between the core diameter **2***a* and the optical properties when the hole occupancy rate S is 30.1% and the hole diameter d is 3.3 μm. Here, FIG. **38**A illustrates the cut-off wavelength and the zero-dispersion wavelength, and FIG. **38**B illustrates the bending loss and the MFD. As illustrated in FIGS. **38**A and **38**B, if the hole diameter d is 3.3 μm, when the core diameter **2***a* is in a range of 7.8 μm to 8.4 μm, a bending loss of equal to or less than 0.1 dB/turn, a cut-off wavelength of equal to or less than 1260 nm, an MFD of in a range of 8.6 μm to 9.5 μm at a wavelength of 1310 nm, and a zero-dispersion wavelength of in a range of 1300 nm to 1324 nm can be realized.

FIGS. **39**A and **39**B are views each illustrating a relationship between the hole diameter d and the optical properties when the hole occupancy rate S is 30.1% and the core diameter **2***a* is 6.6 μm. Here, FIG. **39**A illustrates the cut-off wavelength and the zero-dispersion wavelength, and FIG. **39**B illustrates the bending loss and the MFD. As illustrated in FIGS. **39**A and **39**B, when the core diameter **2***a* is 6.6 μm, there exists no range of the hole diameter d in which a bending loss of equal to or less than 0.1 dB/turn, a cut-off wavelength of equal to or less than 1260 nm, an MFD of in a range of 8.6 μm to 9.5 μm at a wavelength of 1310 nm, and a zero-dispersion wavelength of in a range of 1300 nm to 1324 nm can be realized.

FIGS. **40**A and **40**B are views each illustrating a relationship between the hole diameter d and the optical properties when the hole occupancy rate S is 30.1% and the core diameter **2***a* is 7.8 μm. Here, FIG. **40**A illustrates the cut-off wavelength and the zero-dispersion wavelength, and FIG. **40**B illustrates the bending loss and the MFD. As illustrated in FIGS. **40**A and **40**B, if the core diameter **2***a* is 7.8 μm, when the hole diameter d is in a range of 2.9 μm to 3.4 μm, a bending loss of equal to or less than 0.1 dB/turn, a cut-off wavelength of equal to or less than 1260 nm, an MFD of in a range of 8.6 μm to 9.5 μm at a wavelength of 1310 nm, and a zero-dispersion wavelength of in a range of 1300 nm to 1324 nm can be realized.

As a result illustrated in FIGS. **37**A and **37**B to FIGS. **40**A and **40**B, if the hole occupancy rate S is 30.1%, when the core diameter **2***a* is in a range of 7.8 μm to 8.4 μm and the hole diameter d is in a range of 2.9 μm to 3.4 μm, a bending loss of equal to or less than 0.1 dB/turn, a cut-off wavelength of equal to or less than 1260 nm, an MFD of in a range of 8.6 μm to 9.5 μm at a wavelength of 1310 nm, and a zero-dispersion wavelength of in a range of 1300 nm to 1324 nm can be realized.

Next, the hole occupancy rate S is fixedly set to 35.7%. FIGS. **41**A and **41**B are views each illustrating a relationship between the core diameter **2***a* and the optical properties when the hole occupancy rate S is 35.7% and the hole diameter d is 2.6 μm. Here, FIG. **41**A illustrates the cut-off wavelength and the zero-dispersion wavelength, and FIG. **41**B illustrates the bending loss and the MFD. As illustrated in FIGS. **41**A and **41**B, when the hole diameter d is 2.6 μm, there exists no range of the core diameter **2***a* in which a bending loss of equal to or less than 0.1 dB/turn, a cut-off wavelength of equal to or less than 1260 nm, an MFD of in a range of 8.6 μm to 9.5 μm at a wavelength of 1310 nm, and a zero-dispersion wavelength of in a range of 1300 nm to 1324 nm can be realized.

FIGS. **42**A and **42**B are views each illustrating a relationship between the core diameter **2***a* and the optical properties when the hole occupancy rate S is 35.7% and the hole diameter d is 2.7 μm. Here, FIG. **42**A illustrates the cut-off wavelength and the zero-dispersion wavelength, and FIG. **42**B illustrates the bending loss and the MFD. As illustrated in FIGS. **42**A and **42**B, if the hole diameter d is 2.7 μm, when the core diameter **2***a* is in a range of 6.6 μm to 7.2 μm, a bending loss of equal to or less than 0.1 dB/turn, a cut-off wavelength of equal to or less than 1260 nm, an MFD of in a range of 8.6 μm to 9.5 μm at a wavelength of 1310 nm, and a zero-dispersion wavelength of in a range of 1300 nm to 1324 nm can be realized.

FIGS. **43**A and **43**B are views each illustrating a relationship between the core diameter **2***a* and the optical properties when the hole occupancy rate S is 35.7% and the hole diameter d is 2.9 μm. Here, FIG. **43**A illustrates the cut-off wavelength and the zero-dispersion wavelength, and FIG. **43**B illustrates the bending loss and the MFD. As illustrated in FIGS. **43**A and **43**B, if the hole diameter d is 2.9 μm, when the core diameter **2***a* is in a range of 6.4 μm to 7.4 μm, a bending loss of equal to or less than 0.1 dB/turn, a cut-off wavelength of equal to or less than 1260 nm, an MFD of in a range of 8.6 μm to 9.5 μm at a wavelength of 1310 nm, and a zero-dispersion wavelength of in a range of 1300 nm to 1324 nm can be realized.

FIGS. **44**A and **44**B are views each illustrating a relationship between the core diameter **2***a* and the optical properties when the hole occupancy rate S is 35.7% and the hole diameter d is 3.3 μm. Here, FIG. **44**A illustrates the cut-off wavelength and the zero-dispersion wavelength, and FIG. **44**B illustrates the bending loss and the MFD. As illustrated in FIGS. **44**A and **44**B, when the hole diameter d is 3.3 μm, there exists no range of the core diameter **2***a* in which a bending loss of equal to or less than 0.1 dB/turn, a cut-off wavelength of equal to or less than 1260 nm, an MFD of in a range of 8.6 μm to 9.5 μm at a wavelength of 1310 nm, and a zero-dispersion wavelength of in a range of 1300 nm to 1324 nm can be realized.

FIGS. **45**A and **45**B are views each illustrating a relationship between the hole diameter d and the optical properties when the hole occupancy rate S is 35.7% and the core diameter **2***a* is 6.6 μm. Here, FIG. **45**A illustrates the cut-off wavelength and the zero-dispersion wavelength, and FIG. **45**B illustrates the bending loss and the MFD. As illustrated in FIGS. **45**A and **45**B, if the core diameter **2***a* is 6.6 μm, when the hole diameter d is in a range of 2.7 μm to 3.1 μm, a bending loss of equal to or less than 0.1 dB/turn, a cut-off wavelength of equal to or less than 1260 nm, an MFD of in a range of 8.6 μm to 9.5 μm at a wavelength of 1310 nm, and a zero-dispersion wavelength of in a range of 1300 nm to 1324 nm can be realized. Furthermore, when the hole diameter d is in a range of 2.4 μm to 4.0 μm, a bending loss of equal to or less than 1 dB/turn and a cut-off wavelength of equal to or less than 1550 nm can be realized.

FIGS. **46**A and **46**B are views each illustrating a relationship between the hole diameter d and the optical properties when the hole occupancy rate S is 35.7% and the core diameter **2***a* is 7.1 μm. Here, FIG. **46**A illustrates the cut-off wavelength and the zero-dispersion wavelength, and FIG. **46**B illustrates the bending loss and the MFD. As illustrated in FIGS. **46**A and **46**B, if the core diameter **2***a* is 7.1 μm, when the hole diameter d is in a range of 2.8 μm to 3.1 μm, a bending loss of equal to or less than 0.1 dB/turn, a cut-off wavelength of equal to or less than 1260 nm, an MFD of in a range of 8.6 μm to 9.5 μm at a wavelength of 1310 nm, and a zero-dispersion wavelength of in a range of 1300 nm to 1324 nm can be realized.

As a result illustrated in FIGS. **41**A and **41**B to FIGS. **46**A and **46**B, if the hole occupancy rate S is 36%, when the core diameter **2***a* is in a range of 6.4 μm to 7.4 μm and the hole diameter d is in a range of 2.7 μm to 3.2 μm, a bending loss of equal to or less than 0.1 dB/turn, a cut-off wavelength of equal to or less than 1260 nm, an MFD of in a range of 8.6 μm to 9.5 μm at a wavelength of 1310 nm, and a zero-dispersion wavelength of in a range of 1300 nm to 1324 nm can be realized. Furthermore, when the hole diameter d is in a range of 2.7 μm to 4.0 μm, a bending loss of equal to or less than 1 dB/turn and a cut-off wavelength of equal to or less than 1550 nm can be realized.

Next, the hole occupancy rate S is fixedly set to 38.0%. FIGS. **47**A and **47**B are views each illustrating a relationship between the core diameter **2***a* and the optical properties when the hole occupancy rate S is 38.0% and the hole diameter d is 2.7 μm. Here, FIG. **47**A illustrates the cut-off wavelength and the zero-dispersion wavelength, and FIG. **47**B illustrates the bending loss and the MFD. As illustrated in FIGS. **47**A and **47**B, if the hole diameter d is 2.7 μm, when the core diameter **2***a* is in a range of 6.2 μm to 6.5 μm, a bending loss of equal to or less than 0.1 dB/turn, a cut-off wavelength of equal to or less than 1260 nm, an MFD of in a range of 8.6 μm to 9.5 μm at a wavelength of 1310 nm, and a zero-dispersion wavelength of in a range of 1300 nm to 1324 nm can be realized.

FIGS. **48**A and **48**B are views each illustrating a relationship between the core diameter **2**a and the optical properties when the hole occupancy rate S is 38.0% and the hole diameter d is 2.9 μm. Here, FIG. **48**A illustrates the cut-off wavelength and the zero-dispersion wavelength, and FIG. **48**B illustrates the bending loss and the MFD. As illustrated in FIGS. **48**A and **48**B, if the hole diameter d is 2.9 μm, when the core diameter **2**a is in a range of 6.2 μm to 7.1 μm, a bending loss of equal to or less than 0.1 dB/turn, a cut-off wavelength of equal to or less than 1260 nm, an MFD of in a range of 8.6 μm to 9.5 μm at a wavelength of 1310 nm, and a zero-dispersion wavelength of in a range of 1300 nm to 1324 nm can be realized.

FIGS. **49**A and **49**B are views each illustrating a relationship between the hole diameter d and the optical properties when the hole occupancy rate S is 38.0% and the core diameter **2**a is 6.6 μm. Here, FIG. **49**A illustrates the cut-off wavelength and the zero-dispersion wavelength, and FIG. **49**B illustrates the bending loss and the MFD. As illustrated in FIGS. **49**A and **49**B, if the core diameter **2**a is 6.6 μm, when the hole diameter d is in a range of 2.8 μm to 3.1 μm, a bending loss of equal to or less than 0.1 dB/turn, a cut-off wavelength of equal to or less than 1260 nm, an MFD of in a range of 8.6 μm to 9.5 μm at a wavelength of 1310 nm, and a zero-dispersion wavelength of in a range of 1300 nm to 1324 nm can be realized. Furthermore, when the hole diameter d is in a range of 2.4 μm to 4.0 μm, a bending loss of equal to or less than 1 dB/turn and a cut-off wavelength of equal to or less than 1550 nm can be realized.

FIGS. **50**A and **50**B are views each illustrating a relationship between the hole diameter d and the optical properties when the hole occupancy rate S is 38.0% and the core diameter **2**a is 7.0 μm. Here, FIG. **50**A illustrates the cut-off wavelength and the zero-dispersion wavelength, and FIG. **50**B illustrates the bending loss and the MFD. As illustrated in FIGS. **50**A and **50**B, if the core diameter **2**a is 7.0 μm, when the hole diameter d is in a range of 2.9 μm to 3.0 μm, a bending loss of equal to or less than 0.1 dB/turn, a cut-off wavelength of equal to or less than 1260 nm, an MFD of in a range of 8.6 μm to 9.5 μm at a wavelength of 1310 nm, and a zero-dispersion wavelength of in a range of 1300 nm to 1324 nm can be realized. Furthermore, when the hole diameter d is in a range of 2.7 μm to 4.0 μm, a bending loss of equal to or less than 1 dB/turn and a cut-off wavelength of equal to or less than 1550 nm can be realized.

As a result illustrated in FIGS. **47**A and **47**B to FIGS. **50**A and **50**B, if the hole occupancy rate S is 38.0%, when the core diameter **2**a is in a range of 6.2 μm to 7.5 μm and the hole diameter d is in a range of 2.7 μm to 3.1 μm, a bending loss of equal to or less than 0.1 dB/turn, a cut-off wavelength of equal to or less than 1260 nm, an MFD of in a range of 8.6 μm to 9.5 μm at a wavelength of 1310 nm, and a zero-dispersion wavelength of in a range of 1300 nm to 1324 nm can be realized. Furthermore, when the hole diameter d is in a range of 2.7 μm to 4.0 μm, a bending loss of equal to or less than 1 dB/turn and a cut-off wavelength of equal to or less than 1550 nm can be realized.

Next, the hole occupancy rate S is fixedly set to 42.0%. FIGS. **51**A and **51**B are views each illustrating a relationship between the core diameter **2**a and the optical properties when the hole occupancy rate S is 42.0% and the hole diameter d is 2.9 μm. Here, FIG. **51**A illustrates the cut-off wavelength and the zero-dispersion wavelength, and FIG. **51**B illustrates the bending loss and the MFD. As illustrated in FIGS. **51**A and **51**B, if the hole diameter d is 2.9 μm, when the core diameter **2**a is 6.0 μm, a bending loss of equal to or less than 0.1 dB/turn, a cut-off wavelength of equal to or less than 1260 nm, an MFD of in a range of 8.6 μm to 9.5 μm at a wavelength of 1310 nm, and a zero-dispersion wavelength of in a range of 1300 nm to 1324 nm can be realized.

FIGS. **52**A and **52**B are views each illustrating a relationship between the core diameter **2**a and the optical properties when the hole occupancy rate S is 42.0% and the hole diameter d is 3.2 μm. Here, FIG. **52**A illustrates the cut-off wavelength and the zero-dispersion wavelength, and FIG. **52**B illustrates the bending loss and the MFD. As illustrated in FIGS. **52**A and **52**B, when the hole diameter d is 3.2 μm, there exists no range of the core diameter **2**a in which a bending loss of equal to or less than 0.1 dB/turn, a cut-off wavelength of equal to or less than 1260 nm, an MFD of in a range of 8.6 μm to 9.5 μm at a wavelength of 1310 nm, and a zero-dispersion wavelength of in a range of 1300 nm to 1324 nm can be realized.

FIGS. **53**A and **53**B are views each illustrating a relationship between the hole diameter d and the optical properties when the hole occupancy rate S is 42.0% and the core diameter **2**a is 6.0 μm. Here, FIG. **53**A illustrates the cut-off wavelength and the zero-dispersion wavelength, and FIG. **53**B illustrates the bending loss and the MFD. As illustrated in FIGS. **53**A and **53**B, if the core diameter **2**a is 6.0 μm, when the hole diameter d is 2.9 μm, a bending loss of equal to or less than 0.1 dB/turn, a cut-off wavelength of equal to or less than 1260 nm, an MFD of in a range of 8.6 μm to 9.5 μm at a wavelength of 1310 nm, and a zero-dispersion wavelength of in a range of 1300 nm to 1324 nm can be realized.

FIGS. **54**A and **54**B are views each illustrating a relationship between the hole diameter d and the optical properties when the hole occupancy rate S is 42.0% and the core diameter **2**a is 7.0 μm. Here, FIG. **54**A illustrates the cut-off wavelength and the zero-dispersion wavelength, and FIG. **54**B illustrates the bending loss and the MFD. As illustrated in FIGS. **54**A and **54**B, when the core diameter **2**a is 7.0 μm, a bending loss of equal to or less than 0.1 dB/turn, a cut-off wavelength of equal to or less than 1260 nm, an MFD of in a range of 8.6 μm to 9.5 μm at a wavelength of 1310 nm, and a zero-dispersion wavelength of in a range of 1300 nm to 1324 nm can be realized. Furthermore, when the hole diameter d is in a range of 2.7 μm to 4.0 μm, there exists no range of the hole diameter d in which a bending loss of equal to or less than 1 dB/turn and a cut-off wavelength of equal to or less than 1550 nm can be realized.

As a result illustrated in FIGS. **51**A and **51**B to FIGS. **54**A and **54**B, if the hole occupancy rate S is 42.0%, when the core diameter **2**a is 6.0 μm and the hole diameter d is 2.9 μm, a bending loss of equal to or less than 0.1 dB/turn, a cut-off wavelength of equal to or less than 1260 nm, an MFD of in a range of 8.6 μm to 9.5 μm at a wavelength of 1310 nm, and a zero-dispersion wavelength of in a range of 1300 nm to 1324 nm can be realized.

FIGS. **55**A and **55**B are views each illustrating a relationship between the combination of the structural parameters and the optical properties when the hole occupancy rate S is 30.1%, the structural parameters being illustrated in FIGS. **37**A and **37**B to **40**A and **40**B. FIGS. **55**C and **55**D are views each illustrating a relationship between the combination of the structural parameters and the optical properties when the hole occupancy rate S is 35.7%, the structural parameters being illustrated in FIGS. **41**A and **41**B to FIGS. **46**A and **46**B. FIGS. **55**E and **55**F are views each illustrating a relationship between the combination of the structural parameters and the optical properties when the hole occupancy rate S is 38.0%, the structural parameters being illustrated in FIGS. **47**A and **47**B to FIGS. **50**A and **50**B. FIGS. **55**G and **55**H are views each illustrating a relationship between the combination of the structural parameters and the optical properties when the hole occupancy rate S is 42.0%, the structural parameters being illustrated in FIGS. **51**A and **51**B to FIGS. **54**A and **54**B.

In the structural parameters illustrated in FIGS. **55**A to **55**H, the core diameter **2***a* is in a range of 6.0 μm to 8.4 μm, the relative refractive index difference **Δ1** is in a range of 0.23% to 0.32%, the inner cladding layer outside diameter **2***b* is equal to or less than 50 μm, the relative refractive index difference **Δ2** is equal to or more than −0.15%, the hole diameter d is in a range of 2.7 μm to 3.4 μm, and the hole occupancy rate S is equal to or less than 42%. The hole-assisted optical fiber having the above-mentioned structural parameters realizes a bending loss of equal to or less than 0.1 dB/turn, a cut-off wavelength of equal to or less than 1260 nm, an MFD of in a range of 8.6 μm to 9.5 μm at a wavelength of 1310 nm, and a zero-dispersion wavelength of in a range of 1300 nm to 1324 nm.

Furthermore, FIG. **56** is a view illustrating a relationship between the combination of the hole occupancy rate and the other structural parameters, and the optical properties of the hole-assisted optical fiber according to the first embodiment. In the structural parameters illustrated in FIG. **56**, the core diameter **2***a* is in a range of 3 μm to 9.8 μm, the relative refractive index difference **Δ1** is in a range of 0.11% to 0.45%, the inner cladding layer outside diameter **2***b* has a value larger than a core diameter and equal to or less than 53 μm, the relative refractive index difference **Δ2** has a negative value more than −0.30%, the hole diameter d is in a range of 2.4 μm to 4.0 μm, and the hole occupancy rate S is in a range of 17% to 48%. The hole-assisted optical fiber having the above-mentioned structural parameters realizes such a bending loss of equal to or less than 1 dB/turn and a cut-off wavelength of equal to or less than 1550 nm as illustrated in FIG. **56**.

Next, FIG. **57** is a view illustrating a relationship between another combination of the hole occupancy rate and the other structural parameters, and the optical properties of the hole-assisted optical fiber according to the first embodiment. In the structural parameters illustrated in FIG. **57**, the core diameter **2***a* is in a range of 6.0 μm to 8.4 μm, the relative refractive index difference **Δ1** is in a range of 0.23% to 0.32%, the inner cladding layer outside diameter **2***b* has a value larger than a core diameter **2***a* and equal to or less than 36 μm, the relative refractive index difference **Δ2** has a negative value more than −0.15%, the hole diameter d is in a range of 2.5 μm to 3.4 μm, and the hole occupancy rate S is in a range of 17% to 42%. The hole-assisted optical fiber having the above-mentioned structural parameters realizes such a bending loss of equal to or less than 1 dB/turn, a cut-off wavelength of equal to or less than 1260 nm, an MFD of in a range of 8.6 μm to 9.5 μm at a wavelength of 1310 nm, and a zero-dispersion wavelength of in a range of 1300 nm to 1324 nm as illustrated in FIG. **57**. Furthermore, the hole-assisted optical fiber also realizes a zero-dispersion slope of equal to or less than 0.092 ps/nm^2/km thus realizing an optical fiber compliant with the ITU-T G.652.

Here, in the above-mentioned first embodiment, the number of holes is 10. However, the number of holes may be set to any value equal to or more than 4, and it is particularly preferable that the number of holes be set to an even value since the arrangement of the holes is high in symmetry. In this case, even when the number of holes is set to a value other than 10, a hole-assisted optical fiber having a hole occupancy rate S of a value same as that of the hole-assisted optical fiber according to the first embodiment has properties same as the case of the hole-assisted optical fiber according to the first embodiment.

In some embodiments, the hole-assisted optical fiber includes the inner cladding layer, thus achieving the hole-assisted optical fiber which is excellent in bending loss characteristics, suitable for use as an optical communication-use optical fiber, and high in productivity.

Although the invention has been described with respect to specific embodiments for a complete and clear disclosure, the appended claims are not to be thus limited but are to be construed as embodying all modifications and alternative constructions that may occur to one skilled in the art that fairly fall within the basic teaching herein set forth.

What is claimed is:

1. A hole-assisted optical fiber comprising:

a core portion; and

a cladding portion that includes an inner cladding layer formed around an outer periphery of the core portion and having a refractive index lower than that of the core portion, an outer cladding layer formed around an outer periphery of the inner cladding layer and having a refractive index higher than that of the inner cladding layer and lower than that of the core portion, and a plurality of holes formed around the core portion, wherein

a diameter of the core portion is in a range of 3 μm to 9.8 μm, a relative refractive index difference of the core portion relative to the outer cladding layer is in a range of 0.11% to 0.45%, an outside diameter of the inner cladding layer is equal to or less than 53 μm, a relative refractive index difference of the inner cladding layer relative to the outer cladding layer is a negative value equal to or more than −0.30%, a diameter of each of the plurality of holes is in a range of 2.4 μm to 4.0 μm, a hole occupancy rate is in a range of 17% to 48%, a bending loss at a wavelength of 1625 nm when bent at a radius of 5 mm is equal to or less than 1 dB/turn, and a cut-off wavelength is equal to or less than 1550 nm, and

the hole occupancy rate S (%) is defined by the following expression (1):

$$S=N\pi(d/2)^2/[\pi(R+d)^2-\pi R^2] \quad (1)$$

where N is the number of the plurality of holes, d (μm) is the diameter of each of the plurality of holes, and R (μm) is a radius of an inscribed circle which is brought into internal contact with each of the plurality of holes.

2. The hole-assisted optical fiber according to claim **1**, wherein the diameter of the core portion is in a range of 6.0 μm to 8.4 μm, the relative refractive index difference of the core portion relative to the outer cladding layer is in a range of 0.23% to 0.32%, the outside diameter of the inner cladding layer is equal to or less than 50 μm, the relative refractive index difference of the inner cladding layer relative to the outer cladding layer is equal to or more than −0.15%, the diameter of each of the plurality of holes is in a range of 2.5 μm to 3.4 μm, the hole occupancy rate is equal to or less than 42%, the cut-off wavelength is equal to or less than 1260 nm, a mode field diameter at a wavelength of 1310 nm is in a range of 8.6 μm to 9.5 μm, and a zero-dispersion wavelength is in a range of 1300 nm to 1324 nm.

3. The hole-assisted optical fiber according to claim **2**, wherein the diameter of the core portion is in a range of 6.0 μm to 8.4 μm, the relative refractive index difference of the core portion relative to the outer cladding layer is in a range of 0.23% to 0.32%, the outside diameter of the inner cladding layer is equal to or less than 50 μm, the relative refractive index difference of the inner cladding layer relative to the outer cladding layer is equal to or more than −0.15%, the diameter of each of the plurality of holes is in a range of 2.7 μm to 3.4 μm, the hole occupancy rate is equal to or less than

42%, the cut-off wavelength is equal to or less than 1260 nm, the mode field diameter at a wavelength of 1310 nm is in a range of 8.6 μm to 9.5 μm, the zero-dispersion wavelength is in a range of 1300 nm to 1324 nm, and the bending loss at a wavelength of 1625 nm when bent at a radius of 5 mm is equal to or less than 0.1 dB/turn.

* * * * *